Development and application of novel proteomics methods in proteomics research

Hao, Piliang

2015

Hao, P. (2015). Development and application of novel proteomics methods in proteomics research. Doctoral thesis, Nanyang Technological University, Singapore.

https://hdl.handle.net/10356/62181

https://doi.org/10.32657/10356/62181

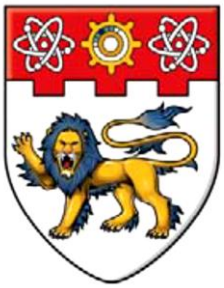

NANYANG TECHNOLOGICAL UNIVERSITY

DEVELOPMENT AND APPLICATION OF NOVEL PROTEOMICS METHODS IN PROTEOMICS RESEARCH

PILIANG HAO

SCHOOL OF BIOLOGICAL SCIENCES

SINGAPORE CENTER ON ENVIRONMENTAL LIFE SCIENCES ENGINEERING

2014

Development and application of novel proteomics methods in proteomics research

Piliang Hao

School of Biological Sciences

Singapore Centre on Environmental Life Sciences Engineering

A thesis submitted to the Nanyang Technological University in fulfillment of the requirement of the degree of Doctor of Philosophy

2014

Acknowledgements

It would not be possible to write this doctoral thesis without the generous help and support from the people around me. I would like to express my sincere gratitude to all of them.

First, my deepest gratitude goes to Dr. Siu Kwan Sze, my Ph.D. supervisor, for his expert guidance and inspiration. His aspiration for novel ideas and persistence in technical innovation has been very important to the success of my research projects. More importantly, it inspires my creativity in solving scientific problems. It is invaluable experience to learn mass spectrometry and proteomics from him during the past five years as a research associate and a Ph.D. student.

I would like to acknowledge the Singapore Centre on Environmental Life Sciences Engineering (SCELSE) for offering me the Ph.D. scholarship to support my studies and life in Singapore. My sincere gratitude goes to many people from SCELSE: Prof. Staffan Kjelleberg has been very supportive in my Ph.D. application and studies; Prof. Yehuda Cohen and Prof. Sanjay Swarup have been very kind to me and teach me how to get along well with people around me; Dr. Grace Chong Hui Ying has been very kind, helpful and timely in processing many issues related to my Ph.D. studies.

I would like to thank my thesis advisory committee, Dr. Zbynek Bozdech and Dr. Rohan Benjamin Hugh Williams, for their constructive criticism and good suggestions during the TAC meetings. I would also like to express my sincere gratitude to Prof. Gerhard Gruber and Prof. Ho Sup Yoon for their fairness and friendly attitude in solving controversial problems. I also thanks Ms. Chong Chye Hong May from graduate office for her kind support during my Ph.D. studies.

Acknowledgements

I would also like to acknowledge the kind support from my current and former laboratory colleagues, such as Wei Meng, Jingru Qian, Dr. Xin Li, Dr. Tiannan Guo, Dr. Yi Zhu, Sim Kae Hwan, Cheow Sok Hwee Esther, Dr. Hongbin Zhu, Dr. Yang Sun, Qi Zhang, Dr. Aida Serra Maqueda, Gallart Palau Xavier, Dr. Bamaprasad Dutta, Dr. Arnab Datta, Dr. Sunil Adav, for their kind help and discussion.

Last, my most gratitude goes to my family for their continuous support and encouragement during my Ph.D. studies. Dr. Yan Ren, my wife, has given me many invaluable comments, suggestions and insightful discussions on my research projects. More importantly, she has spent nearly all of her spare time on taking care of our two kids so that I can spend most of my time on my research work. Ren Yan's parents have also spent most of their time in helping to take care of our kids in the past 5 years. The love and encouragement from my parents have accompanied me and made me a righteous and strict person.

Table of Contents

Table of Contents

Table of Contents

Table of Contents

Table of Contents

List of figures

List of figures

List of tables

Abbreviations

2-DE	Two Dimensional gel Electrophoresis
ABB	Ammonium Bicarbonate
ACN	Acetonitrile
AUC	Area Under the Curve
BCA	BicinChoninic Acid
BSA	Bovine Serum Albumin
CEA	Carotid Endarterectomy
CID	Collision-Induced Dissociation
DTT	Dithiothreitol
ECM	Extracellular Matrix
EDTA	Ethylenediaminetetraacetic Acid
ELISA	Enzyme-Linked Immunosorbent Assay
ERLIC	Electrostatic Repulsion-Hydrophilic Interaction Chromatography
FDR	False Discovery Rate
FWHM	Full Width at Half-Maximum
GO	Gene Ontology
HCD	Higher-energy Collisional Dissociation
HILIC	Hydrophilic Interaction Liquid Chromatography
HPLC	High Performance Liquid Chromatography
ICAT	Isotope Coded Affinity Tag
IAA	Iodoacetamide
IPA	Ingenuity Pathway Analysis
IPI	International Protein Index
iTRAQ	Isobaric Tags for Relative and Absolute Quantification
LC	Liquid Chromatography
LC-MS/MS	Liquid Chromatography coupled to Tandem Mass Spectrometry
LTQ	Linear Quadrupole ion Trap
MALDI	Matrix-Assisted Laser Desorption/Ionization
MDLC	Multidimensional Liquid Chromatography

Abbreviations

MGF	Mascot Generic File
MMP	Matrix Metalloproteinases
MMTS	Methyl Methanethiosulfonate
MRM	Multiple reaction monitoring
mRNA	Messenger RNA
MS	Mass Spectrometry
MudPIT	Multidimensional Protein Identification Technology
NCE	Normalized Collision Energy
NH4Ace	Ammonium Acetate
PBS	Phosphate-Buffered Saline
*p*I	Isoelectric Point
PIMT	Protein L-isoaspartyl-O-methyltransferase
PRM	Parallel Reaction Monitoring
PSM	Peptide Spectrum Match
PTM	Post-Translational Modification
ROC	Receiver Operating characteristic
RPLC	Reverse-phase Liquid Chromatography
RT	Room Temperature
SAX	Strong Anion Exchange
SCX	Strong Cation Exchange
SDS-PAGE	Sodium Dodecyl Sulfate Polyacrylamide Gel Electrophoresis
SILAC	Stable Isotope Labeling by Amino Acids in Cell Culture
SRM	Selected Reaction Monitoring
TCEP	Tris 2-Carboxyethyl Phosphine Hydrochloride
TEAB	Triethylammonium Bicarbonate
TFA	Trifluoroacetic Acid
TMT	Tandem Mass Tags
TOF	Time-of-Flight
Tris	2-Amino-2-hydroxymethyl-propane-1, 3-diol
WAX	Weak Anion Exchange
XIC	Extracted Ion Chromatogram

Abstract

The sensitivity, throughput and accuracy of proteomics have improved considerably in the past years due to the development of novel technologies. However, characterization of protein post-translational modifications remains challenging, especially those less studied ones. Protein deamidation is reported to be involved in aging and many diseases, but so far is less studied due to technical challenges. The existing challenges for accurately identifying and quantifying protein deamidation sites in proteomics include tremendous false positive identifications of deamidated peptides from database searches, substantial interference of artificial deamidation from sample preparation, difficulties in differentiating and quantifying the isomeric n-Asp and isoAsp deamidation products in proteome scale, and inability of validating quantification of deamidated peptides by either ELISA or multiple reaction monitoring. In this thesis, novel proteomic methods were developed to overcome these challenges and facilitate the large-scale characterization of protein deamidation. The accurate and reliable characterization of endogenous protein deamidation becomes feasible with both false positive identifications and artificial deamidation minimized while using our new data analysis strategy and sample preparation protocols. High-resolution parallel reaction monitoring enables the accurate validation of deamidated peptides in unfractionated individual samples. In addition to the validation of these methods using both model proteins and complex tissue samples, we also applied them to the study of protein deamidation in human carotid atherosclerotic plaques from aged patients for predicting secondary cerebrovascular events. The biomarker candidates of deamidated peptides and proteins obtained from label-free quantification on pool samples were validated in 38 individual plaques using parallel reaction monitoring for their applicability as biomarkers. None of them reached the criterion as a clinically usable biomarker possibly due to the small sample size and high individual variation. However, these newly developed technologies open a door for scientists who are interested in understanding the role of protein deamidation in aging and many diseases.

Chapter 1

General Introduction

1 General Introduction

1.1 Recent Development in Proteomics and Existing Challenges

The term "proteomics" was first coined in 1997 and was defined as the large-scale characterization of the entire protein complement of a cell line, tissue, or organism.(1) Proteome is the entire set of proteins produced or modified by an organism or system. (2, 3) Proteomics has developed quickly since the complete sequencing of human genome was achieved in 2003. Database search has been the most prevalent peptide and protein identification methods in proteomics, (4) and it relies on a complete protein database predicted from the genome sequences. *De novo* peptide and protein sequencing is also used under certain circumstance, (5) but it does not become a commonly used method since peptides do not fragment sequentially, and it is generally impossible to get a complete set of b ions and y ions (fragment ions generated by cleavages at the peptide CO-NH bonds) in an MS/MS spectrum.

Proteomics has many unique advantages over traditional protein analytical methods and other "omics" technologies. For example, it can sequence a single protein in a dramatically shorter time than Edman sequencing and identify hundreds of proteins from a complex samples; (6) it can quantify several thousand protein groups among a group of samples with different treatments, which cannot be achieved by genomics or transcriptomics due to the inconsistence between mRNA and protein expression; (7) it can simultaneously identify and quantify thousands of site-specific protein post-translational modifications (PTMs) from complex samples, while the antibody-based PTM studies generally can only study one site-specific PTM at a time. (8) Protein PTMs cannot be studied using other "omics" technologies because they are not encoded by the genome or mRNA.

Two dimensional gel electrophoresis (2-DE) followed by protein identification using Matrix-Assisted Laser Desorption/Ionization Time-of-Flight (MALDI-TOF) was the first widely used proteomics method, and it was believed to be able to resolve the complete proteome in the early days of proteomics. (9, 10) However, after a few years of practice,

many researchers realized that mainly high-abundance proteins were repeatedly identified from the 2-DE method with hydrophobic proteins and low-abundance proteins always missing. (11) To overcome these limitations, shotgun proteomics was developed, in which protein identification and quantification were based on peptides derived from proteolytic digestion of intact proteins. (12, 13) In shotgun proteomics, online or offline multidimensional liquid chromatography (MDLC) can be used to reduce sample complexity and increase dynamic range and sensitivity of peptide identification. (14) For offline MDLC, reverse phase liquid chromatography is mostly used as the last dimension before mass spectrometry (MS) analysis due to its outstanding resolving power and high compatibility with MS. (15)

Nowadays, it is achievable to identify 4000 to 5000 protein groups from a single reverse phase liquid chromatography coupled to tandem mass spectrometry (LC-MS/MS) using mass spectrometers with high sensitivity and high scanning speed, (16, 17) and over 10,000 protein groups can be identified via MDLC-MS/MS. (18) Relative quantification of several thousand proteins between controls and samples can be achieved using label-free quantification, SILAC, ICAT, iTRAQ, TMT, and so on. (19-23) However, it rarely leads to the successful identification of biomarkers suitable for clinical use. (24, 25) A good biomarker can be used as an endpoint to predict clinical benefit or harm for clinical decision-making. The possible reasons include, 1) the relatively insufficient sensitivity of shotgun proteomics in comparison to the extremely low concentration of most clinically used biomarkers; 2) the mask of low-abundance proteins by high-abundance proteins due to the wide dynamic range of complex samples; 3) the low reproducibility of shotgun proteomics; 4) the lack of validation methods for potential biomarkers without ELISA (enzyme-linked immunosorbent assay) kits.

To overcome or alleviate the above-mentioned challenges in biomarker discovery and validation, targeted proteomics with improved sensitivity and reproducibility, such as selected reaction monitoring (SRM) and parallel reaction monitoring (PRM), have been widely used in the area of proteomics in recent years. (26-28) In addition to the change of protein expression, protein PTMs are also found to be related to the progression and

development of various diseases, such as cancer, diabetes, neurodegenerative disease and atherosclerosis, (29-34) which may potentially be more specific biomarkers than protein abundance. Shotgun proteomics can identify and quantify thousands of novel site-specific PTMs in one study, (35-37) and targeted proteomics with high sensitivity and specificity is the method of choice for further validation. In contrast, the traditional antibody based assays, such as Western Blot and ELISA, cannot be used in the discovery and validation of novel PTMs due to the lack of commercially available antibodies with high specificity.

1.2 Biological Significance of Protein Post-translational Modifications (PTMs)

Post-translational modifications (PTMs) are covalent processing events that change the properties of a protein by addition of a modifying group to one or more amino acids or by proteolytic cleavage of regulatory subunits or degradation of entire proteins after proteins have been completely translated and released from the ribosome. (8) By now, over 400 different types of PTMs have been reported. The most common PTM is the enzymatic or nonenzymatic addition of a functional group to proteins *in vivo*, such as phosphorylation and glycosylation; (38) some artificial PTMs can be added nonenzymatically *in vitro*; some PTMs add other proteins or peptides to proteins, such as SUMOylation and ubiquitination; (39, 40) some PTMs can change the chemical nature/composition of amino acids, such as citrullination, deamidation and carbamylation; (41, 42) some PTMs can change the structure of proteins, such as the formation of disulfide bridges between two cysteines and proteolytic cleavage. (43)

PTMs extend the functions and diversity of proteins and can influence almost all aspects of normal cell biology and pathogenesis. Kinases, phosphatases, transferases and ligases can add functional groups, such as proteins, lipids and sugars, to amino acid side chains or remove them, and proteases can cleave peptide bonds to remove specific sequences or regulatory subunits. PTMs play an important role in functional proteomics, because they regulate cellular activity, localization and interaction with other cellular molecules such as proteins, nucleic acids, lipids, and cofactors. For example, phosphorylation is a dynamic and reversible modification involved in the regulation of many biological processes including metabolism, cell division, signal transduction and enzymatic activity;

(44-46) glycosylation plays important roles in many biological processes including embryonic development, cell-to-cell interactions, cell division, and protein regulation and interaction. (47) Aberrant glycosylation has been found to be related to various diseases, such as cancer, inflammation and metabolic disorders. (48-50) Acetylation occurs in nearly all eukaryotic proteins through both irreversible and reversible mechanisms. Acetylation at the ε-NH2 of lysine (termed lysine acetylation) on histone N-termini regulates gene transcription, and it also occurs on cytoplasmic proteins. (51) Furthermore, crosstalk between acetylation and other post-translational modifications, including phosphorylation, ubiquitination and methylation, can modify the biological function of the acetylated protein. (52, 53) However, the functions of most other PTMs remain to be uncovered.

1.3 Current Status of PTM Studies in Proteomics

The analysis of PTMs is particularly important for the study of heart disease, cancer, neurodegenerative diseases and diabetes. (29, 54-56) However, the characterization of PTMs is very challenging due to their low stoichiometry and dynamic changes, but it may provide invaluable insight into the cellular functions underlying etiological processes. The main technical challenges in studying post-translationally modified proteins are the development of specific purification, enrichment and detection methods. In the past years, many novel proteomics technologies have been developed to study different PTMs.

Although over 400 different types of protein PTMs have been reported, only a few of them have been extensively studied due to the low throughput of traditional biological methods and technical limitations in proteomics methods. Since most PTMs occur on some specific amino acids on their target proteins, the modified proteins or peptides have to be enriched before MS analysis in order to avoid the interference from unmodified proteins or peptides. (27) Generally, immunoprecipitation can be used to enrich proteins with known PTMs using commercially available antibodies, but it cannot be used for enriching proteins with novel PTMs due to the lack of antibodies. (57) In addition, according to the physicochemical property of the PTM, affinity chromatography or other

chromatographic methods, such as strong cation exchange (SCX), strong anion exchange (SAX), weak anion exchange (WAX) and hydrophilic interaction liquid chromatography (HILIC), may be used to enrich or separate modified peptides. (58-63)

According to the statistics about protein PTMs in Swiss-Prot knowledgebase from PTM Statistics Curator, (64) phosphorylation, acetylation and N-glycosylation are the top 3 PTMs with experimental evidences, i.e. validation with traditional biological methods other than proteomics methods. Data from large-scale proteomics analysis are not regarded as experimental evidences without further validation. However, most other PTMs are insufficiently studied. For example, s-nitrosylation and deamidation are the 19th and 20th most extensively studied PTMs, respectively, but only 81 s-nitrosylation sites and 63 deamidation sites are reported with experimental evidences. Therefore, there is an urgent need to study PTMs other than phosphorylation and N-glycosylation since many of these less studied PTMs have been reported to have important biological functions. (65-68)

1.4 Protein Deamidation

Deamidation is a chemical reaction in which an amide functional group is removed from an organic compound. Protein deamidation occurs nonenzymatically both *in vivo* and *in vitro* with the conversion of asparagine and glutamine into aspartic acid and glutamic acid, respectively. Deamidation occurs relatively slowly in intact proteins with the half-time of 1-500 days for Asn and 100-5000 days for Gln. (69) However, the rate of deamidation can increase dramatically when amino acid residues are exposed under denatured condition during proteolytic digestion. (70) *In vivo*, protein deamidation has been reported to be related to Alzheimer's disease (AD) and cataracts. (65-67) *In vitro*, deamidation affects the purity and stability of therapeutic proteins during production and storage. (71, 72)

As shown in Figure 1.1, under physiological conditions or at elevated pH, the peptide bond nitrogen (reactive anion) of the N + 1 amino acid attacks the carbonyl carbon of the asparagine or aspartate side chain forming a succinimide ring intermediate that is quickly

hydrolyzed at either the alpha or beta carbonyl group to produce isoAsp and n-Asp at a ratio of about 3:1. (73) Isomerization of Asp residues occurs through the dehydration of Asp via a similar mechanism at neutral or acidic pH. Gln deamidation occurs at a similar mechanism with Asn deamidation except the formation of a six-ring glutarimide intermediate. Identification and quantification of deamidation sites and isomerization sites in proteins are necessary to assess their biological significance. Mass spectrometry (MS) is a powerful tool for large-scale study of deamidation due to its high sensitivity, speed and specificity of detection. The mass increase of 0.984 Dalton resulted from deamidation can be easily detected using high-resolution MS, and deamidation site can be identified and localized using MS/MS.

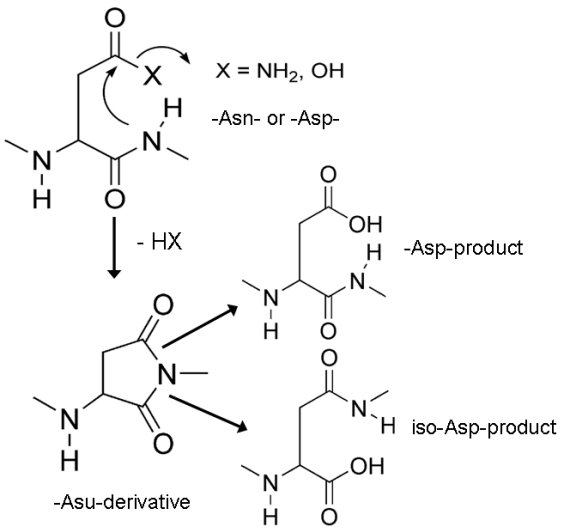

Figure 1.1: Deamidation of asparaginyl residues and isomerization of aspartyl residues through a succinimide intermediate

1.4.1 General Proteomics Workflow for Studying Protein Deamidation

For large-scale proteomic analysis of protein deamidation, shotgun proteomics is currently the method of choice due to its high throughput and sensitivity. Since protein deamidation does not introduce any functional groups, there are no specific methods to enrich deamdiated proteins or peptides. Therefore, a common shotgun proteomics workflow for whole proteome analysis can also be used for the analysis of protein deamidation. However, the separation of deamidated peptides from their undeamidated counterparts does improve the identification and quantification of them. The identification of deamidated peptides is adversely affected if they are co-eluted with their undeamidated counterparts since they are to be co-fragmented with the commonly used isolation width of 2 Th. The co-elution also makes the label-free quantification of deamidated peptides using extracted ion chromatography (XIC) very difficult since

deamidated peptides only has a slight mass difference of 19.34 mDa with the ^{13}C peaks of the corresponding unmodified peptides.

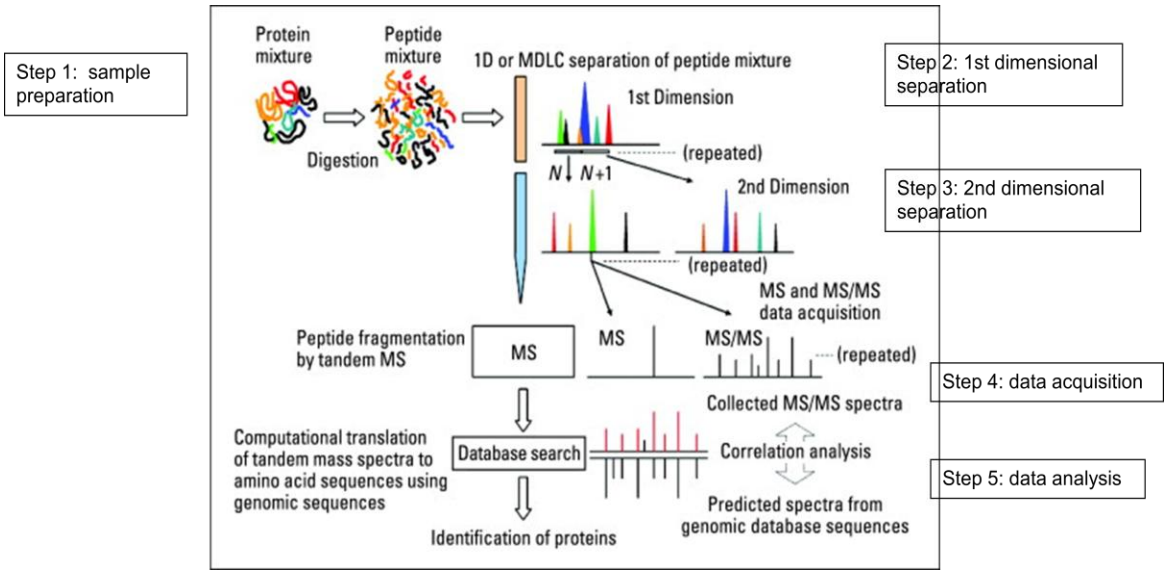

Figure 1.2: A flowchart of multidimensional LC-MS/MS for large-scale analysis of protein deamidation in proteomics (modified from Ref. (74))

Figure 1.2 shows a commonly used flowchart of multidimensional LC-MS/MS for proteomic analysis of whole proteome including protein deamidation using shotgun proteomics. In the step 1 of sample preparation, protein mixtures are digested using a protease into proteolytic peptides ranging from 1000 Da to 5000 Da, which can be detected with MS at much higher sensitivity and fragmented with MS/MS much more efficiently than intact proteins. Multidimensional liquid chromatography (MDLC) including two orthogonal dimensional separations (step 2 and step 3) is usually employed to reduce sample complexity and increase dynamic range and sensitivity of peptide identification by minimizing the undersampling and ion suppression problems. (14) In an offline MDLC, peptides that cannot be separated efficiently and thus collected in the same fraction in the first dimension are to be separated more evenly in the second dimension. The 2nd dimensional separation is directly coupled to mass spectrometry so that the eluted peptides are detected by MS and fragmented by MS/MS using a top N method in step 4 of data acquisition. The peak capacity and resolving power of MDLC are directly related to the sensitivity and dynamic range of peptide identification in LC-

MS/MS as it simplifies the complexity of peptide ions entering mass spectrometry to minimize undersampling. (74) In step 5 of data analysis, the collected MS/MS spectra were generally compared with the predicted MS/MS spectra from protein sequences deduced from genome sequences using database search software, such as Mascot, Sequest and Andomeda so that the sequence and deamidation site of deamidated peptides can be identified (75-78). The false discovery rate (FDR) of peptide identification can be evaluated using either the target-decoy method or Percolator. (79, 80) The accuracy of deamidation site localization can be evaluated automatically using MaxQuant. (77) The relative quantification of deamidated peptides between different samples can be achieved using label-free quantification based on extracted ion chromatography (XIC).

1.4.2 Challenges in Proteome-scale Study of Protein Deamidation

As a less studied PTM, there are still many challenges in studying protein deamidation using large-scale proteomic methods. Database search may return the identification of many false positive deamidated peptides due to the incapability to differentiate the slight mass difference of 19.34 mDa between deamidated peptides and the ^{13}C peaks of their undeamidated counterparts. Since deamidation occurs nonenzymatically both *in vivo* and *in vitro*, artificial deamidation occurring during proteomic sample preparation may prevent the accurate identification and quantification of endogenous deamidation. Now, it is still a challenging task to distinguish between the n-Asp and isoAsp deamidation products using large-scale proteomics methods since they are structural isomers with identical composition, mass and charge (Figure 1.1).

During the identification of deamidated peptides, database searches usually return many false-positive identifications due to the wrong assignment of the ^{13}C peaks of unmodified peptides as the corresponding deamidated peptides. (81, 82) The possible reason is that the ^{13}C or $^{13}C_2$ peaks of unmodified peptides are selected as the precursor masses by peak-picking software, and the MS/MS is not accurate enough to differentiate them from corresponding deamidated ones unambiguously. This is still a serious problem for data acquired with a high resolution mass spectrometer. (83) This issue compromises the LC-MS/MS method for accurate characterization of protein deamidation.

Deamidation takes place relatively slowly in intact proteins with a half life of 1-500 days for Asn and 100-500 days for Gln.(69) However, nonenzymatic deamidation occurs readily under the condition of trypsin digestion, i.e. prolonged incubation in mildly alkaline buffers at 37ºC, which results in the identification of many artificial Asn-deamidation sites and N-glycosylation sites when N-glycosylation site assignment is based on the detection of Asn deamidation in the consensus sequence N-X-S/T (with X not proline).(84-86) Shotgun proteomics is powerful in detecting deamidation sites in proteome scale due to its high sensitivity, accuracy and throughput, (27, 87) and trypsin has been the most widely used protease in proteomics research. Under mildly alkaline conditions, Asn deamidation happens mainly through the formation of a succinimide ring intermediate that is quickly hydrolyzed to *d,l*-Asp and *d,l*-isoAsp with isoAsp predominating.(73) Deamidation of Gln (Gln deamidation) is as much as ten times slower because it is thermodynamically less favorable to form a six-member glutarimide ring.(88) Therefore, to accurately identify and quantify Asn deamidation sites occurring *in vivo*, there is an urgent need to develop a novel sample preparation protocol to minimize the occurrence of artificial Asn deamidation during sample preparation.

Different tandem MS peptide sequencing methods, such as collisional activated dissociation (CAD), higher-energy collisional dissociation (HCD) and negative electrospray ionization have occasionally been observed to distinguish between the isomeric n-Asp and isoAsp products based on specific reporter ions, but the results are non-specific, highly variable and unreliable. The powerful soft peptide backbone-fragmenting techniques electron capture dissociation (ECD) and electron transfer dissociation (ETD) are reported to be capable of distinguishing between the isomeric Asp and isoAsp peptides based on a pair of c+57 and z-57 reporter ions, but the limitation is that the reporter ions of isoAsp are usually very weak and buried in the background noise, which results in many false positive identifications.(89) More challenging is that under typical RP-MS/MS conditions, the isomeric Asp and isoAsp peptides coelute from RP columns, making their quantification rather difficult.(90)

Because of the unavailability of commercial antibodies with high specificity, the quantification

of novel PTM sites is usually validated using multiple reaction monitoring (MRM). (91, 92) However, protein deamidation cannot be validated using MRM due to the slight mass difference of 19.34 mDa between deamidated peptides and the ^{13}C peaks of their undeamidated counterparts. Generally, deamidation does not occur at 100% on most deamidation sites. When triple quadrupole mass spectrometers collects precursor and product ions for each transition in validating deamidated peptides, the ^{13}C peaks of their undeamidated counterparts are also collected with the commonly used isolation width of 0.7 Th. However, it is impossible to differentiate them at the low resolution of triple quadrupole mass spectrometers. Therefore, the quantification of deamidated peptides cannot be validated using the low-resolution MRM. It is necessary to develop novel technologies to validate the quantification of deamidated peptides.

1.5 Objectives and the Overview of the Thesis

Protein deamidation has been reported to be related to many diseases, such as cataracts, celiac disease, heart diseases, neurodegenerative diseases and atherosclerosis. (54, 66, 93-95) It is essential to identify and quantify deamidation sites in proteins in order to better understand their biological roles. However, as mentioned above, there are currently many challenges in accurately identifying and quantifying deamidation sites in proteins, 1. Database search returns many false positive identifications of deamidated peptides; 2. Proteomic sample preparation results in much artificial deamidation; 3, It is challenging to differentiate and quantify the isomeric n-Asp and isoAsp deamidation products in proteome scale; 4. The quantification of deamidated peptides cannot be validated using either ELISA or MRM. In the present thesis, in order to overcome these obvious challenges, novel proteomic methods are to be developed and applied to the study of protein deamidation in human carotid atherosclerotic plaques for predicting secondary cerebrovascular events.

To achieve these objectives, my PhD research work is divided into five phases as described in Figure 1.3. In the phase I, a new database search strategy and a novel

proteomic sample preparation protocol were developed to minimize false positive identification of deamidated peptides and artificial deamidation from sample preparation so that endogenous protein deamidation can be identified and quantified accurately. In the phase II, the newly developed trypsin digestion buffer was compared with 3 commonly used trypsin digestion buffers in in-solution digestion of rat kidney tissues on peptide identification and artificial deamidation; In the phase III, a novel RP-ERLIC-MS/MS strategy was developed to separate, identify and quantify the triad of deamidation-derived products, i.e. unmodified peptides and the isomers of n-Asp and isoAsp containing deamidated peptides; In the phase IV, the recently introduced parallel reaction monitoring (PRM) were applied to the validation of the quantification of deamidated peptides. In the phase V, with the challenges in large-scale analyzing deamidation overcome, the developed technologies were applied to the study of protein deamidation in human carotid atherosclerotic plaques for predicting secondary cerebrovascular events. Similarly, the developed technologies can also be applied to the proteomic study of protein deamidation in any other samples or diseases in the future.

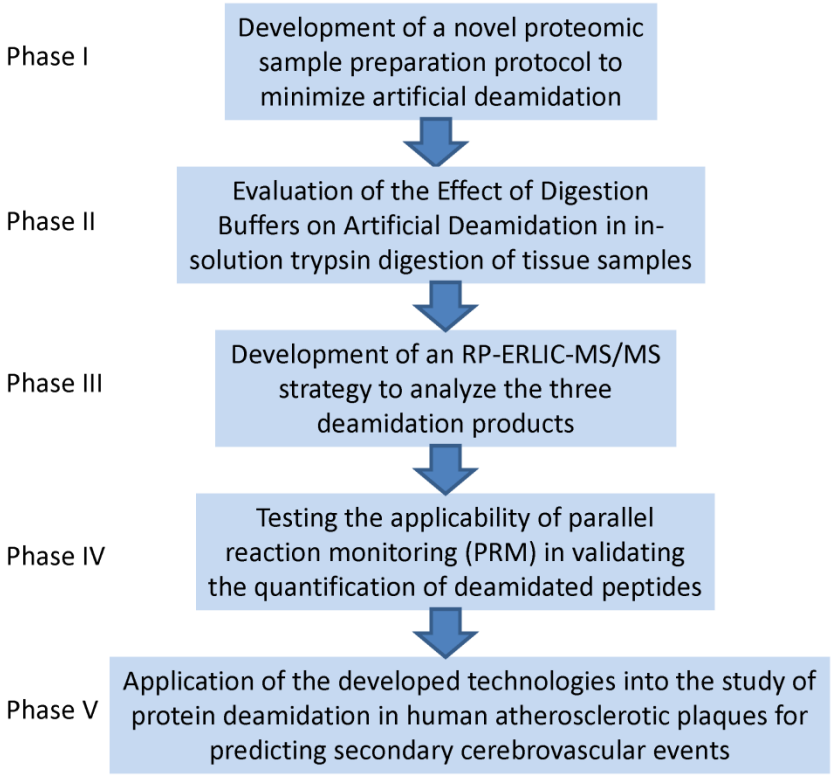

Figure1.3: Schematic work flow of my PhD works

Chapter 2

Detection, Evaluation and Minimization of Nonenzymatic Deamidation in Proteomic Sample Preparation

Chapter 2

2.1 Abstract

Identification of N-linked glycosylation sites generally depends on the detection of Asn deamidation in the consensus sequence N-X-S/T. Characterization of protein deamidation is also important to evaluate its *in vivo* biological roles. Nonenzymatic deamidation occurs readily on peptides under the commonly used proteomic sample preparation conditions, but its impact has not been evaluated systematically. In addition, database search returns many false positive deamidated peptides due to the misassignment of the ^{13}C peaks of unmodified peptides as deamidated peptides. In this chapter, the 19.34 mDa mass difference between them is proposed to be used to minimize the resulting false positive identifications in large-scale proteomic analysis. We evaluated 5 groups of proteomic data and found that nonenzymatic asparagine deamidation occurred on 4-9% of the peptides, resulting in the identification of many false positive N-glycosylation sites. With a comprehensive study of the potential factors in proteomic sample preparations, the mild alkaline pH and prolonged incubation at 37ºC were proven to be the major causes of nonenzymatic deamidation. Thus, an improved protocol of trypsin digestion at pH 6 and deglycosylation at pH 5 was proposed, and significant decrease of nonenzymatic asparagine deamidation was achieved without affecting peptide identification. In addition, we found that the sensitivity of deamidation detection can be improved significantly by increasing the sample loading amount in LC-MS/MS. This greatly increased the identification of glutamine deamidation sites, which tended to occur with sequence motifs different from those for asparagine deamidation: -Q-V-, -Q-L- and -Q-G- and, to a lesser extent, -Q-A- and -Q-E-.

2.2 Introduction

Accurate identification of protein deamidation sites is important to understanding its role in human diseases and aging and in the correct localization of N-glycosylation using the PNGase F deglycosylation method. However, determination of protein deamidation with LC-MS/MS is compromised by current methods of proteomics sample preparation and database searching. Nonenzymatic deamidation of Asn and Gln occurs spontaneously on

proteins and peptides both *in vivo* and *in vitro*. *In vivo*, deamidation is reported to be related to Alzheimer's disease (AD) and cataracts.(65-67) It has also been proposed as a molecular clock in studies of aging.(96, 97) *In vitro,* deamidation leads to the degradation of therapeutic proteins during production and storage.(71, 72) It takes place relatively slowly in intact proteins with a half life of 1-500 days for Asn and 100-5000 days for Gln.(69) However, the deamidation rate of peptides increases significantly under conditions typical of trypsin digestion, *i.e.*, incubation in digestion buffers at pH 8 for 8-16 h at 37ºC.(85) Under mildly alkaline conditions, Asn deamidation happens mainly through the formation of a succinimide ring intermediate that is quickly hydrolyzed to *d,l*-Asp and *d,l*-isoAsp with isoAsp predominating.(73) Deamidation of Gln (Gln deamidation) is as much as ten times slower because it is thermodynamically less favorable to form a six-member glutarimide ring.(88)

Most of the published papers about deamidation have focused on its mechanism and how to detect it in specific proteins.(98-100) Recently, several papers have been published about distinguishing deamidation *in vivo* from that happening during sample preparation.(101, 102) Interest is also increasing in distinguishing *l*-isoAsp from *l*-Asp in synthesized peptides or biological samples.(89, 90) The deamidation of peptides with -Asn-Gly- sequences has been evaluated during proteomic sample preparation(70) but the general impact of nonenzymatic deamidation has not been evaluated comprehensively, although it is known to be facilitated by the conditions of trypsin digestion, the workhorse digestion method of proteomics.

Since nonenzymatic deamidation could potentially occur on every Asn and Gln residue at various rates,(98, 103) all peptides containing either residue could exhibit deamidated counterparts after trypsin digestion, which would reduce the intensities of native peptides and complicate peptide identification. It is especially harmful when the peptides containing either residue are of low abundance. In addition, for large-scale proteomic analysis, the convention for identification of N-linked glycosylation sites generally depends on the detection of Asn deamidation in the consensus sequence N-X-S/T (with X not proline) in peptides after PNGase F treatment. Since nonenzymatic deamidation can

also occur on the Asn in the consensus sequence if it is not occupied by a glycan prior to PNGase F treatment (which is also customarily performed at pH 8), this results in the identification of some artificial N-glycosylation sites. $H_2{}^{18}O$ has been used in differentiating native deamidation sites from those occurring during sample preparation,(101, 102) but this approach cannot distinguish the nonenzymatic deamidation that occurs in the consensus sequence during the PNGase F treatment from the real glycosylation sites. Our preliminary inspection of a large data set (Table 2.2) revealed that the incidence of such false positive identifications was not negligible. There is a pressing need, then, to reduce this artifact in proteomic sample preparation.

The pH of digestion buffers, the temperature and the digestion time are three major factors that control the deamidation rate during proteolytic digestion.(85) To minimize digestion-induced deamidation, two improved digestion protocols have been proposed. Endoproteinase Lys-C digestion at pH 6.0 and 4ºC for 24-120 h was used to reduce nonenzymatic deamidation for several model proteins.(104) The protocol is effective but is difficult to apply to routine proteomic sample preparation due to the prolonged digestion time and the impact of the 4ºC temperature on the digestion efficiency for complex samples. Another protocol minimized nonenzymatic deamidation by reducing the trypsin digestion time to 0.5h with detergents for denaturing proteins omitted.(85) However, this also has not been widely used in proteomic sample preparation, due perhaps to the same consideration of digestion efficiency for complex samples. Since the temperature and incubation time are essential for efficient digestion, we proposed to solve the problem by digesting samples at lower pH in this study.

During the identification of deamidated peptides, database searches usually return many false-positive identifications due to the wrong assignment of the ^{13}C peaks of unmodified peptides as the corresponding deamidated peptides.(81, 82) A possible reason is that the ^{13}C or $^{13}C_2$ peaks of unmodified peptides are selected for matching by peak-picking software, and the MS/MS is not accurate enough to differentiate them from corresponding deamidated ones unambiguously. This is still a serious problem for data acquired with a high resolution mass spectrometer. This issue further compromises the

LC-MS/MS method for accurate characterization of Asn deamidation. Here, the resulting false-positive identifications were eliminated based on the accurate mass difference between the ^{13}C peaks of unmodified peptides and the corresponding deamidated ones. We have also evaluated a number of factors that might affect the deamidation rate and proposed an improved protocol for sample preparation.

2.3 Materials and Methods

2.3.1 Reagents

Unless indicated, all reagents used in this study were purchased from Sigma-Aldrich, USA. Protease inhibitor (Cat no.: 05 892 791 001) was purchased from Roche, Basel, Switzerland; Modified sequencing grade trypsin (V5111) was purchased from Promega, Madison, WI; Unmodified trypsin (T8802) was purchased from Sigma-Aldrich, St. Louis, MO. Sep-Pak C18 cartridges were purchased from Waters, Milford, MA; PNGase F was purchased from New England Biolabs, Ipswich, MA; Bicinchoninic acid (BCA) assay kit was purchased from Pierce, Rockford, IL.

2.3.2 Sample Preparation

Male Sprague Dawley rats were handled in accordance with the guidelines of NTU Institutional Animal Care and Use Committee (NTU-IACUC), NTU, Singapore. Rat livers were snap-frozen in liquid nitrogen immediately after collection and kept at -80ºC until use. The tissue was cut into small pieces and ground into fine powder in liquid nitrogen with a pestle. The powder was then suspended in 4% SDS. The suspension was sonicated for 10 s thrice on ice and centrifuged at 20000 X g at room temperature (RT) for 30 min. The protein concentration of the supernatant was then determined by the bicinchoninic acid (BCA) assay. Rat kidneys were treated in the same way as rat livers.

2.3.3 Traditional In-Gel Trypsin Digestion and PNGase F Treatment

Rat liver samples were run on an SDS-PAGE gel. Protein bands were cut out and transferred to Eppendorf tubes. They were washed with Milli-Q water, mixed with 50% ACN/50% 25mM NH_4HCO_3 via vigorous vortexing for 30 min and dehydrated with 100% ACN until the gel particles became white. They were then reduced with 10 mM DTT at 56ºC for 1 h and alkylated with 55 mM IAA at room temperature for 45 min in the dark followed by successive washes with 25 mM NH_4HCO_3 and 50% ACN/50% 25mM NH_4HCO_3. Finally, they were dehydrated with 100% ACN and dried in vacuum. Trypsin (V5111, Promega, Madison, WI) was added in the approximate weight ratio of 1:30. V5111 is modified (side-chain protected) sequencing grade porcine trypsin. All of the trypsin used in this chapter is from Promega unless otherwise specified. After the trypsin solution was completely absorbed by gel particles, 25 mM NH_4HCO_3 was added to completely cover the particles. They were then incubated at 37ºC overnight.

Peptides were extracted from gel particles with 50% ACN containing 0.1% TFA under sonication for 20 minutes twice. The combined extracts were dried in vacuum and redissolved in 25 mM NH_4HCO_3. To the solution, PNGase F (P0705L, New England Biolabs Inc.) was added as per the manufacturer's instructions and incubated at 37ºC for 6h for complete deglycosylation.

2.3.4 Improved In-Gel Trypsin digestion and PNGase F Treatment

The improved In-Gel trypsin digestion and PNGase F treatment were conducted using the same procedures as the traditional one except that 50 mM CH_3COONH_4, pH 6 and 50 mM CH_3COONH_4, pH 5 were used instead of 25 mM NH_4HCO_3, respectively.

2.3.5 LC-MS/MS

LC-MS/MS was done as previously described.(105) Briefly, peptides were separated and analyzed on a Shimadzu UFLC system coupled to a LTQ-FT Ultra (Thermo Electron,

Bremen, Germany). Mobile phase A (0.1% formic acid [FA] in H_2O) and mobile phase B (0.1% FA in ACN) were used to establish the 60 min gradient comprised of 45 min of 8-35% B, 8 min of 35-50% B and 2 min of 80% B followed by re-equilibration at 5% B for 5 min. Peptides were then analyzed on LTQ-FT with an ADVANCE™ CaptiveSpray™ Source (Michrom BioResources) at an electrospray potential of 1.5 kV. A gas flow of 2, ion transfer tube temperature of 180°C and collision gas pressure of 0.85 mTorr were used. The LTQ-FT was set to perform data acquisition in the positive ion mode as previously described (25). Briefly, a full MS scan (350-1600 m/z range) was acquired in the FT-ICR cell at a resolution of 100,000 and a maximum ion accumulation time of 1000 msec. The AGC target for FT was set at 1e+06 and precursor ion charge state screening was activated. The linear ion trap was used to collect peptides and to measure peptide fragments generated by collision-activated dissociation (CAD). The default AGC setting was used (full MS target at 3.0e+04, MS^n1e+04) in linear ion trap. The 10 most intense ions above a 500 counts threshold were selected for fragmentation in CAD (MS^2), which was performed concurrently with a maximum ion accumulation time of 200 msec. Dynamic exclusion was activated for the process, with a repeat count of 1 and exclusion duration of 20 s. Single charged ions were excluded from MS/MS. Isolation width was 2 Da, and default charge state was 5. For CAD, normalized collision energy was set to 35%, activation Q was set to 0.25, and activation time 30 ms. Spectra were acquired in centroid format in raw data files with XCalibur (version 2.0 SR2).

2.3.6 Data Analysis

The raw data were first converted into the dta format using the extract_msn (version 4.0) in Bioworks Browser (version 3.3, Thermo Fisher Scientific, Inc.), and then the dta files were converted into Mascot Generic File (MGF) format using an in-house program. Intensity values and fragment ion m/z ratios were not manipulated. The IPI rat protein database (version 3.40, 40381 sequences, 20547209 residues) and its reversed complement were combined and used for database searches. The database search was performed using an in-house Mascot server (version 2.2.04, Matrix Science, Boston, MA, USA) with MS tolerance of 5.1 ppm, #^{13}C of 2 and MS/MS tolerance of 0.5 Da. Two

missed cleavage sites of trypsin were allowed. Carbamidomethylation (C) was set as a fixed modification, and oxidation (M), phosphorylation (S, T and Y) and deamidation (N and Q) were set as variable modifications. The obtained peptide/protein list for each fraction was exported to Microsoft Excel or processed using an in-house script for further analysis. The dta files of peptides for which the Mascot score was over 20 in each fraction were combined and converted into Mascot generic file format using an in-house program. It was then searched again using Mascot to generate the protein and peptide list.

For high confidence peptide identification, only peptides with an E-value of less than 0.05 were used for statistical calculation. The FDR of peptide identification was estimated to be less than 1% (FDR = 2.0 × decoy_hits/total_hits). The FDR rate is based on the assigned spectra. Peptides identified with a consensus N-X-S/T (with X not proline) and a modification of deamidation at the asparagine were regarded as N-linked glycopeptides, and those identified with a modification of deamidation at glutamine or at asparagine but not in the consensus sequence were regarded as nonenzymatically deamidated peptides.

2.3.7 Evaluation of the Ratio of Deamidation in 5 Groups of Proteomic Data

Electrostatic Repulsion-Hydrophilic Interaction Chromatography (ERLIC) has recently been shown to be both effective and convenient for fractionation of complex tryptic digests in a sequence with RP.(105) The ratio of deamidation was evaluated in 5 groups of proteomic data obtained from rat kidney tissue, i.e. ERLIC1-RP, ERLIC2-RP, ERLIC3-RP, ERLIC4-RP and In-Gel-RP. For ERLIC-RP, tryptic peptides were obtained as described. (105) Each of 2 mg peptides were fractionated using a PolyWAX LP anion-exchange column (4.6 × 200 mm, 5 μm, 300 Å, PolyLC, Columbia, MD) using the ERLIC gradients in Table 2.1, and one third of the collected fractions was used for LC-MS/MS. For In-Gel-RP, 300 μg proteins were run on a SDS-PAGE gel, which was then cut into 21 slices. In-Gel trypsin digestion was done as described above using the traditional protocol.

Table 2.1 Detailed Information about the Four ERLIC Fractionation Methods Used

	ERLIC1	ERLIC2	ERLIC3	ERLIC4
Mobile phase A	90% ACN/0.1% acetic acid		80% ACN/0.1% FA	
Mobile phase B	30% ACN/0.1% FA		10% ACN/2% FA	
Gradient	Forty-six fractions were collected with a 140 min gradient of 100% Mobile phase A for 10 min, 0-8% Mobile phase B for 20 min, 8-27% B for 30 min, 27-45% B for 10 min, 45-81% B for 20 min, and 81-100% B for 20 min followed by 30 min at 100% B at a flow rate of 0.5 mL/min.			
PNGase F treatment of each fraction	No	No	No	Yes

2.3.8 Evaluation of Factors Potentially Affecting Deamidation during Sample Preparation

Six hundred μg of proteins from rat liver tissue were run on an SDS-PAGE gel, and then about one third of the gel slice was cut from the middle part and digested with trypsin in 25 mM NH_4HCO_3 at 37ºC for 8 h. Peptides were extracted and divided into 18 aliquots. To evaluate the effect of trypsin digestion time on deamidation, 2 aliquots were incubated at 37ºC an additional 4 h, and another 2 aliquots were incubated at 37ºC an additional 8 h. Since both In-Gel and in-solution digested samples have to be dried in vacuum after peptide extraction or desalting, several commonly used vacuum drying conditions were evaluated. Two milliliters of 70% ACN/0.1% TFA or 50% ACN/2% FA were added to the peptide aliquot, which was then put in a SpeedVac (Thermo Electron, Waltham, MA) at RT for 12 h or at 60ºC for 6 h. In order to keep peptides in the solution for the long duration, the buffers were topped up before drying. Since PNGase F was used for deglycosylation during the determination of N-glycosylation sites, we also investigated its effect on the deamidation ratio. Two aliquots of peptides were incubated in 25 mM NH_4HCO_3 at 37ºC for 6 h with PNGase F added for deglycosylation, and another two similarly treated as the control without addition of PNGase F. LC-MS/MS was performed in duplicate on each aliquot.

2.3.9 Comparison of the Digestion Efficiency of Trypsin at pH6 and pH8 using bovine serum albumin (BSA) as the Substrate

BSA was dissolved in 8M urea and 1% SDS at a concentration of 8 mg/mL. The protein was reduced with 10mM DTT at 56ºC for 1 h and alkylated with 55mM IAA for 45 min at room temperature in the dark. The concentration of urea was diluted to 1M with 25 mM NH_4HCO_3, pH 8, or 50 mM CH_3COONH_4, pH 6, before trypsin was added in a weight ratio of 1:30. Similarly, the concentration of SDS was diluted to 0.1% before trypsin was added. It was then incubated at 37ºC for 2h, 4h, 8h and 24h, respectively. Each portion of 5 µg protein digest was run on an SDS-PAGE gel in order to compare the difference in trypsin digestion efficiency at different time points. For comparison, unmodified trypsin (T8802) from Sigma-Aldrich (St. Louis, MO) was also tested in the same way.

2.3.10 Comparison of the Deamidation Rate at pH6 and pH8 using Synthetic Peptides

The peptide DGNGYISAAELR was synthesized at the Peptide Synthesis Core Facility, Nangyang Technological University. It was incubated in 25 mM NH_4HCO_3, pH 8, or 50 mM CH_3COONH_4, pH 6, for 2h, 4h, 8h and 24h at 37ºC. The mass spectra of the untreated and treated peptide were acquired with an ABI 4800 MALDI-TOF/TOF (Applied Biosystems). Both the untreated and treated peptides were analyzed using a PolySULFOETHYL A column (4.6 × 200 mm, 5 µm, 200 Å, PolyLC, Columbia, MD) on a Shimadzu Prominence UFLC system. Buffer A was 0.1% FA in 80% ACN and buffer B was 30 mM CH_3COONH_4 in 30% ACN. Twenty fractions were collected during a 30 min gradient: 5-50% buffer B for 5 min, 50-100% buffer B for 20 min, and 100% B for 5 min at a flow rate of 1 mL/min. The absorbance was monitored at 280 nm. The identifications of the peptide and two deamidated products were verified with MALDI-TOF/TOF. The reporter ion of $y_n - 46$ is used to distinguish between the two deamidated products. (106)

2.3.11Comparison of the Traditional and Improved Sample Preparation Protocol

One hundred µg of proteins from rat liver tissue were run on each lane of an SDS-PAGE gel, and about one tenth of the gel was cut from the middle part and transferred to Eppendorf tubes. To evaluate the effect of pH 6 on trypsin digestion efficiency and the deamidation ratios, gel particles were digested in 50mM CH_3COONH_4, pH 6, and 25mM NH_4HCO_3, pH 8, for both 8h and 16h time courses. To evaluate whether the deglycosylation at pH 5 reduces the deamidation ratio significantly compared with that at pH 8, tryptic peptides were treated with PNGase F for 6h in 50mM CH_3COONH_4, pH 5, or 25mM NH_4HCO_3, pH 8. Each test was performed in duplicate, and LC-MS/MS was performed in duplicate on each test sample.

2.3.12 Enhanced Detection of Nonenzymatic Deamidation from Complex Samples

Two mg of proteins from rat kidney tissue were run on an SDS-PAGE gel which was then cut into 20 slices. In-Gel trypsin digestion and PNGase F treatment were done as described above using the traditional protocol. LC-MS/MS was done as described above; the loading amount was about 100 µg per injection. This approach is hereafter referred to as In-Gel-RP-En.

2.4 Results and Discussion

2.4.1 The Reliable Identification of Deamidated Peptides in Database Searches

LC-MS/MS is the method of choice for determination of protein deamidation. However, database searches can return some false-positive identification of deamidated peptides since the ^{13}C peaks of unmodified peptides can be wrongly assigned as the monoisotopic peaks of the corresponding deamidated peptides. This problem is still severe even when deamidated peptides are identified from complex proteomic samples using mass spectrometers with high resolution. Thus, we need to find a way to differentiate the real deamidated peptides from such false positive ones. In this study, LC-MS/MS was done

on an LTQ-FT Ultra with sufficiently good mass accuracy to solve the problem based on the mass difference between the ^{13}C peaks of unmodified peptides and the corresponding deamidated ones. As shown in Figure 2.1A, the mass difference between the first isotopic peak M and the ^{13}C peak M' of an unmodified peptide is 1.00335 Da; the mass difference between peak M and the first isotopic peak N of the corresponding deamidated peptide is 0.98401 Da; the mass difference between peak M' and N is 19.34 mDa. In order to differentiate peak N from peak M' in database searches, a mass error of 5.1 ppm was used here. Thus, deamidated peptides with mass of less than 3868 Da (19.34 mDa/5.1 ppm) could be identified unambiguously. The lower limit of mass error that can be used depends on the mass accuracy of the mass spectrometer in use. Please be noted that #^{13}C must be set to 2 in Mascot in order to correctly identify ^{13}C or $^{13}C_2$ peaks and reduce the mismatch of them as deamidated peptides. The 19.34 mDa mass difference has been used in differentiating the unmodified and deamidated forms of synthetic peptides or intact proteins using FTMS.(81, 107) In this study we have extended its application to automated database searches in large-scale proteomic analysis. Jung et al has also developed several programs to aid the accurate assignment of monoisotopic precursor masses to MS/MS data.(108)

Since nonenzymatic deamidation usually does not run to completion with peptides, the experimental mass difference between the unmodified peptides and the corresponding deamidated ones can also be used in determining the false positive identification of deamidated peptides. An example of wrong assignment of the ^{13}C peak of the unmodified peptide as deamidated peptides is shown in Figure 2.1B. It was determined based on the mass difference between the experimental mass of the assumed deamidated peptide and the unmodified one, i.e. 3118.4132-3117.4159 = 0.9973. This is nearer to 1.00335 than 0.98401, so the putative deamidated peptide is actually the ^{13}C peak of the unmodified peptide. The mass difference can also be used in determining false positive identifications of deamidated peptides over 3868 Da. An example of a correctly assigned deamidated peptide is shown in Figure 2.1C. The mass difference between the experimental masses of the assumed deamidated peptide and the unmodified one was 0.9831 Da, which is

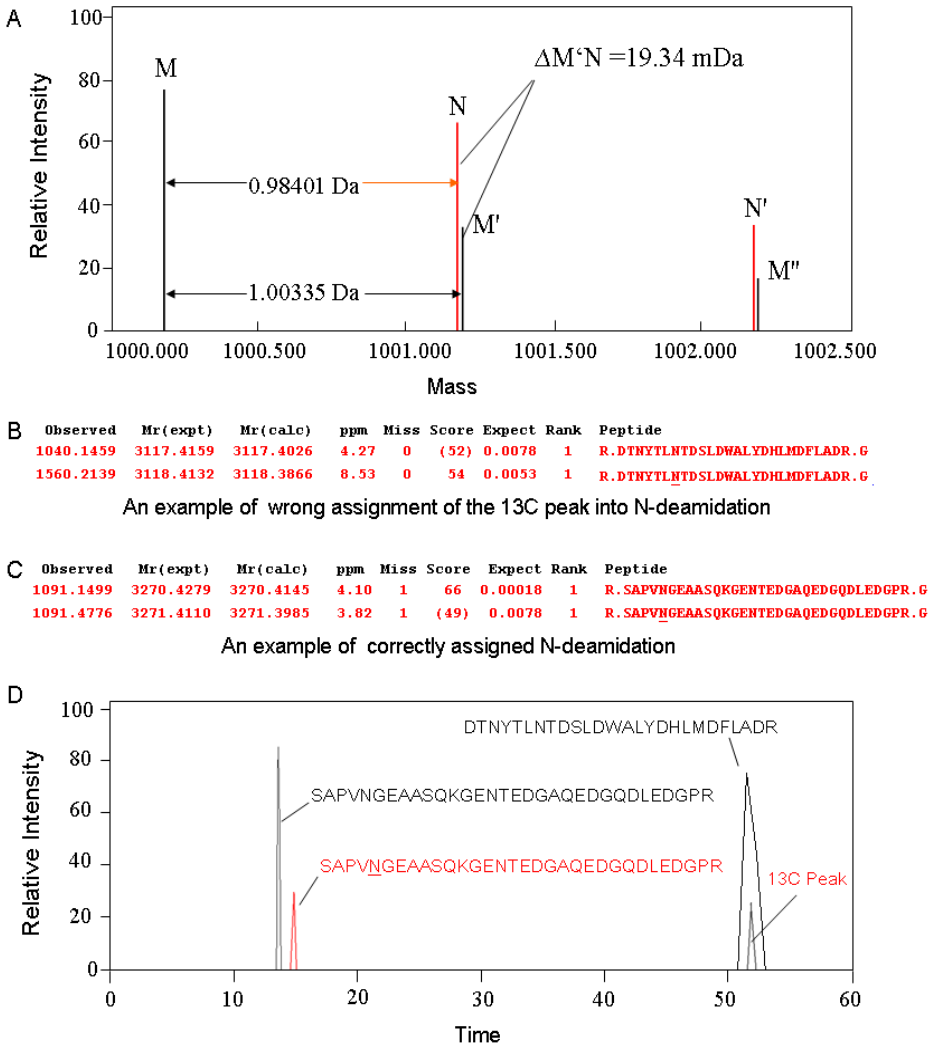

Figure 2.1: The reliable identification of deamidated peptides. (A) Schematic mass spectrum of an unmodified peptide and its corresponding deamidated peptide. Peak M is the first isotopic peak of the unmodified peptide; M' and M'' are its ^{13}C and $^{13}C_2$ peaks, respectively. Peak N is the first isotopic peak of the corresponding deamidated peptide. The mass difference between M' and N is 19.34 mDa. (B) An example of the wrong assignment of the ^{13}C peak as the Asn deamidation product in Mascot database searches; (C) An example of correctly assigned Asn deamidation in Mascot database searches; (D) The XICs of the peptides identified in Fig 2.1B and 2.1C, in the form of a chromatogram obtained via reversed-phase.

nearer to 0.98401 than 1.00335. In addition, the identification of deamidated peptides can also be confirmed based on the retention time. As shown in Figure 2.1D, an unmodified

peptide and its ^{13}C peak have the same retention time in RP chromatography, but a deamidated peptide has a different retention time than that of the corresponding unmodified peptide. This has been used in the reliable identification of deamidated peptides.(70, 109) However, the method we propose here is decidedly more convenient since it can be achieved easily by merely changing the parameters in database searches.

2.4.2 Evaluation of the Ratio of Deamidation in 5 Groups of Proteomic Data

To investigate the effect of nonenzymatic deamidation on proteomic sample preparation, the extent of deamidation was evaluated in 5 groups of proteomic data using the above-mentioned data analysis method. As shown in Table 2.2, Asn deamidation occurs to some extent with 4-9% of all peptides, evidence of a significant effect of proteomic sample preparation conditions. Gln deamidation occurs at a lower ratio: 1-4%. Since Gln deamidation happens via a mechanism similar to Asn deamidation (formation of a glutarimide ring intermediate) but at a slower rate, we focus mainly on Asn deamidation here. It is worthy of notice that all N-glycopeptides identified in ERLIC1-RP, ERLIC2-RP, ERLIC3-RP and In-Gel-RP are false positive ones since these samples were not treated with PNGase F to remove N-glycans. As the only difference between ERLIC3-RP and ERLIC4-RP was that each fraction from ERLIC was deglycosylated with PNGase F in ERLIC4-RP, the number of their false positive N-glycopeptides should be nearly identical. Thus, about 13.7% (107/781) of the N-glycopeptides in ERLIC4-RP are false positive identifications due to nonenzymatic deamidation, confirming the desirability of reducing the occurrence of this artifact in the identification of N-glycopeptides. To the best of our knowledge, this is the first report about the large-scale evaluation of nonenzymatically deamidated peptides in complex proteomic samples. The information listed in Table 2.2 can be obtained from them using an in-house PERL program.

It may be noted that the modifications to the mobile phase that distinguish ERLIC3 and ERLIC4 from ERLIC1 and ERLIC2 conditions were designed to improve the isolation and identification of peptides with PTM's at the expense of resolution of unmodified

peptides. Thus, in Table 2.2, appreciably more glycopeptides were identified using ERLIC4 and significantly less unmodified peptides.

Table 2.2 Estimation of Nonenzymatic Deamidated Peptides and N-Glycopeptides in 5 Groups of Proteomic Data

	ERLIC1-RP[3]	ERLIC2-RP[3]	ERLIC3-RP[4]	ERLIC4-RP[4]	In-Gel-RP
Unique peptides	17003	16518	10396	11939	5267
Unique glycopeptides[1]	96	108	107	781	35
Unique Asn-deamidated peptides	815	845	821	1020	288
Ratio of Asn deamidation[2]	4.79%	5.12%	7.90%	8.54%	5.45%
Unique Gln-deamidated peptides	320	366	307	418	89
Ratio of Gln deamidation[2]	1.88%	2.22%	2.95%	3.50%	1.69%

Note:

1. It should be noted that all N-glycopeptides identified in ERLIC1-RP, ERLIC2-RP, ERLIC3-RP and In-Gel-RP are false positive ones since these samples were not treated with PNGase F to remove N-glycans.
2. Ratio of deamidation is calculated as the number of unique deamidated peptides divided by that of all identified unique peptides in the run.
3. ERLIC1-RP and ERLIC2-RP were two replicates for whole proteome analysis.
4. ERLIC3-RP and ERLIC4-RP were used for the concurrent analysis of proteome, phosphoproteome and glycoproteome. The only difference between them was that ERLIC4-RP was deglycosylated with PNGase F, but ERLIC3-RP was not.

2.4.3 Evaluation of Factors Potentially Affecting Deamidation during Sample Preparation

Since nonenzymatic deamidation occurs at a high ratio in proteomics samples and results in the false positive identification of many N-glycopeptides, it is instructive to determine how it happens and how to prevent it. Deamidation proceeds readily under typical trypsin

digestion conditions, *i.e.*, incubation of proteins in digestion buffers of pH 8 at 37ºC for 8-16 h. We first evaluated the effect of trypsin digestion time on deamidation with gel-separated rat liver tissue proteins. As shown in Figure 2.2A, the deamidation ratio increases significantly during trypsin digestion for 16h compared with that for 8h, indicating that many deamidation sites were newly induced or became detectable during trypsin digestion (P=0.006). Thus, deamidation can be reduced by shortening trypsin digestion time or improving the digestion conditions. It should be noted that the number of detectable deamidated peptides is closely related to the sensitivity of the mass spectrometer used. Because this may change slightly with time, it is preferable to do the LC-MS/MS on samples consecutively for comparing the deamidation ratio.

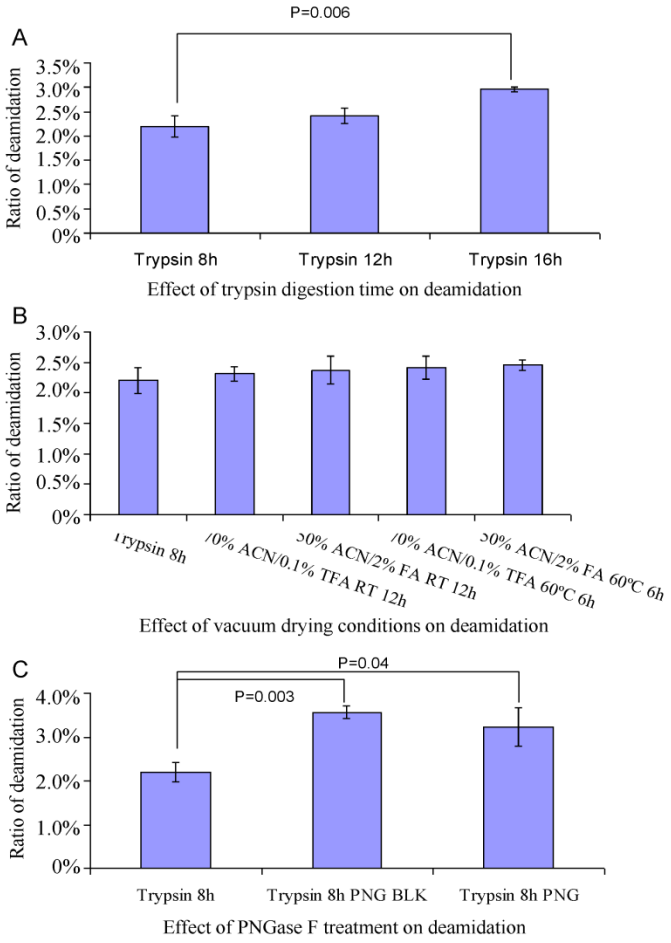

Figure 2.2 Effect of trypsin digestion time (A), vacuum drying condition (B) and PNGase F treatment (C) on Asn deamidation. BLK = Blank; the control corresponding to treatment using PNGase F conditions but without the PNGase F, as described in Materials and Methods. Proteins extracted from rat liver tissue were used in the test.

Tryptic peptides were also subjected to some other treatments before LC-MS/MS. Generally, 50% ACN, 2% FA was used in the extraction of peptides from gel particles, and 70% ACN, 0.1% TFA was used in the elution of desalted peptides. Both steps were followed by vacuum drying. Thus, we tested whether the vacuum drying with these

solutions significantly affected the deamidation ratio. As shown in Figure 2.2B, compared with untreated samples, the deamidation ratio did not significantly increase in the four tested vacuum drying conditions, *i.e.*, with 70% ACN/0.1% TFA at RT for 12h, 50% ACN/2% FA at RT for 12h, 70% ACN/0.1% TFA at 60ºC for 6h and 50% ACN/2% FA at 60ºC for 6h. This indicates that nonenzymatic deamidation proceeds slowly under acidic conditions even at 60ºC.

The effect of PNGase F treatment on the deamidation ratio is shown in Figure 2.2C. Compared with untreated samples, the deamidation ratio increased significantly in both PNGase F treated samples (P=0.04) and the control (P=0.003), the two being comparable. This indicates that the incubation of tryptic peptides with 25 mM NH_4HCO_3 is responsible for the increase of deamidation, not the PNGase F treatment itself, and suggests that the incubation conditions could be improved in order to reduce the occurrence of deamidation.

2.4.4 Improved Protocol for N-Glycosylation Site Determination from Complex Samples

Based on our results, the standard trypsin digestion and deglycosylation protocol induce a significant degree of nonenzymatic deamidation due to the mildly alkaline pH of the reaction buffers. As shown by the schematic in Figure 2.3, we propose to solve this problem via an improved protocol that involves conducting protein reduction, alkylation, and trypsin digestion in 50 mM CH_3COONH_4, pH 6 and performing the deglycosylation in 50 mM CH_3COONH_4, pH

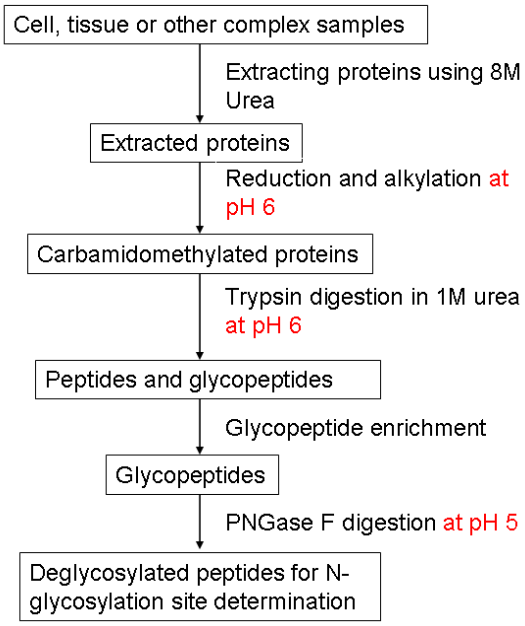

Figure 2.3 Proposed improved trypsin digestion and PNGase F treatment protocol for N-glycosylation site determination.

5. The deamidation rate is minimal at pH 5,(101) but trypsin digestion cannot be performed at so low a pH according to the instructions from the manufacturer. Accordingly, we evaluated trypsin digestion at pH 6. For the deglycosylation of N-glycopeptides, the suggested reaction buffer for PNGase F is 50 mM Na_2HPO_4, pH 7.5, or 25 mM NH_4HCO_3, but the enzyme activity was found not to be compromised at a pH as low as 5.(110) Accordingly, we proposed to do the deglycosylation at pH 5 in this study.

2.4.5 Comparison of the Digestion Efficiency of Trypsin at pH6 and pH8 using Bovine Serum Albumin (BSA) as the Substrate

The digestion efficiency of trypsin at pH 6 was evaluated with BSA before it was applied to complex samples. As shown in Figure 2.4A and 2.4C, when urea is used as the denaturant, five µg BSA disappeared completely after being digested with either unmodified or modified (side-chain protected) trypsin for 2-24h, indicating that even 2h digestion at pH 6 at 37ºC was enough for complete digestion. However, when SDS was used as the denaturant, the band of BSA remained unchanged even after 24h digestion at pH 6 at 37ºC if unmodified trypsin was used (Figure 2.4B), indicating that it was completely deactivated at pH 6. BSA was digested into large fragments at pH 8 if SDS and unmodified trypsin were used. In contrast, modified trypsin performed much better than unmodified when SDS was used as the denaturant. As shown in Figure 2.4D, although it only digested BSA into large fragments after 24h at pH 6 at 37ºC, digestion was complete at pH 8 in 2h. Thus, it was preferable to use urea as the denaturant when the trypsin digestion was done at pH 6, and the resulting activity of trypsin was good enough for proteomic analysis. The difference in the performance of V5111 and T8802 trypsin is possibly due to that V5111 trypsin is modified by reductive methylation, rendering it more resistant to SDS denaturation. Since most researchers are using modified trypsin to prevent autolysis, its high activity at pH 6 seems to be an additional benefit in reducing digestion-induced deamidation.

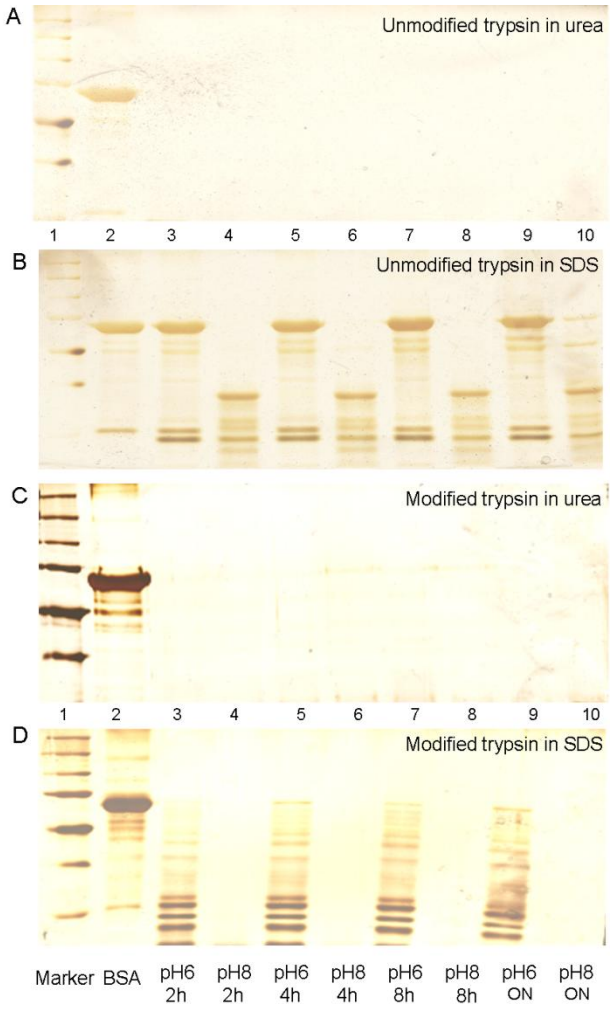

Figure 2.4 SDS-PAGE images of trypsin digested BSA at pH 6 and pH 8 for different time periods using urea or SDS as the denaturant. (A) SDS-PAGE image of unmodified trypsin-digested BSA at pH 6 and pH 8 in urea buffer; (B) SDS-PAGE image of unmodified trypsin digested BSA at pH 6 and pH 8 in SDS buffer; (C) SDS-PAGE image of modified trypsin digested BSA at pH 6 and pH 8 in urea buffer; (D) SDS-PAGE image of modified trypsin digested BSA at pH 6 and pH 8 in SDS buffer. Lane 1, MW mark; 2, BSA without adding trypsin; 3, digestion at pH6 for 2h; 4, digestion at pH8 for 2h; 5, digestion at pH6 for 4h; 6, digestion at pH8 for 4h; 7, digestion at pH6 for 8h; 8, digestion at pH8 for 8h; 9, digestion at pH6 for 24h; 10, digestion at pH8 for 24h.

2.4.6 Comparison of the Deamidation Rate at pH6 and pH8 using Synthetic Peptides

The deamidation rate at pH 6 and pH 8 at 37ºC was determined using the synthetic peptide DGNGYISAAELR. As shown in Figure 2.5, the SCX chromatograms showed the gradual transformation of the undeamidated peptide into two deamidation products containing -βDG- and –DG- at pH 8. The identification of the peptide and two deamidated products was verified with MALDI-TOF/TOF. The deamidation ratio was calculated as the area of the two deamidation products divided by the sum of the area of both deamidated and undeamidated peptides. It was estimated to be 5.7%, 11.4%, 25.8% and 64.8% after 2h, 4h, 8h and 24h incubation at pH 8 at 37ºC. However, the chromatograms remained unchanged when the synthetic peptide was incubated at pH 6 at 37ºC for 2h, 4h and 8h [*data not shown*]. Even after 24h incubation at pH 6 at 37ºC, the deamidation ratio was estimated to be only 0.52%. The same trend was also semiquantitatively reflected in the MALDI-TOF mass spectra of the solution at different time points shown in the insets of Figure 2.5. This confirms that deamidation happens much more slowly at pH 6 than that at pH 8. Krokhin et al reported that the half-life of the deamidation of peptides with –NG- was ~8h in 100 mM NH_4HCO_3 at 37ºC.(70) This is two times faster than the deamidation rate

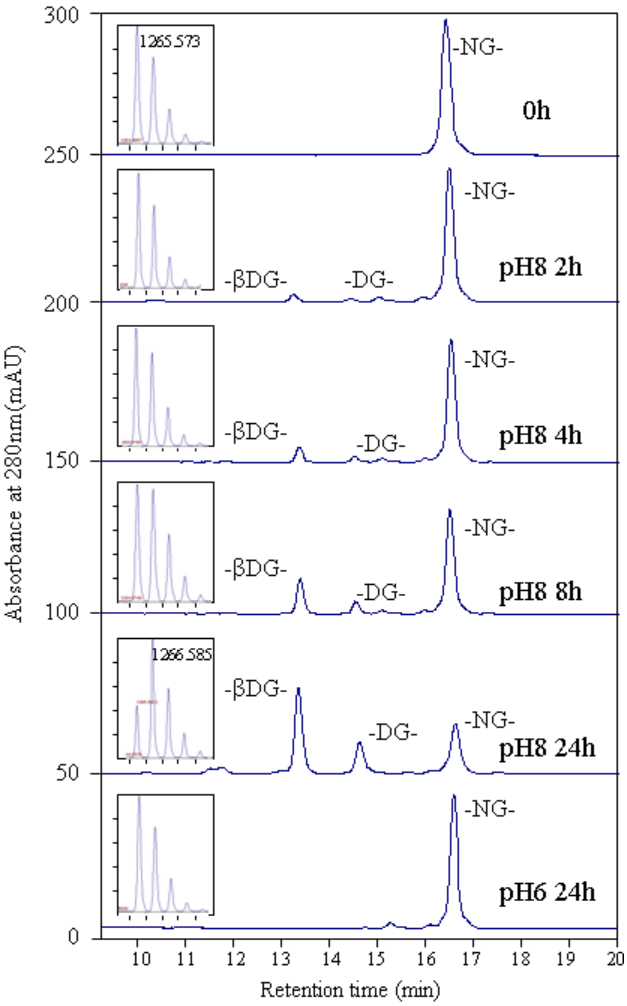

Figure 2.5 Monitoring the deamidation of the synthetic peptide DGNGYISAAELR at pH 6 and pH 8 by HPLC and MALDI-TOF. Solutions of the synthetic peptide in 50 mM CH_3COONH_4, pH 6, or 25 mM NH_4HCO_3 were incubated at 37ºC for 2h, 4h, 8h and 24h, respectively. They were resolved with a SCX column with UV detection at 280nm. Each unfractionated mixture was also analyzed semi-quantitatively with MALDI-TOF with the mass spectra shown in the insets.

in 25 mM NH_4HCO_3 at 37ºC detected in this study. The difference might be due to some difference in the incubation buffer and/or the peptide sequence.

2.4.7 Comparison of the Traditional and Improved Sample Preparation Protocol using Complex Samples

Gel-separated rat liver tissue proteins were used in testing the improved sample preparation protocol. The digestion efficiency of trypsin was compared at pH 6 and 8. While the kinetics of trypsin digestion were slower at pH 6, the number of peptides actually identified in the four test groups was comparable (Figure 2.6A). This suggests that a pH of 6 can be used without sacrificing the extent of proteomic identification. However, this comparison should be performed anew if different samples are used since their properties may affect the digestion efficiency. In addition, we tried using Glu-C from two companies (Sigma-Aldrich and Roche Diagnostics [Basel, Switzerland]) in digesting proteins at pH 4-6. A significant decrease in the deamidation ratio was observed, but the digestion efficiency in both cases was much lower than that of trypsin [*data not shown*].

The deamidation ratio was also compared among the four tested trypsin digestion conditions. Trypsin digestion at pH 6 for 8h and 16h produced comparable deamidation ratios, which were slightly less than that at pH 8 for 8h (Figure 2.6B). This indicates that some deamidations exist *in vivo* in the native proteins or occur easily in the first 8h of trypsin digestion, but incubation of tryptic peptides with the reaction buffer of pH 6 did not lead to a significant increase in deamidation after the initial 8h digestion time. Apparently, prolonged trypsin digestion at pH 6 can be used safely with complex samples in order to ensure thorough digestion. However, trypsin digestion at pH 8 for 16h produced a significantly higher deamidation ratio than in the other groups ($P=0.002$, Figure 2.6B), further confirming the liability to deamidation from prolonged incubation with reaction buffers of pH 8. Thus, decreasing trypsin digestion time is an alternative solution for reducing deamidation while maintaining digestion efficiency.

The effect of PNGase F treatment on deamidation was evaluated at various pH values as well. As shown in Figure 2.6C, when tryptic peptides obtained from 8h digestion at pH 6 were treated with PNGase F in 25 mM NH_4HCO_3, pH 8, at 37ºC for 6h, the deamidation ratio increased 40.1% (P=0.05). However, it showed slight decrease when they were treated with PNGase F in 50 mM CH_3COONH_4, pH 5, at 37ºC for 6h. Since nonenzymatic deamidation is believed to be irreversible, the decrease may be due to analytical variations in LC-MS/MS. The number of N-glycopeptides identified from these two different treatments was comparable. It appears that the PNGase F treatment at pH 5 is much better than that at pH 8 in reducing nonenzymatic deamidation while maintaining adequate enzyme activity. The deamidation ratio was 1.07% ± 0.20% when samples were prepared using the improved sample preparation protocol, i.e. trypsin digestion at pH 6 for 8h and PNGase F treatment at pH 5 for 6h, a 58.7% decrease compared with the results from the traditional sample preparation protocol, *i.e.*, trypsin digestion at pH 8 for 8h and PNGase F treatment at pH 8 for 6h (P=0.0002). Actually, many labs routinely perform trypsin digestion and PNGase F treatment overnight (8h-16h) in order to ensure complete digestion, in which case the deamidation ratio could be even higher.

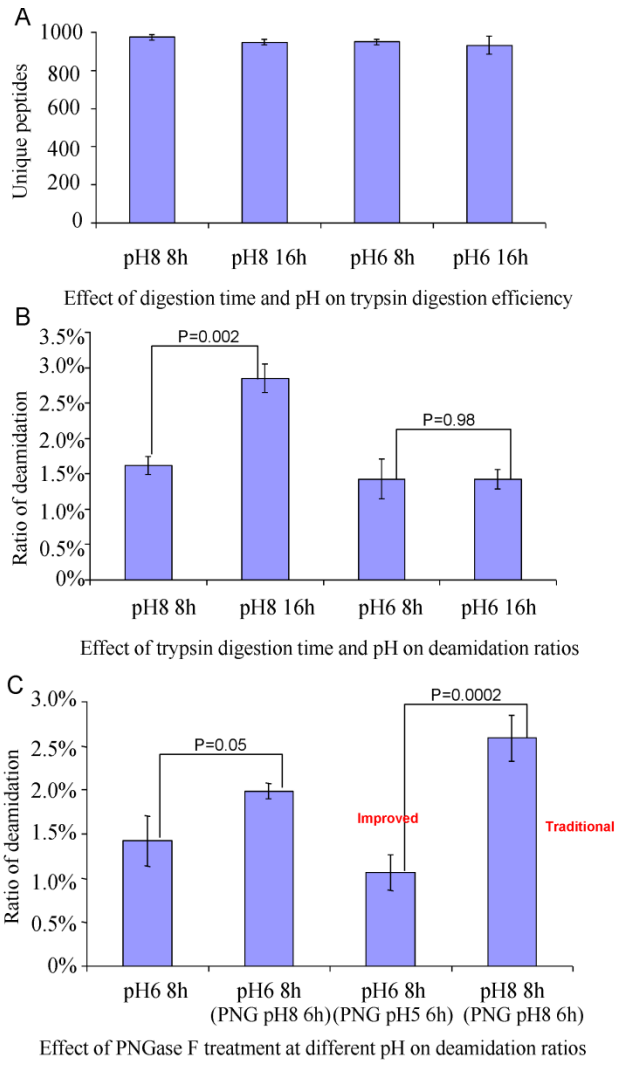

Figure 2.6 Comparison of the traditional and improved trypsin digestion and PNGase F treatment protocol. (A) Effect of digestion time and pH on trypsin digestion efficiency; (B) Effect of trypsin digestion time and pH on deamidation ratios; (C) Effect of PNGase F treatment at different pH on deamidation ratios. Proteins extracted from rat liver tissue were used in the test.

2.4.8 Comparison of the Motifs of Asn Deamidation and Gln Deamidation

Many papers have been published on various aspects of the deamidation of peptides and proteins, most of them about Asn deamidation. Asn deamidation is particularly prone to occurring with the sequences -N-G- and -N-S-. As best we know, no large-scale analysis of Gln-deamidated peptides in complex samples has been done yet, and the relevant motifs of susceptible sequences remain undiscovered. The rate of Gln deamidation is ten times slower than that of Asn deamidation, making it more difficult to analyze. In this study, we occasionally found that an increase in the amount of sample loaded in LC-MS/MS was helpful for the detection of deamidated peptides. When the loading amount per LC-MS/MS injection increases from about 7.5 µg (In-Gel-RP) to about 100 µg (In-Gel-RP-En), the figure for the ratio of Asn deamidation increases from 5.45% to 10.10%, and the figure for the ratio of Gln deamidation increases from 1.69% to 10.41%. Obviously there has been a dramatic increase in the ability to identify Gln-deamidated peptides of low abundance, presumably due to enhancement of mass signals, as well as a less dramatic increase in identification of Asn-deamidated peptides. However, the increase in the loading amount does not have a significant effect on the identification of unmodified peptides. With 794 Gln-deamidated peptides identified in In-Gel-RP-En, motifs for Gln deamidation susceptibility could be compiled and compared with those for Asn deamidation in ERLIC4-RP, in which 1020 Asn-deamidated peptides were identified. As shown in Figure 2.7, Asn deamidation tends to occur at -N-G-, -N-S-, and -N-D- sequences, consistent with previous studies. Gln deamidation tends to occur at -Q-V-, -Q-L- and -Q-G- sequences, and to a lesser extent at Q-A- and Q-E-. This contrasts with Asn deamidation motifs. Gln deamidation proceeds through a mechanism similar to that of Asn deamidation except that a six-member glutarimide ring is formed. Presumably the effect of steric hindrance on the formation of a glutarimide ring is not as strong as that on the formation of a five-member ring so that the kinetics of Gln deamidation are comparatively rapid with -Q-V- and -Q-L- sequences. Interesting, -Q-V-, -Q-L-, -Q-A- and -Q-I- have relatively high deamidation rate. We speculate that the electron-donating property of alkyl- groups (of V, L, A and I residues) promotes the nucleophilic attack that results in the intermediate glutarimide ring; the inductive effect makes it easier for the

attacking nitrogen to push its unshared pair of electrons onto the electropositive carbonyl that gets attacked to form the ring.

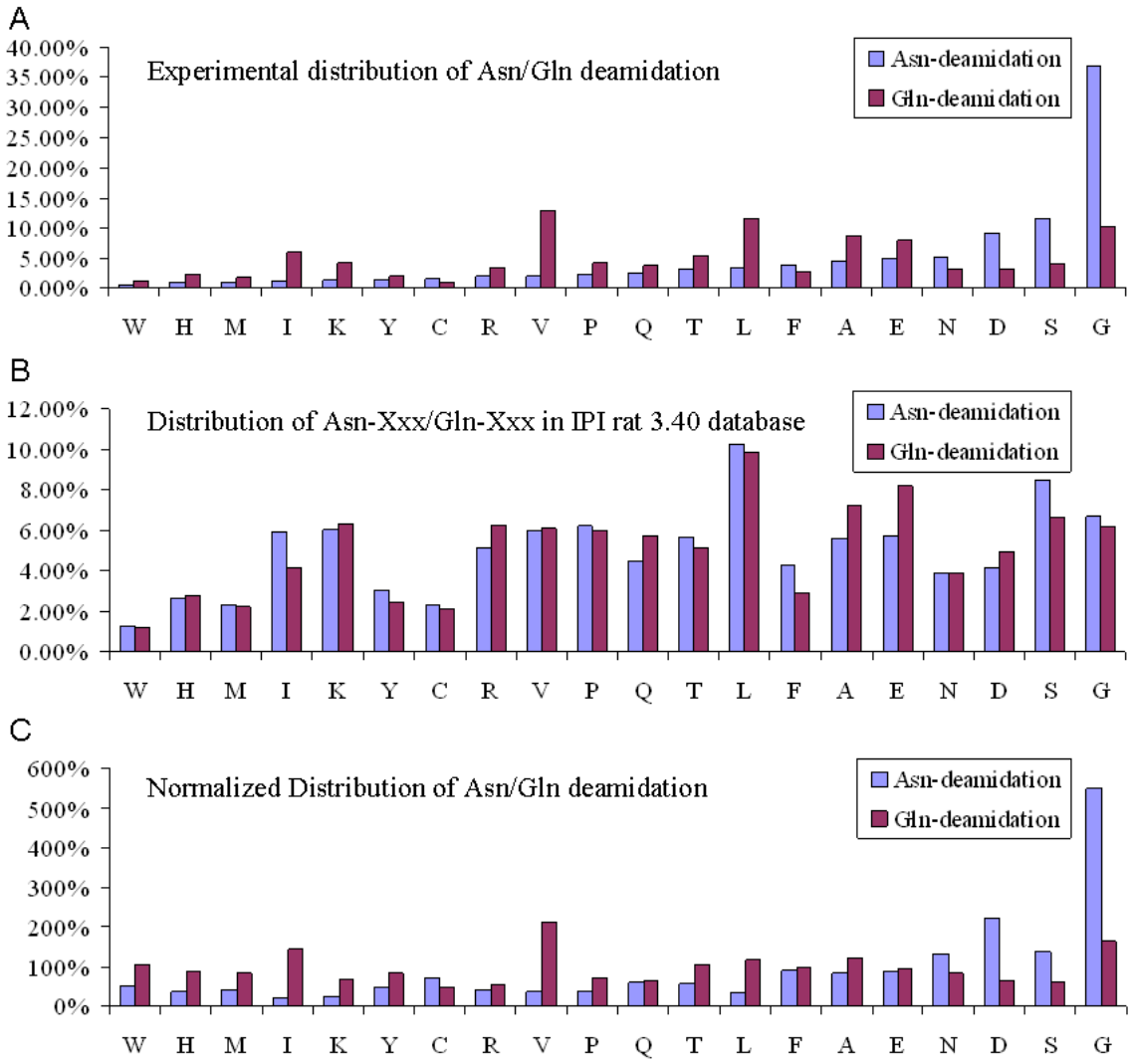

Figure 2.7 Comparison of the incidence of Asn deamidation and Gln deamidation in proteomic samples. (A) Experimental distribution of Asn deamidation and Gln deamidation; (B) Distribution of Asn-Xxx/Gln-Xxx in IPI rat 3.40 database; (C) Normalized Distribution of Asn/Gln deamidation (the experimental distribution of Asn deamidation and Gln deamidation divided by the distribution of Asn-Xxx/Gln-Xxx in IPI rat 3.40 database). The X-axis lists the residue on the C-terminal side of the deamidated N- or Q-residue.

2.5 Conclusion

Nonenzymatic asparagine deamidation was found to occur to some extent in 4-9% of all peptides during workup of samples for proteomic analysis and results in the false positive identification of numerous N-glycopeptides. An improved protocol of trypsin digestion at pH 6 and PNGase F treatment at pH 5 was proposed and validated in order to solve this problem. The minimization of nonenzymatic deamidation will not only improve the reliability of N-glycopeptide identification but also be helpful for the identification of low-abundance peptides from complex samples. It should be noted that nonenzymatic deamidation during sample preparation cannot be avoided completely even with the improved protocol (unless the minimal deamidation in question was present *in vivo*). In the future, $H_2{}^{18}O$ could also be used during PNGase F treatment in the improved protocol to reduce further the false positive identification of N-glycopeptides.

Chapter 3

Evaluation of the Effect of Digestion Buffers on Artificial Deamidation in In-solution Trypsin Digestion

Chapter 3

3.1 Abstract

Nonenzymatic deamidation occurs readily under the condition of trypsin digestion, resulting in the identification of many artificial deamidation sites. To evaluate the effect of trypsin digestion buffers on artificial deamidation, we compared the commonly used buffers of Tris-HCl (pH 8), ammonium bicarbonate (ABB) and triethylammonium bicarbonate (TEAB), and ammonium acetate (pH 6) which was reported to reduce Asn deamidation. iTRAQ quantification on rat kidney tissue digested in these four buffers indicates that artificial Asn deamidation is produced in the order of ammonium acetate<Tris-HCl<ABB<TEAB, and Gln deamidation has no significant differences in all tested buffers. Label-free experiments show the same trend, while protein and unique peptide identification are comparable during using these four buffers. To explain the differences of these four buffers in producing artificial Asn deamidation, we determined the half-time of Asn deamidation in these buffers using synthetic peptides containing –Asn-Gly- sequences. It is 51.4±6.0 days in 50 mM of ammonium acetate (pH 6) at 37ºC, which is about 23, 104 and 137 times of that in Tris-HCl, ABB and TEAB buffers, respectively. In conclusion, ammonium acetate (pH 6) is more suitable than other tested buffers for characterizing endogenous deamidation and N-glycosylation.

3.2 Introduction

Protein deamidation is reported to contribute to Alzheimer's disease and cataracts, (65-67) and it is also proposed as a molecular clock of biological events, such as in protein turnover, development and aging. (96, 97) Shotgun proteomics is powerful in detecting deamidation sites in proteome scale due to its high sensitivity, accuracy and throughput, (27, 87) and trypsin has been the most widely used protease in proteomics research. However, nonenzymatic deamidation occurs readily under the condition of trypsin digestion, i.e. prolonged incubation in mildly alkaline buffers at 37ºC, which results in the identification of many artificial Asn-deamidation sites and N-glycosylation sites when glycosylation site assignment is based on the detection of Asn deamidation in the consensus sequence N-X-S/T (with X not proline).(84-86) Digestion buffers, temperature

and digestion time are three major factors controlling the extent of deamidation during proteolytic digestion.(84, 85) Since overnight trypsin digestion at 37ºC is generally used in most proteomics experiments for complex samples, such as cell, tissue and plasma, it is necessary to comprehensively evaluate the effect of trypsin digestion buffers on artificial deamidation.

In proteomics studies, 25-100 mM ammonium bicarbonate (ABB) has been the most widely used trypsin digestion buffer for both in-gel digestion and in-solution digestion due to its volatility,(111) but it is reported to result in ~70-80% conversion of -Asn-Gly- into -Asp-Gly- or -βAsp-Gly during the overnight digestion. (70) Tris-HCl (pH 8) is another widely used digestion buffer and the recommended buffer from trypsin manufacturers,(112) and it is reported to be a very mild catalyst of deamidation.(69) However, it remains unclear whether Tris-HCl is good enough for reducing artificial deamidation in proteomic studies without a comprehensive evaluation. Triethylammonium bicarbonate (TEAB) is commonly used in trypsin digestion buffers when amine-reactive isobaric tagging reagents, such as isobaric tags for relative and absolute quantitation (iTRAQ) and tandem mass tag (TMT), are used to label proteins or tryptic peptides for protein quantification because it has no primary amines which would interfere with the labeling. (113, 114) Presently, there are no reports about the effect of TEAB on artificial deamidation, but it has already been used in the identification and quantification of N-glycopeptides. (115) The identified N-glycopeptides may include many false positive ones if it is a strong catalyst of deamidation. In addition to these commonly used buffers, we developed an improved trypsin digestion buffer, i.e. ammonium acetate (pH 6), which was shown to significantly reduce artificial Asn deamidation without affecting peptide identification using in-gel digested samples.(84) Due to the difference between in-gel and in-solution digested samples, it is necessary to conduct a comprehensive evaluation on in-solution digestion before widely applying it to proteomics studies. In this study, we comprehensively evaluated 50 mM of ammonium acetate (pH 6), Tris-HCl (pH 8), ABB and TEAB as the buffers for in-solution trypsin digestion of rat kidney tissue using both iTRAQ quantification and label-free experiments, and determined the half-time of Asn deamidation in these buffers using synthetic peptides.

Our results indicate that ammonium acetate (pH 6) significantly outperforms the commonly used trypsin digestion buffers by minimizing artificial deamidation for proteomic study of endogenous deamidation and N-glycosylation.

3.3 Materials and Methods

3.3.1 Reagents

Unless indicated, all reagents used in this study were purchased from Sigma-Aldrich, USA. Protease inhibitor (Cat no.: 05 892 791 001) was purchased from Roche, Basel, Switzerland; Unmodified trypsin (T8802) was purchased from Sigma-Aldrich, St. Louis, MO. Sep-Pak C18 cartridges were purchased from Waters, Milford, MA; 2D-Quant Kit was purchased from Thermo Fisher, MA.

3.3.2 Sample Preparation

Male Sprague−Dawley rats were handled in accordance with the guidelines of NTU Institutional Animal Care and Use Committee (NTU-IACUC), NTU, Singapore. Rat kidneys were snap-frozen immediately in liquid nitrogen after collection, and kept at -80^{o}C until use. The tissue was cut into small pieces and ground into fine powders in liquid nitrogen with a pestle. The powders were then suspended in lysis buffer (8 M urea, 50 mM Tris-HCl, pH 8) with protease inhibitor (05 892 791 001, Roche) added (10 ml/tablet). The suspension was sonicated for 10 seconds thrice on ice and centrifuged at 20,000g at 4^{o}C for 20 min. The protein concentration of the supernatant was then determined by the bicinchoninic acid (BCA) assay. About 5 mg tissue lysate was diluted to 4 mg/ml using the lysis buffer, reduced with 10 mM DTT at 37^{o}C for 2 h and alkylated with 40 mM iodoacetamide at room temperature for 45 min in the dark. After the concentration of urea was diluted to 1M with 50mM Tris-HCl (pH 8), trypsin (T8802, Sigma) was added at a weight ratio of 1:50. It was then incubated at 37^{o}C for 15 h. The obtained tryptic peptides were desalted using a Sep-Pak® C18 cartridge (Waters, Milford, MA, USA) and dried in a SpeedVac® (Thermo Electron, Waltham, MA, USA). The trypsin digestion using other digestion buffers was done using the same procedure as

that of Tris-HCl trypsin digestion except for the lysis buffer and digestion buffer. Three technical replicates were done for each step. It should be noted that protein concentration in ammonium acetate (NH4Ace) buffer was quantified using 2D-Quant Kit (Thermo Fisher, MA) since protein precipitation at pH 6 during dilution of urea concentration interfered with BCA quantification.

3.3.3 iTRAQ Labeling

Peptides digested in different buffers were labeled with 4-plex iTRAQ reagents (Applied Biosystems, Foster City, CA) according to the instructions from the manufacturer as follows: ammonium acetate, 114; Tris-HCl, 115; ABB, 116; TEAB, 117. The labeled peptides were pooled and desalted using Sep-Pak C18 cartridges. They were then fractionated using Electrostatic Repulsion-Hydrophilic Interaction Chromatography (ERLIC) as follows.

3.3.4 ERLIC Fractionation of iTRAQ Labeled Peptides

iTRAQ labeled Peptides were fractionated using a PolyWAX LP weak anion-exchange column (4.6 × 200 mm, 5 μm, 300 Å, PolyLC, Columbia, MD) on a Shimadzu Prominence UFLC system. Mobile Phase A (10 mM CH_3COONH_4 in 85% ACN/1% FA) and mobile phase B (30% ACN/0.1% FA) were used to establish a 26 min gradient of 0%–28% buffer B for 19 min, 28%–100% buffer B for 0.1 min and 100% buffer B for 6.9 min at a flow rate of 1 mL/min with 16 fractions collected. The collected fractions were then dried with vacuum centrifuge, pooled into 6 fractions by combining (1-3); (4-5); (6-7); (8-9); (10-11); (12-16), and redissolved in 3% ACN/0.1% FA for LC-MS/MS analysis.

3.3.5 ERLIC Fractionation of Label-free Peptides

Label-free peptides from 1 mg of proteins were fractionated using a PolyWAX LP weak anion-exchange column on a Shimadzu Prominence UFLC system in triplicate. Mobile Phase A (85% ACN/0.1% FA) and mobile phase B (10% ACN/0.4% FA) were used to establish a 30 min gradient of 0%–10% buffer B for 10 min, 8%–35% buffer B for 12 min, 35%–100% buffer B for 2 min and 100% buffer B for 6 min at a flow rate of 1 mL/min with 18 fractions collected. The collected fractions were then dried with vacuum centrifuge, pooled into 5 fractions by combining (1-4); (5-6); (7-8); (9-11); (12-18), and redissolved in 3% ACN/0.1% FA for LC-MS/MS analysis.

3.3.6 LC-MS/MS

Peptides were separated and analyzed on a Dionex Ultimate 3000 RSLCnano system coupled to a Q Exactive (Thermo Fisher, MA). About 1 µg of the peptides from each pooled fraction were injected into an Acclaim peptide trap column (Thermo Fisher, MA) via the auto-sampler of the Dionex RSLCnano system. Peptides were separated in a capillary column (75 µm x 10 cm) packed with C18 AQ (5 µm, 300Å; Bruker-Michrom, Auburn, CA, USA) at room temperature. The flow rate was at 300 nl/min. Mobile phase A (0.1% formic acid in 5% ACN) and mobile phase B (0.1% formic acid in 90% ACN) were used to establish a 60 min gradient. Peptides were then analyzed on Q Exactive with a nanospray source (Thermo Fisher, MA) at an electrospray potential of 1.5 kV. A full MS scan (350-1600 m/z range) was acquired at a resolution of 70,000 at m/z 200 and a maximum ion accumulation time of 100 msec. Dynamic exclusion was set as 30 s. Resolution for HCD spectra was set to 17,500 at m/z 200. The AGC setting of full MS scan and MS^2 was set as 1E6 and 1E5, respectively. The 10 most intense ions above a 1000 counts threshold were selected for fragmentation in HCD with a maximum ion accumulation time of 100 msec. Isolation width of 2 was used for MS^2. Single and unassigned charged ions were excluded from MS/MS. For HCD, normalized collision energy was set to 28%. The underfill ratio was defined as 0.1%.

3.3.7 Data Analysis

The raw data were first converted into .apl files with MaxQuant 1.4.1.2 using the function of "Partial processing" with step 1 to 5, and then the .apl files were converted into Mascot Generic File (MGF) format using an in-house made Perl script. The UniProt rat protein database (release 2013_10, 28855 sequences) concatenated with cRAP contaminants (version 2012.01.01) and their reverse complement were combined and used for database searches. The database search was performed using an in-house Mascot server (version 2.4.0, Matrix Science, Boston, MA, USA) with MS tolerance of 10 ppm, #^{13}C of 2 and MS/MS tolerance of 0.02 Da. Two missed cleavage sites of trypsin were allowed. Carbamidomethylation (C) was set as a fixed modification, and oxidation (M) and deamidation (NQ) were set as variable modifications. For iTRAQ labeled peptides, 4-plex iTRAQ was set as fixed modifications on N-terminal and lysine, and it was set as a variable modification on tyrosine. Only peptides with a Mascot score over 30 and a minimum length of 7 are used for statistical analysis. It results in an FDR of less than 1%.(79) For high confidence protein identification, only protein groups identified with at least 2 unique peptides over 30 are reported, and only peptides of which the search engine rank is 1 and peptides in top scored proteins are counted. A Student's t-Test was used to verify the significance of the differences between each comparison.

3.3.8 Determination of the Half-time of Asn Deamidation in the Four Buffers Using Synthetic Peptides

The peptide DGNGYISAAELR was synthesized at the Peptide Synthesis Core Facility, Nanyang Technological University. It was incubated in 50 mM Tris-HCl, 50 mM ABB and 50 mM TEAB at 37^{o}C for 2h, 4h, 8h and 24h, respectively. Since Asn deamidation occurs slowly in 50 mM ammonium acetate (pH 6),(84) the incubation time is 1d, 3d, 7d and 10 d. After incubation, peptides were analyzed using a PolyWAX LP weak anion-exchange column on a Shimadzu Prominence UFLC system. Mobile phase A (80% ACN/0.1% FA) and mobile phase B (10% ACN/2% FA) were used to establish a 30 min gradient of 0–20% B for 10 min, 20–100% B for 15 min and 100% B for 5 min at a flow rate of 1 ml/min. The absorbance was monitored at 280 nm. The half-time of Asn

deamidation was determined based on the percentage of remaining unmodified peptides over time.

3.4 Results and Discussion

The suitable buffer for studying endogenous deamidation and N-glycosylation should introduce as little as possible artificial deamidation during proteomic sample preparation without significantly affecting protein and peptide identification. Here, we comprehensively evaluated the three commonly used trypsin digestion buffers of Tris-HCl, ABB and TEAB and an improved buffer of ammonium acetate (pH 6) in these aspects. To explain the difference of these four buffers in introducing artificial Asn deamidation, we also determined the half-time of Asn deamidation in these buffers using synthetic peptides.

3.4.1 iTRAQ Based Relative Quantification of Asn-deamidated Peptides and Gln-deamidated Peptides Digested in the Four Buffers

To evaluate the potential of these four buffers in producing artificial deamidation during the course of proteomic sample preparation, we used 4-plex iTRAQ reagents to label tryptic peptides from rat kidneys digested in these four buffers and compared the summed areas of the reporter ions from each labeling with experimental bias normalized. Only Asn-deamidated peptides and Gln-deamidated peptides with reporter ions detected in all four digestion conditions are used for statistical analysis. As shown in Figure 3.1, based on the results from two LC-MS/MS technical replicates, the summed areas of the reporter ions of Asn-deamidated peptides are in the order of ammonium acetate<Tris-HCl<ABB<TEAB, indicating the difference in the rate of Asn deamidation in these four buffers. In contrast, the rate of Gln deamidation is consistent in the four tested buffers. It should be noted that the difference of Asn deamidation between different buffers from iTRAQ experiments may be underestimated due to the following two reasons: 1) TEAB in the dissolution buffer of iTRAQ labeling Kits increases Asn deamidation in all labeled

samples during the course of iTRAQ labeling and vacuum drying of the pooled samples, which reduces the difference of Asn deamidation between different digestion conditions; 2) the ratio compression problem in iTRAQ quantification. (116, 117)

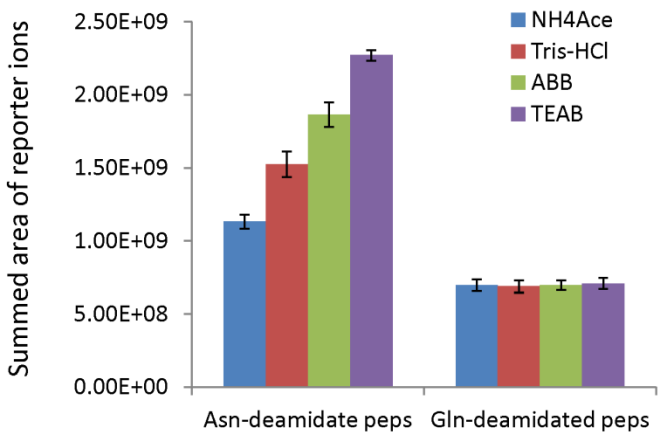

Figure 3.1 The summed area of the reporter ions of Asn-deamidated peptides and Gln-deamidated peptides under different digestion conditions from iTRAQ experiments. Artificial Asn deamidation is produced in the order of ammonium acetate<Tris-HCl<ABB<TEAB; Gln deamidation has no significant differences in all tested buffers.

3.4.2 Identification of Asn-deamidated Peptides, Gln-deamidated Peptides and Artificial N-glycopeptides in Label-free Experiments

Due to the limitation of iTRAQ quantification in comparing the four buffers in producing artificial deamidation, label-free experiments were used as an alternative. To clearly show the effect of different digestion buffers on artificial deamidation, we used an ERLIC gradient that could selectively enrich deamidated peptides. Therefore, the observed ratio of deamidation in this study may be higher than that from other proteomics studies without enriching deamidated peptides. Based on the label-free LC-MS/MS results from three technical replicates, the number of identified unique Gln-deamidated peptides was comparable while using 50 mM of the four digestion buffers, but the number of identified unique Asn-deamidation peptides in Tris-HCl, ABB and TEAB is 2.2, 3.0 and 3.8 times of that from ammonium acetate (pH 6) ($P<0.002$) , respectively (Figure 3.2). As a result, the number of identified unique glycopeptides in Tris-HCl, ABB

and TEAB is 2.3, 3.4 and 4.4 times of that from ammonium acetate (pH 6), respectively ($P<0.01$). As the samples were not treated with PNGase F, all of the identified N-glycopeptides were artificial ones either from endogenous or artificial Asn deamidation. Our results indicate that ammonium acetate (pH 6) is more efficient than the three commonly used trypsin digestion buffers in reducing artificial Asn deamidation, and thus is a suitable buffer for studying endogenous deamidation and N-glycosylation. It is worth noticing that the number of unique Asn-deamidated peptides is less than that of unique Gln-deamidated peptides while using ammonium acetate buffer (pH 6), which is contrary to the results from other large-scale proteomic studies using ABB buffer.(84) It indicates that the identified Asn-deamidated peptides while using ammonium acetate buffer are mainly native ones and the rate of Asn deamidation is controlled *in vivo* since it occurs at a rate of 50 times faster than that of Gln deamidation *in vitro*.(103) Parker et al. used samples without PNGase F treatment to detect and remove false positive N-glycopeptides,(115) but it might not be an efficient way due to the low reproducibility of LC-MS/MS in analyzing complex samples. The ammonium acetate buffer (pH 6) provides a convenient and reliable alternative.

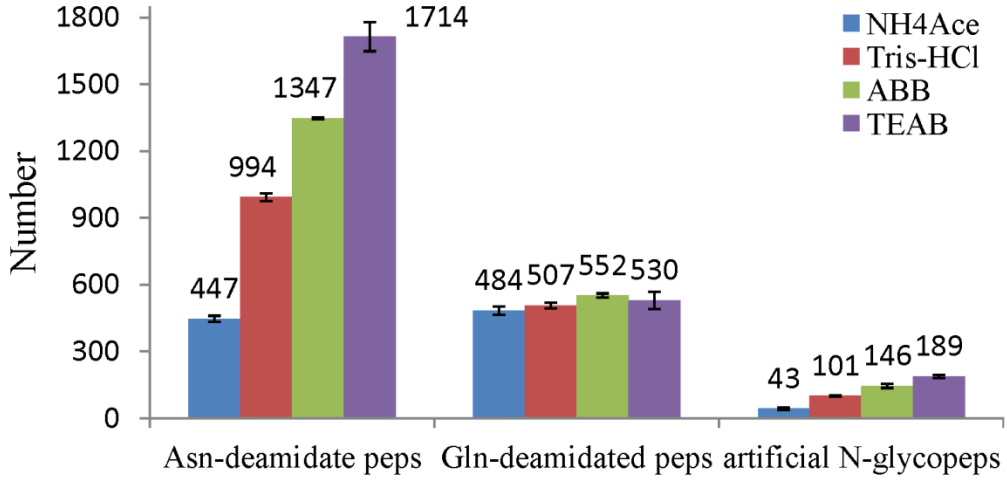

Figure 3.2 Number of unique Asn-deamidated peptides, Gln-deamidated peptides and artificial N-glycopeptides identified from rat kidney tissue digested in 50 mM of ammonium acetate (pH 6), Tris-HCl (pH 8), ABB and TEAB from three technical replicates of label-free experiments. Significantly less Asn-deamidated peptides and artificial N-glycopeptides were identified while using ammonium acetate (pH 6) than other buffers; Gln deamidation was consistent among the four buffers. The low standard deviation indicates good reproducibility between technical replicates.

3.4.3 The Distribution of Asn deamidation and Gln deamidation while Using the Four Trypsin Digestion Buffers

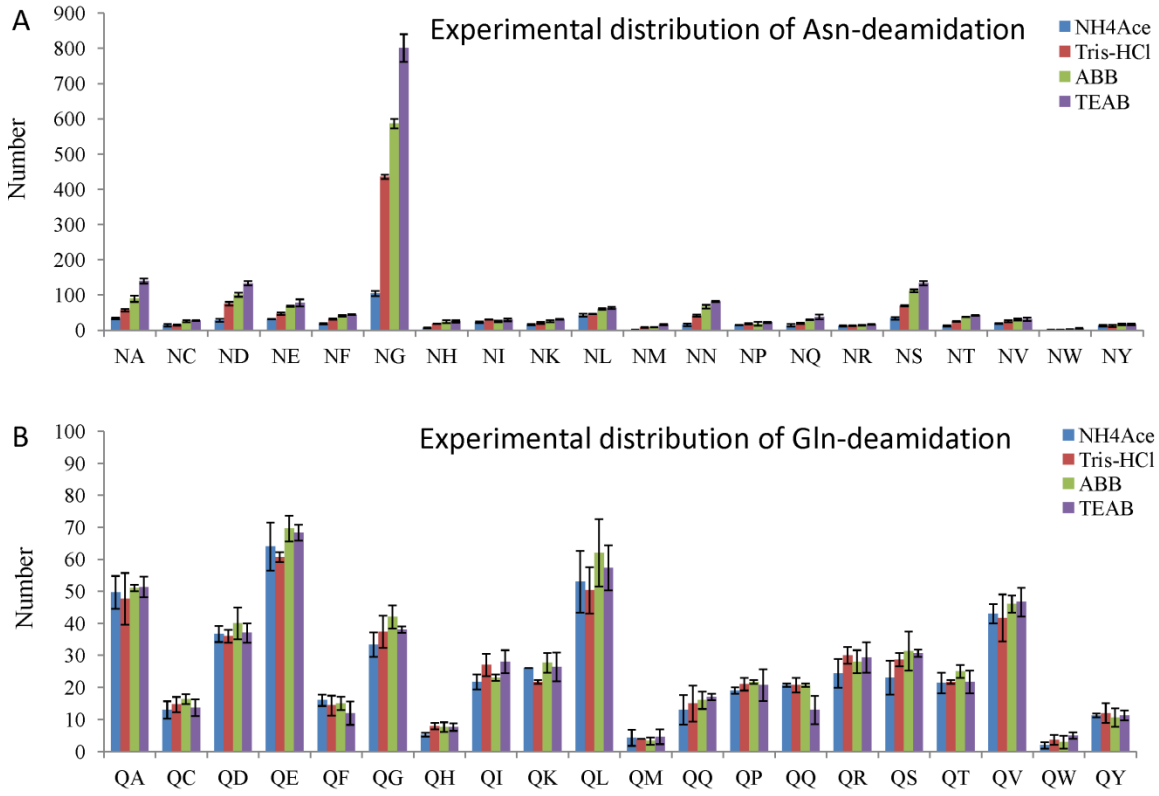

Figure 3.3 Comparison of the distribution of Asn deamidation and Gln deamidation in rat kidney tissue digested in the four buffers. Experimental distribution of Asn deamidation (A) and Gln deamidation (B). The x axis lists the residue on the C-terminal side of the deamidated N- or Q-residue.

To study the effect of different trypsin digestion buffers on nonenzymatic deamidation in details, we reported the number of Asn deamidation and Gln deamidation based on the residues on the C-terminal side of the deamidated Asn/Gln. As shown in Figure 3.3A, the number of Asn deamidation detected at the –N-G- sequence in Tris-HCl (pH 8), ABB and TEAB were 4.2, 5.6 and 7.7 times of that in ammonium acetate (pH 6), respectively, and similar but less remarkable trend occurred on –N-S-, -N-D- and –N-A- sequences. However, trypsin digestion buffers have a negligible effect on those sequences with long deamidation half-time, such as –N-R-, –N-Y-, –N-I- and –N-P-.(103) For Gln

deamidation, the effect of trypsin digestion buffers is negligible on all sequences because of its extremely long half-time (Figure 3.3B).(103) These results indicate that trypsin digestion buffers affect nonenzymatic deamidation of peptides mainly on sequences with short half-time of deamidation.

3.4.4 Protein and Peptide Identifications and Tryptic Miscleavages in Label-free Experiments

Table 3.1 Number of Protein and Peptide Identifications and Percentage of Miscleavaged Peptides from Rat Kidney Tissue Digested in the Four Buffers

	Unique peptides	Proteins	Misscleavaged peptides (%)
Ammonium acetate (pH 6)	19785±128	2447±6	34.4%±0.3%
Tris-HCl (pH 8)	19508±173	2453±25	32.3%±0.1%
ABB	19306±161	2482±40	25.2%±0.1%
TEAB	18894±921	2369±77	26.6%±0.2%

Note: This table shows the results from three technical replicates with individual sample preparations. As detailed in the section of "Materials and Methods", only protein groups with at least 2 unique peptides above 30 (Mascot score) are reported. The low standard deviation indicates good reproducibility between technical replicates.

As shown in Table 3.1, based on the label-free LC-MS/MS results from three technical replicates, protein and unique peptide identifications are comparable while using 50 mM of the four trypsin digestion buffers. However, the percentages of tryptic peptides with miscleavages in ammonium acetate (pH 6) are significantly higher than that in other tested buffers ($P<0.02$), indicating the reduced activities of trypsin in ammonium acetate (pH 6). Surprisingly, Tris-HCl (pH 8) also produces significantly more tryptic peptides

with miscleavages than ABB (P=0.0005) and TEAB (P=0.0012) although it is the recommended buffer from manufacturers. The increase of tryptic miscleavages does not affect protein and peptide identification possibly because many peptides that are too short to be identified with full cleavages become identifiable with miscleavages. Because of the increase of miscleavaged peptides, ammonium acetate (pH 6) and Tris-HCl (pH 8) may not be ideal buffers for SRM assay development in targeted MS analysis.(118) However, targeted SRM validation may still be used with caution if the control and samples are digested in ammonium acetate (pH 6) under completely same conditions. It was worth noticing that the solubility of proteins decreased greatly at pH 6. Therefore, protein concentration was diluted to 0.5 mg/ml during trypsin digestion using all tested buffers to ensure the solubility of proteins.

3.4.5 Determination of the Half-time of Asn deamidation in the Four Buffers Using Synthetic Peptides

The synthetic peptide DGNGYISAAELR was used to determine the half-time of Asn deamidation in 50 mM of ammonium acetate (pH 6), Tris-HCl (pH 8), ABB and TEAB. As shown in Figure 3.4, the ERLIC chromatograms showed the gradual transformation of unmodified peptides into two deamidation products containing –βDG- and –DG-. The half-time of Asn deamidation was determined as 51.4±6.0 days in 50 mM ammonium acetate (pH 6), which was about 23, 104 and 137 times of that in Tris-HCl, ABB and TEAB buffers, respectively. This sufficiently explains the reduced artificial Asn deamidation in ammonium acetate buffer (pH 6) detected using both label-free qualitative experiments and iTRAQ quantification. Deamidation decreased with decreasing pH in the range of pH 12 to 5.(119) For 1 day incubation in 50 mM ammonium acetate buffer (pH 6), 0.56% of the peptides are deamidated, which has a negligible effect on proteomic studies. It was reported that the half-time of Asn deamidation was 1.03 days in 0.15 M Tris-HCl, pH 7.4 at 37ºC,(103) which was about half of ours. The difference might be due to that they used 3 times higher concentration of Tris-HCl than ours, and Asn deamidation accelerated as the concentration of buffers increased.(120) We also determined the half-time of Asn-deamiation in 25 mM ABB buffer, and it was

15.08±2.03 h, i.e. about 1.27 times of that in 50 mM ABB buffer. Thus, a lower concentration of buffers should be used in proteomic sample preparations to reduce artificial deamidation. For example, 25-50 mM may be a good choice to the keep the pH of the buffers stable during trypsin digestion.

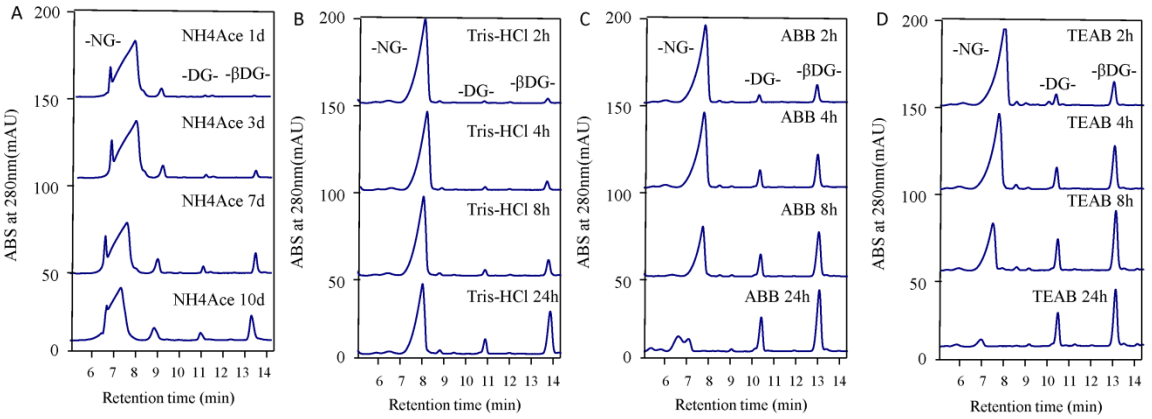

Figure 3.4 Determination of the half-time of Asn deamidation using the synthetic peptide DGNGYISAAELR by HPLC. Solutions of the synthetic peptide in 50 mM CH_3COONH_4, pH 6 were incubated for 1d, 3d, 7d and 10d at 37 °C. The incubation time in other buffers were 2h, 4h, 8h and 24h at 37°C. Peptide mixtures were resolved with an ERLIC column with UV detection at 280 nm. The half-time of Asn deamidation in 50 mM CH_3COONH_4, pH 6 is about 23, 104 and 137 times of that in 50 mM of Tris-HCl (pH 8), ABB and TEAB. A side product with the elution time of around 9 minutes formed during the incubation in 50 mM CH_3COONH_4, but it had no effect on the detection of endogenous Asn deamidation.

3.5 Conclusion

This work comprehensively compared 50 mM of ammonium acetate (pH 6), Tris-HCl (pH 8), ABB and TEAB as in-solution trypsin digestion buffers. Both iTRAQ quantification and label-free results indicate that ammonium acetate (pH 6) is more suitable than other tested buffers for studying endogenous deamidation and N-glycosylation due to the significant decrease of artificial Asn deamidation in comparison to other buffers without affecting protein and peptide identification and Gln deamidation. Determination of the half-time of Asn deamidation in the four buffers further validates the conclusion. Our results also indicate that among the commonly used tryspin digestion

buffers, ABB and TEAB are not suitable for studying Asn deamidation and N-glycosylation, but Tris-HCl may be used if trypsin digestion has to be done at around pH 8.

Chapter 4

Enhanced Separation and Characterization of Deamidated Peptides with RP-ERLIC-based Multidimensional Chromatography Coupled with Tandem Mass Spectrometry

4.1 Abstract

Protein asparagine deamidation produces the mixture of protein isoforms containing asparaginyl, n-aspartyl and isoaspartyl residues at the deamidation sites, which results in function loss and protein degradation. The identification and quantification of the deamidation products are very important to evaluate its biological effects, but it is difficult to distinguish between the n-Asp and isoAsp deamidation products in a proteome-wide analysis because of their similar physicochemical properties. Electron capture dissociation (ECD) and electron transfer dissociation (ETD) are reported to be able to distinguish between the isomeric n-Asp and isoAsp containing peptides using a pair of reporter ions. However, in a proteome-wide analysis, it may result in many false positive identifications of isoAsp containing peptides since the peak intensity of the reporter ions are generally very weak and buried in the background noise. In the common setup of reverse-phase liquid chromatography (RPLC), it is challenging to identify and quantify the isomeric deamidated peptides because of their coelution/poor separation. In this study, a RP-ERLIC-MS/MS approach was proposed to separate and quantify the triad of deamidation products on a proteome-wide scale. The method is featured by the use of offline RPLC in the first dimensional separation and the online coupling of electrostatic repulsion-hydrophilic interaction chromatography (ERLIC) to tandem MS. The three deamidation products from the same peptides are to be co-eluted and thus collected in the same fraction in offline RPLC. In the 2nd dimension of ERILC, they are separated according to both *p*I and GRAVY, facilitating the identification and quantification of them. We confirmed the co-elution of the three deamidation products in RPLC and the excellent separation of them in ERLIC using synthetic peptides, and tested the performance of ERLIC-MS/MS using simple tryptic digests. Using this RP-ERLIC-MS/MS, we identified 302 unique Asn-deamidated peptides from rat liver tissue. 20 of them were identified with all three deamidation-related products, and 70 of them were identified with two deamidation products.

4.2 Introduction

Nonenzymatic deamidation of asparagine and glutamine takes place spontaneously in proteins *in vivo,* which may lead to the structural changes and loss of function in long-life proteins. Because protein deamidation occurs at a constant rate *in vivo,* it was proposed as a "molecular clock" in studies of aging.(96, 97) It is reported that Alzheimer's disease (AD) and cataracts are due to the accumulation of isoaspartyl residues in some proteins with important functions.(65-67) Protein deamidation may result in the degradation of antibodies and therapeutic proteins during their production and storage.(71, 72) As shown in Figure 1.1, under *in vivo* conditions or at alkaline pH, a succinimide ring intermediate was formed during the deamidation of asparagine, and it is quickly hydrolyzed to n-Asp and isoAsp at a ratio of about 1:3.(73) At neutral or low pH, Asp isomerization occurs through the dehydration of Asp via a similar mechanism.(89) In order to uncover the biological significance of protein deamidation, it is necessary to develop an accurate, reliable and high-throughput analytical method to identify and quantify protein deamidation and isomerization sites.

Mass spectrometry (MS) can be used for the fast, sensitive and specific identification of protein deamidation in a proteome scale. The mass difference of 0.984 Da between deamidated peptides and their corresponding undeamidated counterparts can be readily detected using high-resolution MS. (81, 107) However, it is still very difficult to differentiate between the isomeric n-Asp and isoAsp deamidation products since they have identical chemical composition and mass, and similar physiochemical properties (Figure 1.1). It is reported that some tandem MS peptide sequencing methods, such as HCD, CAD and negative electrospray ionization, are able to differentiate between the isomeric deamidation products based on some reporter ions, but the results are unspecific, highly variable and unreliable.(106, 121, 122)

The powerful soft peptide backbone-fragmenting techniques of ECD and ETD are reported to be able to distinguish between the isomeric Asp and isoAsp peptides based on a pair of reporter ions, i.e. c+57 and z-57.(89) LC-ECD-MS/MS has been applied to the large-scale study of deamidated peptides containing isoAsp in cell line sample.(90)

However, many false positive identifications were included if the identification is based solely on the detection of the reporter ions without further manual validation. The possible reason is that the reporter ions of isoAsp containing peptides are generally masked by the background noise due to their relatively low intensity compared with other fragment ions. Under the commonly used RPLC-MS/MS conditions, the XIC based quantification of the isomeric Asp and isoAsp peptides is challenging because they have the same mass and are co-eluted from RP columns. (90) The identification of the deamidation isomers is also challenging while using RP liquid chromatography because of the co-fragmentation of them and their similar fragmentation pattern except for the weak reporter ions. As a result, this reporter ion based identification method cannot be used to identify low-abundance deamdated peptides containing isoAsp from complex samples.

In principle, it is feasible to identify and quantify the triad of deamidation products containing an Asn, n-Asp or isoAsp residue at the same position using LC-MS/MS if they are well separated by liquid chromatography before tandem MS. The typical SCX-RP-based shotgun proteomic approach cannot be used in the identification and quantification of the triad of deamidation products since these three peptides have identical GRAVY values of -3.5, resulting in the co-elution of them in RPLC. However, the triad of peptides can potentially be separated well using ERLIC. The deamidated peptides are eluted later than their unmodified counterparts using ERLIC on an anion-exchange chromatography (AEX) column as the conversion of Asn to Asp introduces a negative charge, enhancing their retention on the column. In addition, ERLIC has been reported to be able to separate peptides based on their *pI*. (105) Therefore, in principle, ERLIC can be used in the separation of the isomeric deamidation products containing Asp and isoAsp as they have different *p*I values. n-Asp residue has a side-chain pKa of around 3.9, but that of isoAsp is around 3.1. Theoretically, the triad of deamidation peptides should be eluted in the order of Asn<n-Asp<isoAsp in ERLIC. Thus, they can be identified based on their elution order even if they have the similar tandem MS fragmentation pattern. Consequently, ERLIC-MS/MS can potentially be an excellent alternative to the commonly used RPLC-MS/MS in separating and characterizing the triads of deamidation

peptides. It is necessary to use volatile mobile phases that are compatible with mass spectrometry in order to minimize clogging and adduct formation in the ionization source. Our recent development of ERLIC introduces volatile solvents that are fully compatible with MS/MS analysis.(105)

For proteome-wide study of complex samples, multidimensional liquid chromatography (MDLC) is generally used to reduce sample complexity and increase sensitivity and dynamic range of peptide identification by minimizing the undersampling and ion suppression problems.(14, 74) In this study, we proposed to develop a RP-ERLIC-MS/MS sequence for the proteome-scale study of deamidation and isomerization sites. The co-elution of the three deamidation-related products from the same peptide in RPLC becomes an advantage when RPLC is used as the first dimension of offline MDLC since they are to be collected into the same fraction. This facilitates the separation and identification of them in the second dimension of ERLIC coupled to MS/MS and subsequent data analysis.

4.3 Materials and Methods

4.3.1 Reagents

Unless indicated, all reagents used in this study were purchased from Sigma-Aldrich, USA. Protease inhibitor (Cat no.: P8340) and unmodified trypsin (T8802) were purchased from Sigma-Aldrich, St. Louis, MO. Sep-Pak C18 cartridges were purchased from Waters, Milford, MA; Bicinchoninic acid (BCA) assay kit was purchased from Pierce, Rockford, IL.

4.3.2 Sample Preparation

Male Sprague Dawley rats were handled in accordance with the guidelines of NTU Institutional Animal Care and Use Committee (NTU-IACUC), NTU, Singapore. Rat

livers were snap-frozen in liquid nitrogen immediately after collection and kept at -80ºC until use. The tissue was cut into small pieces and ground into fine powder in liquid nitrogen with a pestle. The powder was then suspended in 8 M urea with protease inhibitor cocktail (P8340, Sigma) and 10 mM PMSF added in the ratio of 1:50 and 1:20 (v/v), respectively. The suspension was sonicated for 10 s thrice on ice and centrifuged at 20,000 X g at room temperature (RT) for 30 min. The protein concentration of the supernatant was then determined by the bicinchoninic acid (BCA) assay. Trypsin digestion was done as previously described.(105) The obtained tryptic peptides were desalted using a Sep-Pak C18 cartridge (Waters, Milford, MA) and dried in a SpeedVac (Thermo Electron, Waltham, MA). The mixture of BSA (A2153, Sigma-Aldrich) and chicken ovalbumin (A5503, Sigma-Aldrich) was digested and desalted in the same way with rat liver samples.

4.3.3 RPLC Fractionation

Four triads of deamidation-related peptides with different *p*I and GRAVY value were synthesized at the Peptide Synthesis Core Facility, Nangyang Technological University, with the sequences DG(N/D/isoD)GYISAAELR, DS(N/D/isoD)GAILVYDVTDEDSFQK, VT(N/D/isoD)GAFTGEISPGMIK, and IEYDDQ(N/D/isoD)DGSCDVK. These peptides had been identified from a rat liver protein digest in a previous study. (105) The mixture of each triad of peptides was fractionated using a BioBasic C18 column (4.6 × 250 mm, 5 µm, 300 Å, Thermo Scientific, West Palm Beach, FL) on a Shimadzu Prominence UFLC system monitored at 280 nm. Mobile phase A (0.1% formic acid (FA) in H_2O) and mobile phase B (0.1% FA in ACN) were used to establish the 50 min gradient of 5% mobile phase B for 3 min, 5-40% B over 32 min, 40-60% buffer B over 5 min, 60-100% buffer B over 5 min, and 5 min at 100% B, at a flow rate of 1 mL/min. For the fractionation of rat liver whole proteome, 2 mg of peptides were fractionated using the same gradient, with 29 fractions collected. These were then dried *in vacuo* and combined into 24 fractions based on the amplitude of absorbance in the chromatogram as shown in Figure 4.1. Each fraction was redissolved in 200 µL 85% ACN/0.1% NH_4OH for ERLIC-LC-MS/MS analysis.

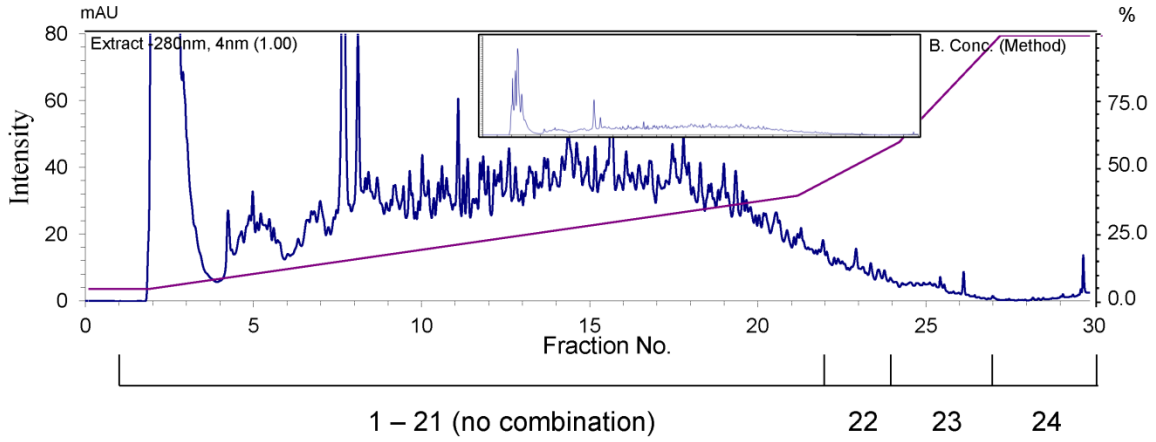

Figure 4.1 RPLC chromatogram of tryptic peptides from rat liver. Twenty nine fractions were collected from offline RPLC and pooled into 24 for subsequent ERLIC-LC-MS/MS analysis. The insert shows the full scale chromatogram, and the strong UV absorption at 2.5 and 7.8 min were from impurities. The UV absorption was monitored at 280nm.

4.3.4 ERLIC Fractionation

The mixture of the above-mentioned triad of peptides was fractionated using a PolyWAX LP anion-exchange column (4.6 × 200 mm, 5 µm, 300 Å, PolyLC, Columbia, MD) on a Shimadzu Prominence UFLC system monitored at 280 nm. Mobile phase A (85% ACN/0.1% acetic acid) and mobile phase B (30%ACN/0.2% FA) were used in a 30 min gradient of 5-30% B over 15 min and 30-100% buffer B over 10 min followed by 5 min at 100% B, at a flow rate of 1 mL/min. The volatile acid in the mobile phases is used to maintain the low pH. Thus, FA is in use when ERLIC is coupled to MS/MS.

4.3.5 RP-LC-MS/MS

The mixture of the triad of synthetic peptides was separated and analyzed on a Shimadzu UFLC system coupled to an LTQ-FT Ultra (Thermo Electron, Bremen, Germany). It was injected into a Zorbax peptide trap column (Agilent, CA) via the autosampler of the Shimadzu UFLC for concentration and desalting. The peptides were separated in a capillary column (200 µm × 10 cm) packed with C18 AQ (5 µm, 300 Å; Bruker-

Michrom, Auburn, CA). The flow rate was maintained at 500 nL/min. Mobile phase A (0.1% FA in H_2O) and mobile phase B (0.1% FA in ACN) were used to establish the 60 min gradient comprised of 45 min of 5-35% B, 8 min of 35-50% B and 2 min of 80% B followed by re-equilibration at 5% B for 5 min. Peptides were then analyzed on the LTQ-FT with an ADVANCE™ CaptiveSpray™ Source (Bruker-Michrom) at an electrospray potential of 1.5 kV. A gas flow of 2, ion transfer tube temperature of 180°C and collision gas pressure of 0.85 mTorr were used. The LTQ-FT was set to perform data acquisition in the positive ion mode as previously described except that the m/z range of 350-1600 was used in the full MS scan. (123)

4.3.6 ERLIC-LC-MS/MS

ERLIC-LC-MS/MS was done on the same UFLC and mass spectrometer system with the following modifications: 1) A PolyWAX LP anion-exchange guard column (PolyLC, Columbia, MD) was used as the trap column and 85% ACN/0.1% NH4OH was used as the desalting solvent; 2) The peptides were separated in a capillary column (200 µm × 15 cm) packed with PolyWAX LP anion-exchange bulk material (5 µm, 300 Å; PolyLC); 3) For the tryptic digest of BSA and chicken ovalbumin, mobile phase A (0.1% FA in ACN) and mobile phase B (0.1% FA in H_2O) were used to establish the 60 min gradient comprised of 45 min of 0-30% B, 5 min of 30-50 % B, 4 min of 50-90% B, and 1 min of 90%-0% B, followed by re-equilibration at 100% A for 5 min; 4) For synthetic peptides and rat liver samples, the same ERLIC mobile phases were used to establish a 90 min gradient comprised of 70 min of 0-30% B, 5 min of 30-50 % B, 3 min of 50-90% B, and 2 min of 90%-0% B followed by re-equilibration at 100% A for 10 min. The flow rate was maintained at 500 nL/min.

4.3.7 Data Analysis

The raw data were first converted into dta format using the extract_msn (version 4.0) in Bioworks Browser (version 3.3, Thermo Fisher Scientific, Inc.), and then the dta files

were converted into MGF format using an in-house program. Intensity values and fragment ion m/z ratios were not manipulated. For BSA and chicken ovalbumin, the Swiss-Prot protein database (Release 57.11) was used for database searches. For synthetic peptides and rat liver samples, the IPI rat protein database (version 3.40, 40381 sequences, 20547209 residues) and its reversed complement were combined and used for database searches. The database search was performed using an in-house Mascot server (version 2.2.04, Matrix Science, Boston, MA, USA) with MS tolerance of 5.1 ppm and MS/MS tolerance of 0.8 Da. Two missed cleavage sites of trypsin were allowed. Carbamidomethylation (C) was set as a fixed modification, and oxidation (M), phosphorylation (S, T and Y) and deamidation (N and Q) were set as variable modifications. The ions score significance threshold was set at 20. The obtained peptide/protein list for each fraction was exported to Microsoft Excel or processed using an in-house script for further analysis. For high confidence peptide identification, only peptides with an E-value of less than 0.05 were used for statistical calculation. The FDR of peptide identification was set to be less than 1% (FDR = 2.0 × decoy_hits/total_hits). The FDR rate is based on the assigned spectra.

4.4 Results and Discussion

4.4.1 A Novel Strategy for Large-scale Study of Protein Deamidation

We propose to use the following shotgun proteomics strategy in studying protein deamidation: 1) Tryptic peptides are first separated based on their polarity using RPLC as the first dimension of offline MDLC. All three deamidation products originating from the same peptides are co-eluted and collected in the same fraction due to their identical GRAVY values; 2) Each RPLC fraction is separated using ERLIC coupled to a mass spectrometer. To be compatible with direct MS analysis, volatile mobile phases are used. In ERLIC, tryptic peptides are eluted based on their *p*I values as well as polarity, (105) and the separation is orthogonal to that of the 1st dimensional RPLC. Therefore, RP-ERLIC is a proper MDLC sequence. As a result, the three peptides in a deamidation triad that are co-eluted and collected in the same fraction in RPLC, can be separated according

to their *p*I values in online ERLIC, facilitating the identification and quantification of them using MS/MS. Figure 4.2 shows the flow chart for the RP-ERLIC-MS/MS sequence. In addition to testing this sequence for study of deamidation events, we also evaluated its applicability in peptide identification for whole proteome analysis using a rat liver tissue. We evaluated every step of the RP-ERLIC-MS/MS strategy using synthetic peptides and simple tryptic peptide mixtures from model proteins before applying it to tissue samples with high complexity.

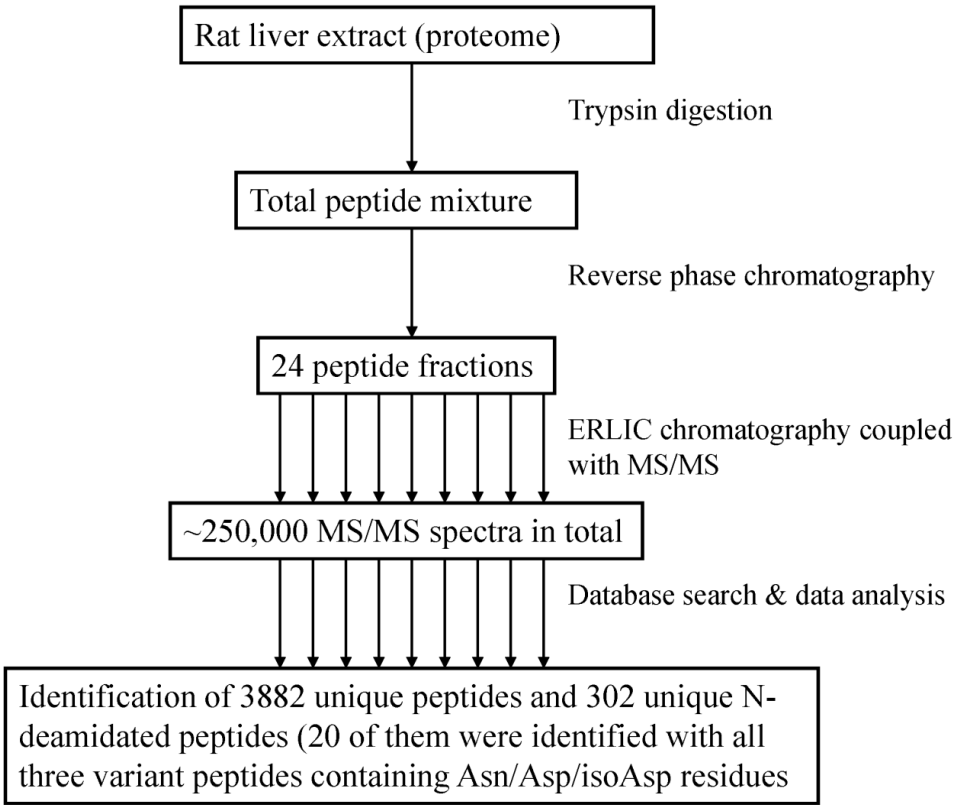

Figure 4.2 Proposed strategy for characterization of whole proteome and deamidated peptides using RP-ERLIC-MS/MS. Two mg tryptic peptides from rat liver extract were separated with offline RP liquid chromatography and pooled into 24 fractions. Each fraction was analyzed using ERLIC chromatography coupled with mass spectrometry. The resulted MS/MS spectra were searched against the IPI rat database using an in-house Mascot server.

4.4.2 Evaluation of RPLC and ERLIC for Separation of Synthetic Peptides

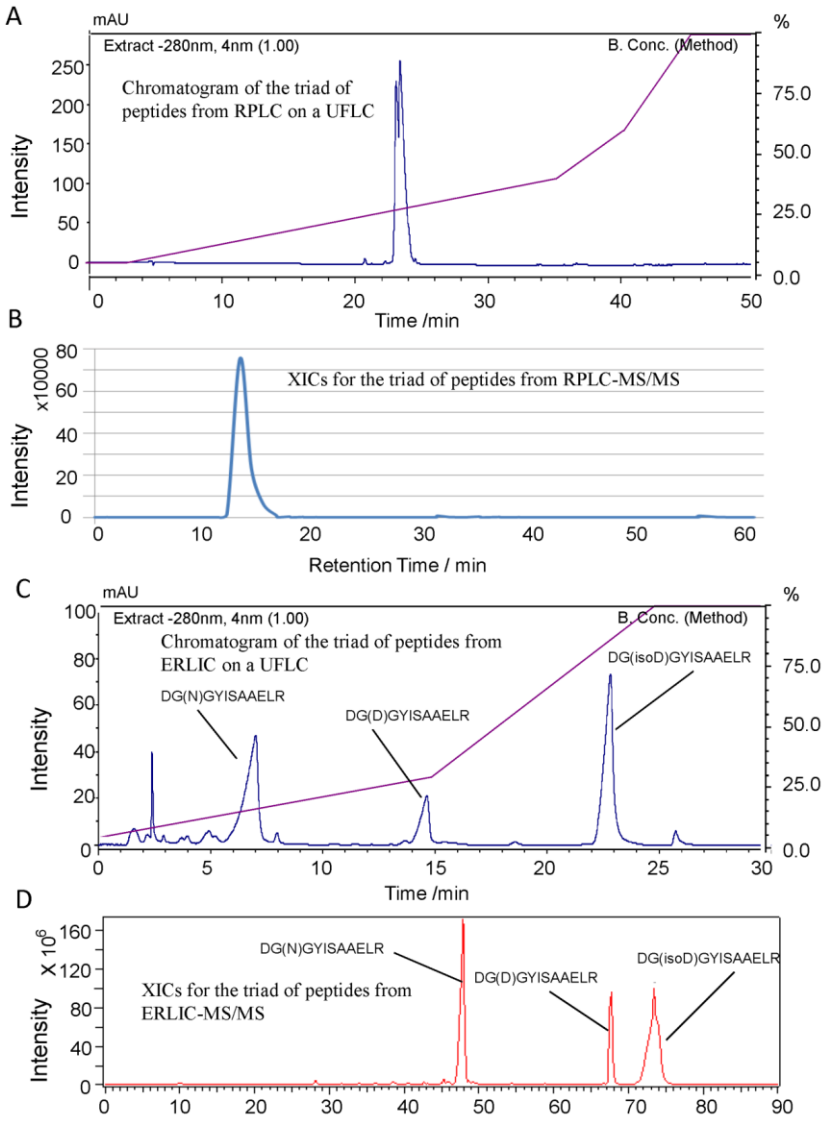

Figure 4.3 Comparison of RPLC and ERLIC for Separation of Synthetic Peptides: the co-elution of the peptide mixture of DG(N/D/isoD)GYISAAELR in C18 RP liquid chromatography with a conventional column (A) and in a C18 capillary coupled to mass spectrometry (B); separation of the peptide mixture of DG(N/D/isoD)GYISAAELR using ERLIC chromatography with a conventional column (C) and with a capillary coupled to mass spectrometry (D). The absorbance was monitored at 280 nm. The co-elution of the three deamidation-related products in RPLC makes it an ideal chromatography for the first dimension of MDLC, since collection of them in the same fraction facilitates their identification as a set when resolved in the second dimension.

To prove the co-elution of the triads of deamidation-related peptides in RPLC, they were separated using a C18 column on a Shimadzu UFLC. As shown in Figure 4.3A, the peptides DG(N)GYISAAELR/ DG(D)GYISAAELR/ DG(isoD)GYISAAELR are co-eluted in a normal RPLC gradient. When RPLC separation was run on a nano-scale C18 column coupled to mass spectrometry, the extracted ion chromatograms (XICs) showed the same co-elution of the triad, which prevents the reliable identification and quantification of the isomeric deamidated peptides (Figure 4.3B). Similar results were obtained from other peptide triads [*data not shown*]. This confirms our hypothesis that RPLC can be ideally used as the first dimension of MDLC for analysis of protein deamidation. Although RPLC has been reported to be capable of separating the three deamidation-related products with some modifications in packing materials or mobile phases, the separation was poor, and their elution order was unpredictable. (70) For comparison, we also tested ERLIC chromatography in the same way in separating the triad of deamidation-related peptides. As shown in Figure 4.3C, they were well separated from each other using a normal ERLIC gradient. In order to confirm the elution order of the three deamidation products within the triad, we also separate each of the peptides separately using the same ERLIC gradient (Figure 4.4) on a Shimadzu UFLC. In addition, we also confirmed the identifications using the MS/MS spectra from MALDI-TOF/TOF and the reporter ion of $y_n - 46$ from isoAsp containing peptides.(106) When the ERLIC separation was done on a nanoscale ERLIC column coupled to mass spectrometry, the XICs showed the same good separation of the triad of deamidation products (Figure 4.3D). In conclusion, ERLIC seems to be suitable for use as the second dimension of MDLC for analysis of deamidation events.

4.4.3 Application of ERLIC-MS/MS to the Simple Tryptic Digest from Two Model Proteins

We tested the capability of ERLIC-MS/MS in distinguishing between the triads of deamidation-related peptides from the tryptic digest of BSA and chicken ovalbumin and further optimized the ERLIC-MS/MS setup before applying it to proteomic samples with high complexity. BSA and chicken ovalbumin were identified at the sequence coverage

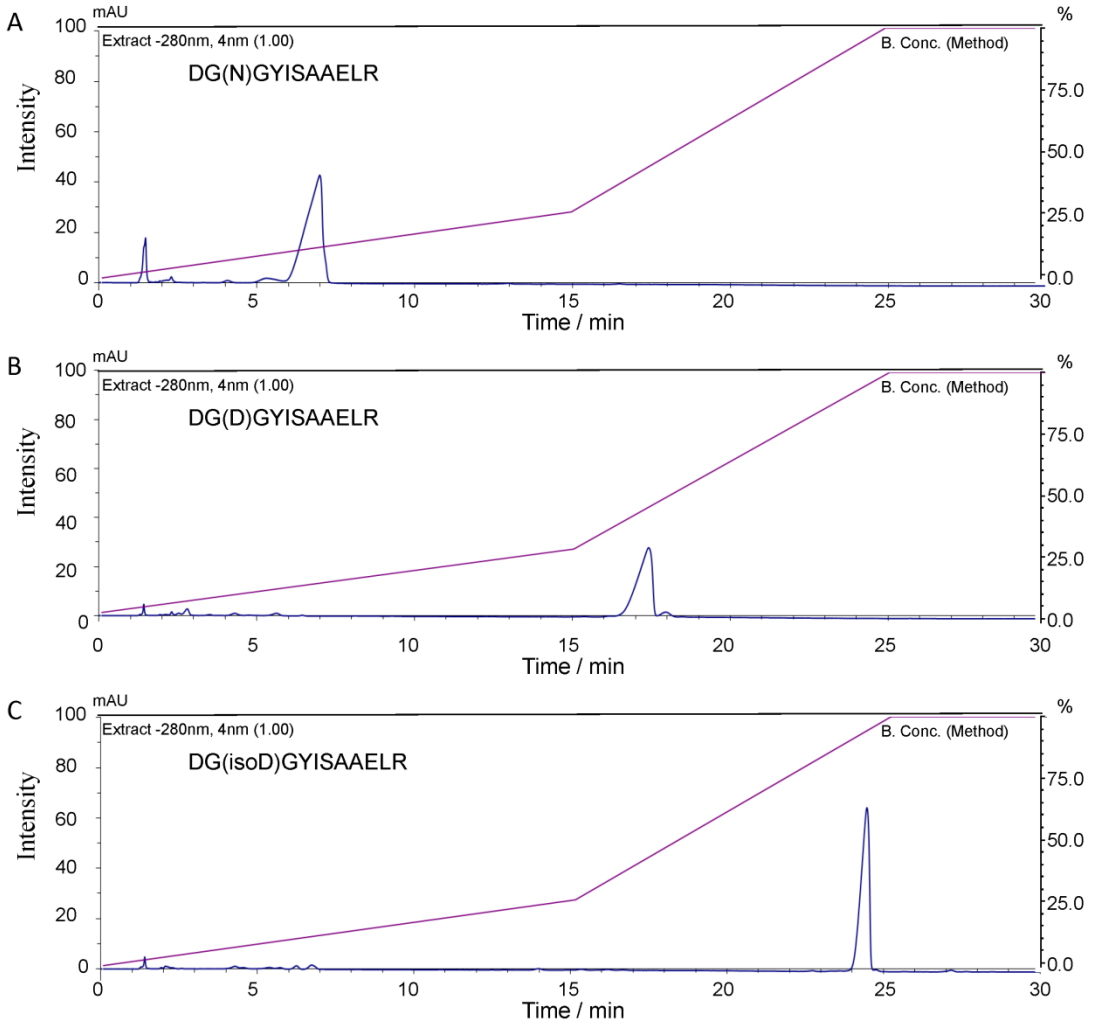

Figure 4.4 ERLIC chromatograms of the peptides of DG(N)GYISAAELR (A), DG(D)GYISAAELR (B) and DG(isoD)GYISAAELR (C) from a Shimadzu UFLC.

of 82% and 78%, respectively, indicating that ERLIC-MS/MS has potential to be used as the last dimension of MDLC for whole proteomes analysis in addition to deamidation events. In total, 15 unique Asn-deamidated peptides were identified, and four of them were identified with all three deamidation-related products. The triads of deamidation-related peptides identified from BSA and chicken ovalbumin are listed in Table 4.1. As with the results from synthetic peptides, the triad peptides were well separated from each other in ERLIC with their retention time differing by at least 5 min (Figure 4.5A and 4.5B). The deamidated peptides can be unambiguously distinguished from their corresponding undeamidated counterparts based on the mass difference of 0.984 Da and the difference in MS/MS spectra. The deamidation site is sandwiched between fragments

Table 4.1 The triads of deamidation-related peptides identified from BSA and chicken ovalbumin

prot_desc	pep_exp_mz	pep_calc_mr	pep_score	pep_seq	pep_var_mod_pos	Retention time (min)	Precursor Intensity	Peptide Type
Bovine serum albumin	722.3254	1442.635	67.81	YICDNQDTISSK		26.99	5879.09	Asn peptide
Bovine serum albumin	722.3236	1442.635	66.11	YICDNQDTISSK		27.32	74372.7	Asn peptide
Bovine serum albumin	722.321	1442.635	74.44	YICDNQDTISSK		27.67	412996	Asn peptide
Bovine serum albumin	722.3218	1442.635	73.8	YICDNQDTISSK		28.04	251903	Asn peptide
Bovine serum albumin	722.3254	1442.635	71.09	YICDNQDTISSK		28.43	21104	Asn peptide
Bovine serum albumin	722.3254	1442.635	64.11	YICDNQDTISSK		28.8	19558	Asn peptide
Bovine serum albumin	722.3253	1442.635	61.35	YICDNQDTISSK		29.17	16680.5	Asn peptide
Bovine serum albumin	722.325	1442.635	60.47	YICDNQDTISSK		29.54	15200.5	Asn peptide
Bovine serum albumin	722.3254	1442.635	44.56	YICDNQDTISSK		29.95	5157.08	Asn peptide
Bovine serum albumin	722.3248	1442.635	52.33	YICDNQDTISSK		30.33	4295.79	Asn peptide
Bovine serum albumin	722.3236	1442.635	51.25	YICDNQDTISSK		34.07	1160.39	Asn peptide
Bovine serum albumin	722.3246	1442.635	44.82	YICDNQDTISSK		34.84	1860.56	Asn peptide
Bovine serum albumin	722.3257	1442.635	49.9	YICDNQDTISSK		35.25	1364.6	Asn peptide
Bovine serum albumin	722.8166	1443.619	43.99	YICDNQDTISSK	0.000040000000.0	38.94	2794.04	n-Asp peptide
Bovine serum albumin	722.8166	1443.619	48.88	YICDNQDTISSK	0.000040000000.0	39.34	3429.17	n-Asp peptide
Bovine serum albumin	722.8167	1443.619	44.93	YICDNQDTISSK	0.000004000000.0	39.73	2945.04	n-Asp peptide
Bovine serum albumin	722.8175	1443.619	44.95	YICDNQDTISSK	0.000040000000.0	48.79	1645.32	isoAsp peptide
Bovine serum albumin	722.8171	1443.619	70.36	YICDNQDTISSK	0.000040000000.0	49.17	5471.99	isoAsp peptide
Bovine serum albumin	722.8176	1443.619	57.2	YICDNQDTISSK	0.000040000000.0	49.55	8084.28	isoAsp peptide
Bovine serum albumin	722.8175	1443.619	59.09	YICDNQDTISSK	0.000040000000.0	49.91	5604.63	isoAsp peptide
Bovine serum albumin	874.3575	1746.698	70.04	YNGVFQECCQAEDK		30.81	1564.05	Asn peptide
Bovine serum albumin	874.3562	1746.698	85.24	YNGVFQECCQAEDK		31.14	17052.5	Asn peptide
Bovine serum albumin	874.3549	1746.698	83.63	YNGVFQECCQAEDK		31.55	58510.4	Asn peptide
Bovine serum albumin	874.355	1746.698	82.02	YNGVFQECCQAEDK		31.94	97366.3	Asn peptide
Bovine serum albumin	874.355	1746.698	95.03	YNGVFQECCQAEDK		32.31	45513.6	Asn peptide
Bovine serum albumin	874.3564	1746.698	73.04	YNGVFQECCQAEDK		32.72	8800.57	Asn peptide

Bovine serum albumin	874.3573	1746.698	62.35	YNGVFQECCQAEDK		33.17	2658.61	Asn peptide
Bovine serum albumin	874.3575	1746.698	49.55	YNGVFQECCQAEDK		34.12	682.736	Asn peptide
Bovine serum albumin	874.8518	1747.682	58.82	YNGVFQECCQAEDK	0.04000000000000.0	42.14	2136.05	n-Asp peptide
Bovine serum albumin	874.851	1747.682	55.37	YNGVFQECCQAEDK	0.04000000000000.0	42.24	2181.45	n-Asp peptide
Bovine serum albumin	874.8487	1747.682	73.09	YNGVFQECCQAEDK	0.04000000000000.0	42.56	9842.72	n-Asp peptide
Bovine serum albumin	874.85	1747.682	66.05	YNGVFQECCQAEDK	0.04000000000000.0	42.93	14802.2	n-Asp peptide
Bovine serum albumin	874.85	1747.682	44.3	YNGVFQECCQAEDK	0.04000000000000.0	43.33	11656.1	n-Asp peptide
Bovine serum albumin	874.851	1747.682	43.18	YNGVFQECCQAEDK	0.00000400000000.0	47.87	1177.11	isoAsp peptide
Bovine serum albumin	874.85	1747.682	68.87	YNGVFQECCQAEDK	0.04000000000000.0	48.24	7853.68	isoAsp peptide
Bovine serum albumin	874.8498	1747.682	70.16	YNGVFQECCQAEDK	0.04000000000000.0	48.66	47125.2	isoAsp peptide
Bovine serum albumin	874.8483	1747.682	74.43	YNGVFQECCQAEDK	0.04000000000000.0	49.07	74047.2	isoAsp peptide
Bovine serum albumin	874.8492	1747.682	91.56	YNGVFQECCQAEDK	0.04000000000000.0	49.46	63364.8	isoAsp peptide
Bovine serum albumin	874.8496	1747.682	60.94	YNGVFQECCQAEDK	0.04000000000000.0	49.81	18378.5	isoAsp peptide
Bovine serum albumin	874.85	1747.682	72.08	YNGVFQECCQAEDK	0.04000000000000.0	50.18	5653	isoAsp peptide
Bovine serum albumin	874.848	1747.682	42	YNGVFQECCQAEDK	0.00000400000000.0	50.55	2768.18	isoAsp peptide
Bovine serum albumin	874.8498	1747.682	65.69	YNGVFQECCQAEDK	0.04000000000000.0	50.97	3916.93	isoAsp peptide
Bovine serum albumin	874.8492	1747.682	61.23	YNGVFQECCQAEDK	0.04000000000000.0	51.34	4249.91	isoAsp peptide
Bovine serum albumin	740.4029	1478.788	69.05	LGEYGFQNAILVR		9.25	1266.04	Asn peptide
Bovine serum albumin	740.4002	1478.788	89.62	LGEYGFQNAILVR		9.54	52801.3	Asn peptide
Bovine serum albumin	493.9366	1478.788	60.34	LGEYGFQNAILVR		9.59	1918.49	Asn peptide
Bovine serum albumin	740.398	1478.788	89.55	LGEYGFQNAILVR		9.88	211045	Asn peptide
Bovine serum albumin	493.9365	1478.788	67.22	LGEYGFQNAILVR		9.89	6951.74	Asn peptide
Bovine serum albumin	740.398	1478.788	83.05	LGEYGFQNAILVR		10.3	508184	Asn peptide
Bovine serum albumin	493.9365	1478.788	73.27	LGEYGFQNAILVR		10.3	17313.3	Asn peptide
Bovine serum albumin	740.399	1478.788	80.07	LGEYGFQNAILVR		10.71	284871	Asn peptide
Bovine serum albumin	493.9365	1478.788	52.02	LGEYGFQNAILVR		10.73	9176.38	Asn peptide
Bovine serum albumin	740.4003	1478.788	80.15	LGEYGFQNAILVR		11.12	44549.1	Asn peptide
Bovine serum albumin	740.4014	1478.788	86.06	LGEYGFQNAILVR		11.55	12861.1	Asn peptide
Bovine serum albumin	740.4011	1478.788	68.82	LGEYGFQNAILVR		11.95	8689.23	Asn peptide

Bovine serum albumin	740.4013	1478.788	73.66	LGEYGFQNAILVR		12.35	5121.25	Asn peptide
Bovine serum albumin	740.401	1478.788	70.38	LGEYGFQNAILVR		12.75	6553.68	Asn peptide
Bovine serum albumin	740.4006	1478.788	60.45	LGEYGFQNAILVR		13.14	3948.58	Asn peptide
Bovine serum albumin	740.4001	1478.788	61.14	LGEYGFQNAILVR		13.54	4542.96	Asn peptide
Bovine serum albumin	740.4008	1478.788	85.83	LGEYGFQNAILVR		13.96	4695.64	Asn peptide
Bovine serum albumin	740.4025	1478.788	61.78	LGEYGFQNAILVR		14.5	2882.27	Asn peptide
Bovine serum albumin	740.4012	1478.788	58.82	LGEYGFQNAILVR		15.97	3460.06	Asn peptide
Bovine serum albumin	740.4027	1478.788	75.02	LGEYGFQNAILVR		17.15	2169.48	Asn peptide
Bovine serum albumin	740.8934	1479.772	79.73	LGEYGFQNAILVR	0.0000000400000.0	15.3	2892.32	n-Asp peptide
Bovine serum albumin	740.8918	1479.772	76.84	LGEYGFQNAILVR	0.0000000400000.0	15.69	3814.02	n-Asp peptide
Bovine serum albumin	740.8933	1479.772	84.32	LGEYGFQNAILVR	0.0000000400000.0	18.38	8873.15	isoAsp peptide
Bovine serum albumin	740.8937	1479.772	74.43	LGEYGFQNAILVR	0.0000000400000.0	18.73	30705.6	isoAsp peptide
Chicken ovalbumin	929.9898	1857.959	96.68	ELINSWVESQTNGIIR		17.61	4962.83	Asn peptide
Chicken ovalbumin	929.9861	1857.959	86.34	ELINSWVESQTNGIIR		17.96	156528	Asn peptide
Chicken ovalbumin	620.326	1857.959	57.55	ELINSWVESQTNGIIR		17.97	141092	Asn peptide
Chicken ovalbumin	620.3262	1857.959	43.02	ELINSWVESQTNGIIR		18.45	7338.95	Asn peptide
Chicken ovalbumin	929.987	1857.959	84.61	ELINSWVESQTNGIIR		18.62	5506.22	Asn peptide
Chicken ovalbumin	930.4782	1858.943	83.36	ELINSWVESQTNGIIR	0.0000000000040000.0	21.94	3879.67	n-Asp peptide
Chicken ovalbumin	930.4789	1858.943	103.47	ELINSWVESQTNGIIR	0.0000000000040000.0	22.29	35516.8	n-Asp peptide
Chicken ovalbumin	620.6548	1858.943	61.01	ELINSWVESQTNGIIR	0.0000000000040000.0	22.3	23006	n-Asp peptide
Chicken ovalbumin	620.655	1858.943	57.4	ELINSWVESQTNGIIR	0.0000000000040000.0	22.68	22715.5	n-Asp peptide
Chicken ovalbumin	930.48	1858.943	83.35	ELINSWVESQTNGIIR	0.0000000000040000.0	22.69	23942.3	n-Asp peptide
Chicken ovalbumin	930.4801	1858.943	78.3	ELINSWVESQTNGIIR	0.0000000000040000.0	23.32	1844.71	n-Asp peptide
Chicken ovalbumin	930.4799	1858.943	86.14	ELINSWVESQTNGIIR	0.0000000000040000.0	23.37	2405.64	n-Asp peptide
Chicken ovalbumin	930.4816	1858.943	71.01	ELINSWVESQTNGIIR	0.0004000000000000.0	24.76	2990.64	isoAsp peptide
Chicken ovalbumin	930.4803	1858.943	77.79	ELINSWVESQTNGIIR	0.0004000000000000.0	24.96	3505.52	isoAsp peptide
Chicken ovalbumin	930.4807	1858.943	81.51	ELINSWVESQTNGIIR	0.0000000000040000.0	26.03	2947.38	isoAsp peptide
Chicken ovalbumin	620.6538	1858.943	52.57	ELINSWVESQTNGIIR	0.0000000000040000.0	26.35	62788.8	isoAsp peptide
Chicken ovalbumin	930.4782	1858.943	103.18	ELINSWVESQTNGIIR	0.0000000000040000.0	26.36	63759.3	isoAsp peptide

Chicken ovalbumin	620.6533	1858.943	53.4	ELINSWVESQTNGIIR	0.0000000000040000.0	26.7	94207.3	isoAsp peptide
Chicken ovalbumin	930.4773	1858.943	86.44	ELINSWVESQTNGIIR	0.0000000000040000.0	26.71	90904.9	isoAsp peptide
Chicken ovalbumin	620.654	1858.943	49.54	ELINSWVESQTNGIIR	0.0000000000040000.0	27.06	75191.2	isoAsp peptide
Chicken ovalbumin	930.4786	1858.943	103.68	ELINSWVESQTNGIIR	0.0000000000040000.0	27.06	63797	isoAsp peptide
Chicken ovalbumin	930.4796	1858.943	97.33	ELINSWVESQTNGIIR	0.0000000000040000.0	27.42	19244.2	isoAsp peptide
Chicken ovalbumin	930.4808	1858.943	104.56	ELINSWVESQTNGIIR	0.0000000000040000.0	27.76	16181.4	isoAsp peptide
Chicken ovalbumin	930.4803	1858.943	103.18	ELINSWVESQTNGIIR	0.0000000000040000.0	28.15	4628.78	isoAsp peptide
Chicken ovalbumin	930.4797	1858.943	78.54	ELINSWVESQTNGIIR	0.0000000000040000.0	28.56	972.912	isoAsp peptide
Chicken ovalbumin	930.4783	1858.943	78.94	ELINSWVESQTNGIIR	0.0000000000040000.0	28.91	1832.38	isoAsp peptide
Chicken ovalbumin	930.4805	1858.943	74.89	ELINSWVESQTNGIIR	0.0000000000040000.0	29.33	866.068	isoAsp peptide
Chicken ovalbumin	930.48	1858.943	65.42	ELINSWVESQTNGIIR	0.0000000000040000.0	29.68	923.214	isoAsp peptide
Chicken ovalbumin	930.48	1858.943	58.72	ELINSWVESQTNGIIR	0.0000000000040000.0	30.12	601.787	isoAsp peptide
Chicken ovalbumin	930.9722	1859.927	70.1	ELINSWVESQTNGIIR	0.0004000000040000.0	33.6	1057.47	2 deamidations
Chicken ovalbumin	930.9702	1859.927	91.65	ELINSWVESQTNGIIR	0.0004000000040000.0	33.8	788.135	2 deamidations
Chicken ovalbumin	930.9699	1859.927	79.32	ELINSWVESQTNGIIR	0.0004000000040000.0	35.88	943.935	2 deamidations
Chicken ovalbumin	930.9724	1859.927	80.68	ELINSWVESQTNGIIR	0.0004000000040000.0	36.27	1514.5	2 deamidations
Chicken ovalbumin	930.9729	1859.927	91.29	ELINSWVESQTNGIIR	0.0004000000040000.0	36.36	1033.9	2 deamidations
Chicken ovalbumin	930.9743	1859.927	90.18	ELINSWVESQTNGIIR	0.0004000000040000.0	36.68	1391.39	2 deamidations
Chicken ovalbumin	930.9711	1859.927	77.21	ELINSWVESQTNGIIR	0.0004000000040000.0	42.61	2231.23	2 deamidations
Chicken ovalbumin	930.9725	1859.927	88.64	ELINSWVESQTNGIIR	0.0004000000040000.0	42.94	5754.02	2 deamidations
Chicken ovalbumin	930.9718	1859.927	97.58	ELINSWVESQTNGIIR	0.0004000000040000.0	43.34	6584.85	2 deamidations
Chicken ovalbumin	930.9716	1859.927	77.65	ELINSWVESQTNGIIR	0.0004000000040000.0	43.74	5415.39	2 deamidations
Chicken ovalbumin	930.9715	1859.927	91.77	ELINSWVESQTNGIIR	0.0004000000040000.0	44.14	3621.74	2 deamidations
Chicken ovalbumin	930.9735	1859.927	91.54	ELINSWVESQTNGIIR	0.0004000000040000.0	44.4	2195.47	2 deamidations

with the deamidated asparagine (aspartic acid), such as b3-5, b7, b11-b13 and y12 (Figure 4.5D), the mass of which was about 0.984 Da higher than that of the corresponding b or y ions detected in the MS/MS spectra of the unmodified peptides (Figure 4.5C). (62, 124) The MS/MS spectra of the isomeric deamidated peptides containing Asp or isoAsp were identical in CAD analysis. As discussed in the section of 4.2, we can distinguish them based on their predictable elution order in ERLIC. As shown in Figure 4.4A and 4.4B, the relative intensity of the last eluted deamidated peptides was about 3 times of the first eluted deamidated peptides, which is consistent with the ratio of isoAsp and n-Asp produced in nonenzymatic deamidation and isomerization. (72, 73, 125) This further confirms their identities. It is evident that the rate of deamidation is much higher for the peptide shown in Figure 4.5A than that in Figure 4.5B, reflecting the rapid kinetics of Asn deamidation at the –N-G- sequence.(126, 127) In conclusion, ERLIC-MS/MS can be effectively used in the identification and relative quantification of deamidated products from the same peptide.

4.4.4 Application of RP-ERLIC-MS/MS to Tryptic Peptides from Rat liver Tissue

To determine the performance of the RP-ERLIC-MS/MS setup in characterizing proteomic samples of high complexity, tryptic peptides from 2 mg rat liver tissue were first distributed into 24 fractions with offline RPLC, and then subjected to ERLIC-MS/MS for characterization of whole proteome and deamidated peptides. As a result, 1305 protein groups were identified with at least 2 unique peptides; 3,882 unique peptides were identified from a total of 23,658 PSMs (peptide spectrum matches); 302 unique Asn-deamidated peptides were identified from 1408 PSMs; 20 unique Asn-deamidated peptides were identified with all three deamidation-related products, and 70 Asn-deamidated peptides were identified with two of them. The identified triads of deamidation-related peptides are shown in Supplemental Table 2 in Ref. (128). For those identified with two deamidation-related products, all of them include the undeamidated peptides. It is infeasible to determine whether the identified deamidated peptides are Asp or isoAsp-containing deamidation products based solely on the elution time. However, the separation of them will surely facilitate the identification and quantification of them

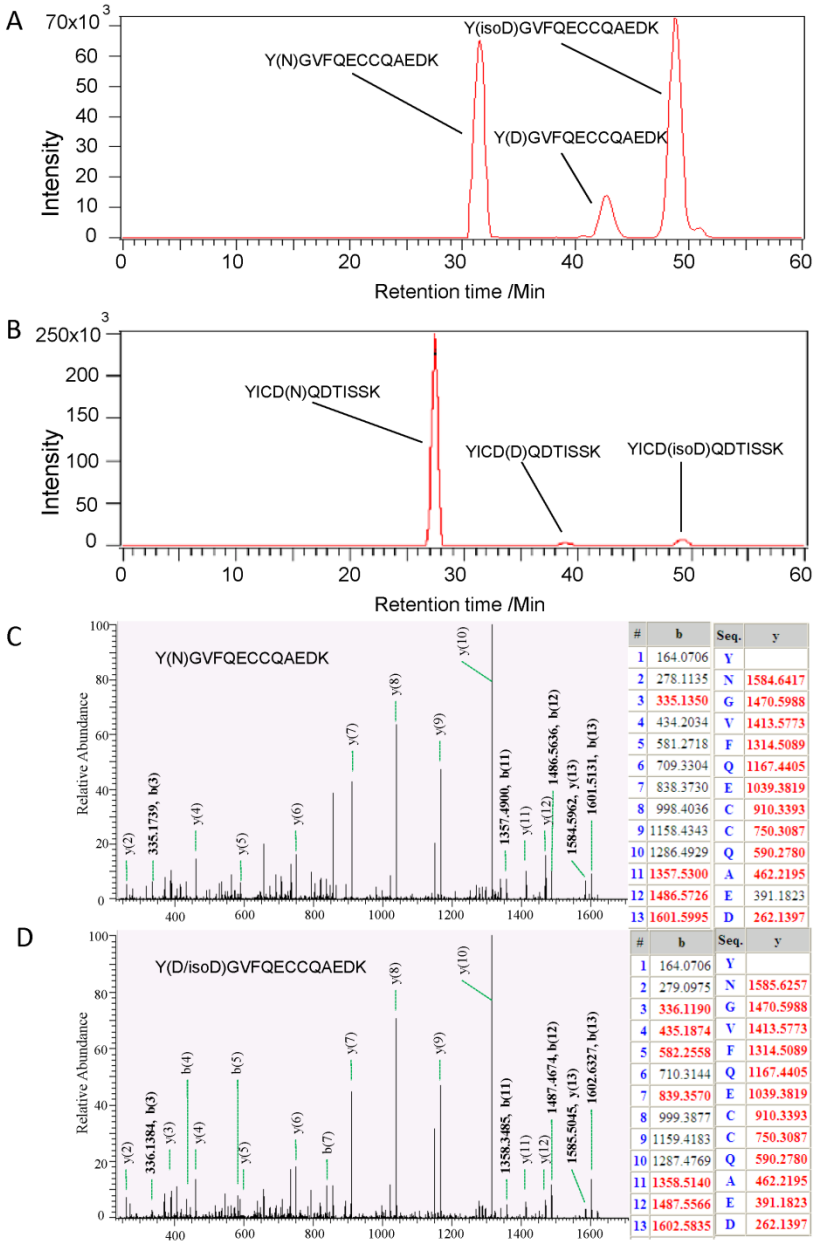

#	b	Seq.	y
1	164.0706	Y	
2	278.1135	N	1584.6417
3	335.1350	G	1470.5988
4	434.2034	V	1413.5773
5	581.2718	F	1314.5089
6	709.3304	Q	1167.4405
7	838.3730	E	1039.3819
8	998.4036	C	910.3393
9	1158.4343	C	750.3087
10	1286.4929	Q	590.2780
11	1357.5300	A	462.2195
12	1486.5726	E	391.1823
13	1601.5995	D	262.1397

#	b	Seq.	y
1	164.0706	Y	
2	279.0975	N	1585.6257
3	336.1190	G	1470.5988
4	435.1874	V	1413.5773
5	582.2558	F	1314.5089
6	710.3144	Q	1167.4405
7	839.3570	E	1039.3819
8	999.3877	C	910.3393
9	1159.4183	C	750.3087
10	1287.4769	Q	590.2780
11	1358.5140	A	462.2195
12	1487.5566	E	391.1823
13	1602.5835	D	262.1397

Figure 4.5 Separation and identification of two groups of deamidation products containing an asparaginyl, aspartyl or isoaspartyl residue at the same position from the tryptic digest of BSA and chicken ovalbumin. (A) XICs of Y(D/isoD)GVFQECCQAEDK and their undeamidated counterpart from ERLIC-LC-MS/MS; (B) XICs of YIC(D/isoD)QDTISSK and their undeamidated counterpart from ERLIC-LC-MS/MS; (C) Tandem mass spectrum for identification of Y(N)GVFQECCQAEDK; (D) Tandem mass spectrum for identification of Y(D/isoD)GVFQECCQAEDK. The unmodifed and deamidated peptides were differentiated based on the difference in MS/MS spectra, while the two isomeric deamidated peptides were differentiated based on their elution times.

when ERLIC are to be used together with ETD or ECD MS/MS in the future. Not all deamidated peptides are identified with all of the three deamidation-related products possibly because of the following causes: 1, Deamidation occurs entirely on the deamidation site either *in vivo* or *in vitro* during the course of sample preparation, and isomerization of deamidation products may also occur; 2, The existing ERLIC-MS/MS setup is not sensitive enough to detect low-abundance deamidation products and needs to be further optimized. Figure 4.6A shows that a potential Asp product is missed from MS/MS because its intensity is lower than 500 counts, i.e. the threshold for MS/MS; 3, Since mass spectrometry generally selects top N high-intensity peptides from a MS1 scan for MS/MS fragmentation in shotgun proteomics, some deamidated peptides may be missed from MS/MS fragmentation if they are co-eluted with some high-abundance peptides. As shown in Figure 4.6B, the XICs of deamidated peptides illustrates that a potential Asp product is missing from MS/MS possibly because it is co-eluted with high-intensity peptides. Manual check of the MS1 full scan at the time point confirms our deduction (Figure 4.6C and 4.6D). For peptides with multiple deamidation sites, the deamidation products are much more complex than those with a single deamidation site since the residue on each deamidation site could possibly be an asparaginyl, n-aspartyl or isoaspartyl residue. Thus, it is difficult to use the proposed strategy to accurately identify all of these products. However, as shown in Supplemental Table 2 in Ref. (128), the retention time of the peptides with two deamidated residues is longer than those with only one deadmidated residue, such as the peptides of SGTTWIQEIVNMIEQNGDVEK and GILGYTENQVVSCNFNSNSHSSTFDAGAGIALDDNFVK. Therefore, this RP-ERLIC-MS/MS strategy may be used in characterizing peptides with multiple deamidation sites when coupled with ECD in the future. The number of identified proteins and unique peptides from RP-ERLIC-MS/MS in this study was significantly less than those identified from the commonly used MDLC of ERLIC-RP and SCX-RP,(129) and the number of identified unique Asn-deamidated peptides was also much less than that from ERLIC-RP, indicating that the RP-ERLIC-MS/MS system still needs to be optimized in future. However, it has been proven to be able to separate and characterize the triads of deamidation-related peptides.

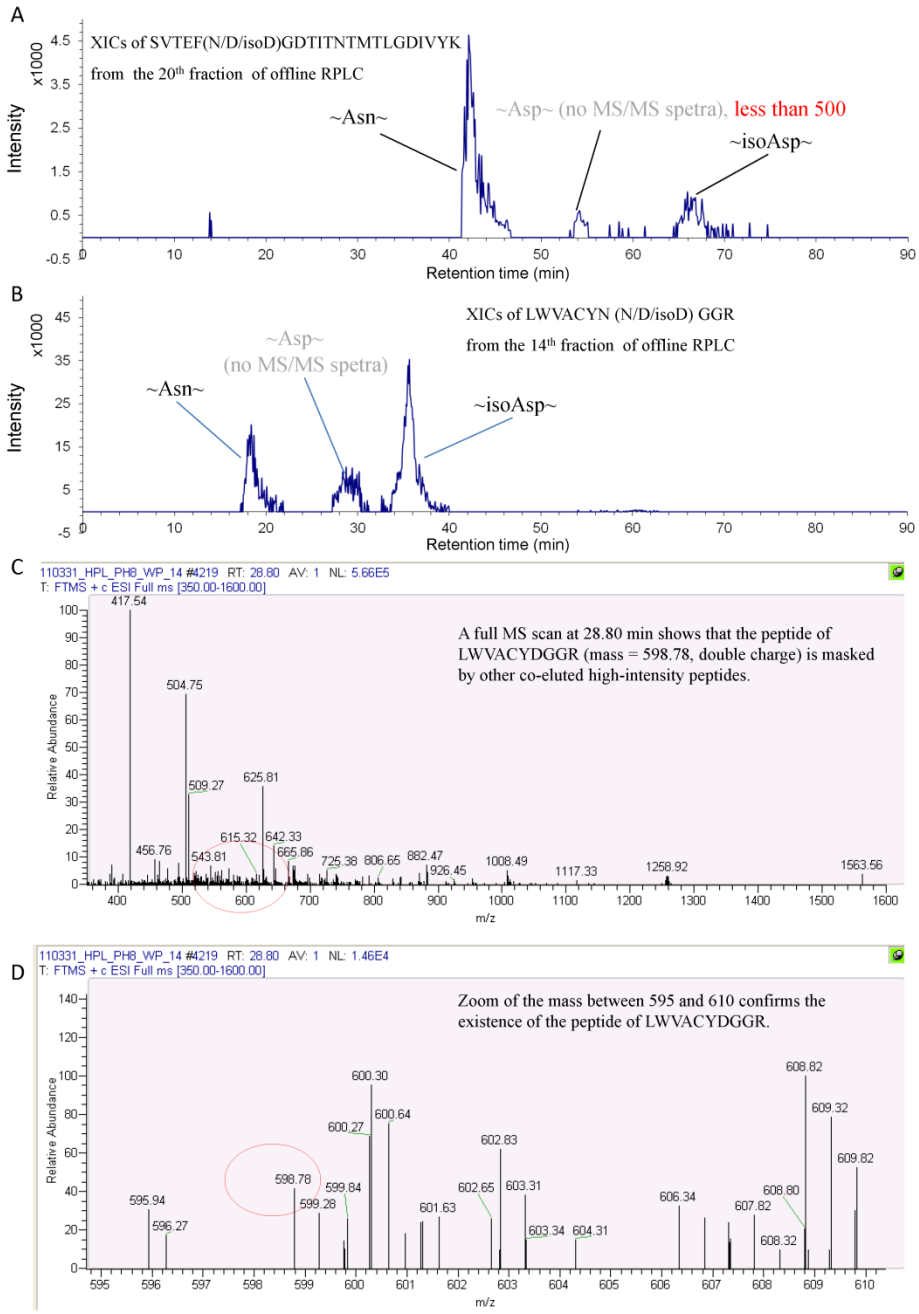

Figure 4.6 XICs of the triads of deamidation-related peptides showing the reason why only one or two of them are identified. (A) XICs of SVTEF(N/D/isoD)GDTITNTMTLGDIVYK; (B) XICs of LWVACYN (N/D/isoD) GGR; (C) A full MS scan at 28.80 min shows that the peptide of LWVACYDGGR (mass = 598.78, double charge) is masked by other co-eluting high-abundance peptides; (D) Zoom of the mass between 595 and 610 confirms the existence of the peptide LWVACYDGGR. The gray font in (A) and (B) signifies that the peptides are not identified by MS/MS.

4.4.5 Considerations for Optimizing RP-ERLIC-MS/MS in the Future

Based on our results, ERLIC-MS/MS has been proven to work effectively on simple peptide mixtures, e.g. the tryptic peptides from BSA and chicken ovalbumin, but it is not sensitive enough to detect low-abundance deamidated peptides from complex tryptic digests. Since it is the first time that we directly coupled ERLIC to MS/MS, it may be further optimized in the future in order to get better sensitivity. In this study, we tested 85% ACN/0.1% NH_4OH, 85% ACN/1 mM NH_4HCO_3 and 90% ACN/0.1% FA as the dissolving and desalting buffer for peptides. The first one got the best result since the retention of peptides on the ERLIC trap column increases as the pH of the mobile phase increases due to the decrease of electrostatic repulsion. Other reasonable solutions may also be tested to optimize peptide trapping efficiency in the future. In this study, a PolyWAX LP guard column was used as the trap column for ERLIC-MS/MS, but a PolyWAX LP trap column designed specifically for peptide trapping may get better performance. Alternatively, peptides may be directly injected into ERLIC columns without using any trap columns. Additionally, different gradients and other mobile phases may be tested in ERLIC-MS/MS, and similar WAX columns from other companies may also be tested for ERLIC-MS/MS. It is highly possible that ERLIC-MS/MS may become sensitive enough to characterize complex samples as the last dimension of MDLC with the above-mentioned optimization.

4.4.6 Calculation of the Intensity Ratio of the isomeric isoAsp and n-Asp peptides

If a deamidated peptide is identified with ERLIC-MS/MS for over three times, the average intensity of the top 3 is used to calculate its relative abundance. Otherwise, the average intensity of all identified ones is used. The aim is to get the approximately highest intensity of the peptides. As shown in Supplemental Table 3 in Ref. (128), the ratio of the isoAsp versus Asp peptides is close to 3:1 in BSA and chicken ovalbumin, i.e. 2.09 to 5.90. It indicates that it may be mainly originated from nonenzymatic deamidation without any repair. However, for rat liver tissue, the ratio of the isoAsp versus Asp peptides is 0.23 to 69.49, indicating that some *in vivo* isoAsp repair/generation

mechanism may work. It proves that the ERLIC-MS/MS strategy can be effectively used in calculating the ratio of isoAsp versus Asp peptides from samples with high complexity.

4.5 Conclusion

The widely used RPLC-MS/MS cannot be effectively used in the separation and characterization of the structural isomers of deamidated peptides containing n-Asp or isoAsp due to their identical polarities, but the newly introduced ERLIC is proven to separate them well based on their different *p*I. Therefore, we here proposed and validated a novel RP-ERLIC-MS/MS strategy for proteome-scale study of protein deamidation. Its sensitivity still needs to be further improved before it can be used in characterizing low-abundance deamidated peptides from complex samples. For more reliable identification of isoAsp deamidation products, RP-ERLIC may be coupled to ECD or ETD in the future. This sequence may also be used for the characterization of whole proteome because of its remarkable resolution and compatibility with mass spectrometry.

Chapter 5

Application of the Developed Technologies into the Study of Protein Deamidation in Human Atherosclerotic Plaques for Predicting Secondary Cerebrovascular Events

Chapter 5

5.1 Abstract

Human carotid atherosclerotic plaques from old patients are good samples to test the applicability of our newly developed proteomic methods since protein deamidation accumulates progressively with ages. The deep proteomic profiling of atherosclerotic plaques is helpful to understand its mechanism, and the identification of prognostic biomarkers may save patients from secondary cerebrovascular events. In this chapter, our newly developed proteomics methods as detailed in previous chapters were employed to ensure the accurate and reliable characterization of endogenous protein deamidation. With the latest proteomics technologies, 3846 proteins were identified with at least 2 unique peptides from atherosclerotic plaques, and many low-abundance proteins with important functions in atherosclerosis were identified confidently using mass spectrometry for the first time. It represents a leap forward in understanding of plaque composition, development and progression. Label-free quantification on pooled plaques from patients with/without secondary cerebrovascular events identified many up-regulated proteins and deamidated peptides that were either known biomarkers for unstable plaques or closely related to the initiation and progression of atherosclerosis as biomarker candidates. These candidates were then evaluated in 38 individual samples using PRM for predicting secondary cerebrovascular events after the applicability of PRM for validation of deamidated peptides was proven using simple tryptic digests. None of them reached the criterion as a clinically usable biomarker possibly due to the small sample size and high individual variation. However, the applicability of our newly developed technologies for studying deamidation has been sufficiently proven. It opens a door for scientists who are interested in understanding the role of protein deamidation in aging and many diseases.

5.2 Introduction

Atherosclerotic cardiovascular disease is a major cause of mortality worldwide, accounting for more than 19 million deaths per year.(130) Atherosclerosis is a chronic inflammatory disease resulting in the narrowing of large and medium-sized arteries with

associated plaque deposition on the intimal layer. Atherosclerotic plaque formation begins with sub-endothelial accumulation of lipids, macrophage foam cells and T cells; in the later stages a necrotic core composed of apoptotic and necrotic cells, cell debris and cholesterol crystals forms. Plaque growth results in the narrowing of arterial lumen and ischemia in the surrounding tissue, while plaque rupture can lead to life-threatening myocardial infarction and ischemic stroke due to the blockage of arteries.(131) Atherosclerotic plaques can be separated into two broad categories: stable and unstable, with the latter associated with high risk of ruptures, leading to primary cardiovascular or cerebrovascular events. (132, 133) Carotid endarterectomy (CEA) is a surgical procedure that can be used to reduce the risk of stroke, by correcting stenosis in the common carotid artery or internal carotid artery of patients with primary cerebrovascular events. The incidence of secondary cerebrovascular events in patients who underwent CEA is 8.2%, (134, 135) and predictive biomarkers may be used to save them from the secondary events. By now, proteomics methods have been the most widely used means to study the composition of plaques for better understanding the mechanism of atherosclerosis and seek biomarkers due to its high sensitivity and throughput. (136, 137)

Defining the proteome of atherosclerotic plaques represents a promising avenue of investigation for understanding the mechanism of atherosclerosis and searching novel therapeutic targets. In fact, proteomics has been used to understand the mechanisms underlying atherosclerosis and to identify biomarkers for many years. Until 2006, 2-DE was the main means to study atherosclerosis in animal models or human arteries, but generally only a few hundred proteins could be identified.(138, 139) In 2007, Bagnato et al. conducted the first large-scale proteomic analysis of human coronary atherosclerotic tissues and successfully identified 806 proteins.(140) In 2009, De Kleijn and colleagues identified approximately 1200 proteins in human carotid atherosclerotic plaques in a proteomic study using multidimensional LC-MS/MS.(141) However, many low-abundance proteins that are known to be important for the development and progression of plaques, such as VCAM1, ICAM1 and TGF-β, and various cytokines and growth factors, still could not be identified from atherosclerotic plaques using mass

spectrometry-based proteomics methods. It is an urgent need to apply the cutting-edge proteomics technologies to the study of human carotid atherosclerotic plaques.

Protein deamidation is reported to be related to aging and many diseases, (65-67, 96, 97) but its role in atherosclerosis remains unclear and less studied. Since nonenzymatic deamidation accumulates progressively with ages in proteins, (142) atherosclerotic plaques from old patients are good samples to test the applicability of our newly developed proteomic methods. Patients were aged between 56 and 83 in this study. In the previous chapters of this thesis, we developed novel data analysis strategy and sample preparation protocols to minimize false positive identifications of deamidated peptides and artificial deamidation so that the accurate and reliable characterization of endogenous protein deamidation becomes feasible. (84) The quantification of protein deamidation between patients with and without secondary cerebrovascular events may identify up-regulated deamidated peptides as biomarker candidates.

To test the applicability of deamidated peptides as biomarkers, it is necessary to validate their levels in each individual sample. The traditional antibody based assays, such as Western Blot and ELISA, cannot be used in the discovery and validation of novel PTMs due to the lack of commercially available antibodies with high specificity. Generally, MRM can be used in the validation of novel PTMs in individual samples. (92, 143) However, it cannot be used in the validation of deamidated peptides in individual samples. With the commonly used full width at half-maximum (FWHM) of 0.7 Th in Q1 for MRM, both deamidated peptides and the ^{13}C peak of the corresponding undeamidated peptides are isolated for fragmentation due to the slight mass difference of 19.34 mDa between them. (84) When the FWHM of 0.7 Th is also used to monitor the MS2 fragments of deamidated peptides in Q3, both the MS2 fragments of deamidated peptides and that of the ^{13}C peaks of their corresponding undeamidated peptides are isolated due to the slight mass difference of 19.34 mDa between them. Therefore, MRM cannot be effectively used to differentiate deamidated peptides from their corresponding undeamidated peptides due to its low resolution, i.e. <2000. Generally, the mass accuracy

of less than 5 ppm which is achievable at the resolution of at least 70,000 is necessary to differentiate the mass difference of 19.34 mDa. Therefore, the newly introduced PRM with a resolution of 70,000 to 140,000 on Q Exactive can theoretically be used in the validation of deamidated peptides in individual samples.

In this chapter, the latest proteomics technologies were applied to the study of human carotid atherosclerotic plaques to increase the proteome coverage and confirm the presence of as many as possible low-abundance proteins. Our newly developed proteomics methods were employed to ensure the accurate characterization of endogenous protein deamidation. Label-free quantification on pooled plaques from patients with/without secondary cerebrovascular events identified many up-regulated proteins and deamidated peptides that were either known biomarkers for unstable plaques or closely related to the initiation and progression of atherosclerosis as biomarker candidates. These candidates were then evaluated in each individual sample using PRM for predicting secondary cerebrovascular events after the applicability of PRM for validation of deamidated peptides was proven using simple tryptic digests.

5.3 Materials and Methods

5.3.1 Reagents

Unless indicated, all reagents used in this study were purchased from Sigma-Aldrich, USA. Protease inhibitor (Cat no.: 05 892 791 001) was purchased from Roche, Basel, Switzerland; Unmodified trypsin (T8802) was purchased from Sigma-Aldrich, St. Louis, MO. Sep-Pak C18 cartridges were purchased from Waters, Milford, MA; 2D-Quant Kit was purchased from Thermo Fisher, MA.

5.3.2 Patient information

Atherosclerotic plaques from 38 patients who underwent carotid endarterectomy (surgical unblocking of the carotid artery) in a Dutch hospital (UMC Utrecht) between 2002 and

2006 were used for proteomics analysis in this study.(141) Patients were aged between 56 and 83, with 32 males and 6 females. The study was approved by the Institutional Review Boards of the hospital and written informed consent was obtained from all patients. In the discovery stage study, plaque lysates from patients with and without secondary cerebrovascular events were pooled into two groups, respectively. Secondary outcome means any major cardiovascular event, such as vascular death, nonfatal myocardial infarction, nonfatal stroke, and nonfatal aneurysm rupture. Definitions and assessment procedures of the outcome events were described previously. (144)

5.3.3 Sample Preparation

Each of 38 atherosclerotic plaques was washed 3 times with 1X PBS, weighed, cut into small pieces and put into microcentrifuge tubes. One volume of SSB14B beads (Next Advance, Inc., NY) and three volumes of lysis buffer (8M Urea, 50 mM ammonium acetate, pH 6) with protease inhibitors added were added into the tubes (Note: 100mg=100ul). The homogenization was done at SPEED 10 for 3 min using Bullet Blender®. After the tubes were centrifuged at 2,000 g for 1 min, the homogenization was repeated once. The suspension was centrifuged at 20,000g at 4^{o}C for 20 min. The protein concentration of the supernatant was then determined using 2D-Quant Kit (Thermo Fisher, MA) since protein precipitation at pH 6 during dilution of urea concentration affected BCA quantification. The plaque lysates from 19 test patients who underwent secondary cerebrovascular events and those from 19 control patients without secondary cerebrovascular events were pooled, respectively. About 3 mg tissue lysate from either individual plaques or pooled sample was reduced with 10 mM DTT at 37^{o}C for 2 h and alkylated with 50 mM iodoacetamide at room temperature for 45 min in the dark. After the concentration of urea was diluted to 1M with 50mM ammonium acetate (pH 6), trypsin (T8802, Sigma) was added at a weight ratio of 1:40. It was then incubated at 37^{o}C for 15 h. The obtained tryptic peptides were desalted using a Sep-Pak® C18 cartridge (Waters, Milford, MA) and dried in a SpeedVac® (Thermo Electron, Waltham, MA).

5.3.4 ERLIC Fractionation of Label-free Peptides from Pooled Plaque Lysates

Peptides from 1 mg of pooled plaque lysates were fractionated using a PolyWAX LP weak anion-exchange column (4.6 × 200 mm, 5 µm, 300 Å, PolyLC) on a Shimadzu Prominence UFLC system. To ensure the solubility of peptides, 200 µl of mobile phase A (85% ACN/0.1% FA) was used to dissolve the peptides. Mobile phase A and mobile phase B (10% ACN/0.4% FA) were used to establish a 40 min gradient of 0% – 8% buffer B for 10 min, 8% – 32% buffer B for 20 min, 32% – 100% buffer B for 2 min and 100% buffer B for 8 min at a flow rate of 1 mL/min with 30 fractions collected. The collected fractions were then dried in vacuum, pooled into 20 fractions and redissolved in 3% ACN/0.1% FA for LC-MS/MS analysis. Fractions 3-17 were not combined, while fractions 1-2, 18-19, 20-22, 23-26 and 27-30 were combined, respectively.

5.3.5 LC-MS/MS for Shotgun Proteomics

Peptides from 20 pooled ERLIC fractions were separated and analyzed on a Dionex Ultimate 3000 RSLCnano system coupled to a Q Exactive (Thermo Fisher, MA) in triplicate. Peptides were separated in a capillary column (75 µm x 10 cm) packed with C18 AQ (5 µm, 300Å; Bruker-Michrom, Auburn, CA, USA) at room temperature. The flow rate was at 300 nl/min. Mobile phase A (0.1% formic acid in 5% ACN) and mobile phase B (0.1% formic acid in 90% ACN) were used to establish a 70 min gradient comprised of 5 min of 5% B, 57 min of 5-40% B, 1 min of 40-80% B and 2 min of 80% B followed by re-equilibration at 5% B for 5 min. Peptides were then analyzed on Q Exactive with a nanospray source (Thermo Fisher, MA) at an electrospray potential of 1.5 kV. A full MS scan (350-1600 m/z range) was acquired at a resolution of 70,000 at m/z 200 and a maximum ion accumulation time of 100 msec. Dynamic exclusion was set as 20 s. Resolution for HCD spectra was set to 17,500 at m/z 200. The AGC setting of full MS scan and MS2 were set as 3E6 and 5E4, respectively. The 10 most intense ions above a 250 counts threshold were selected for fragmentation in HCD with a maximum ion accumulation time of 100 msec. Isolation width of 2 was used for MS2. Single and unassigned charged ions were excluded from MS/MS. For HCD, normalized collision energy was set to 25%. The underfill ratio was defined as 0.1%.

5.3.6 LC-MS/MS for Parallel Reaction Monitoring (PRM)

Peptides from each individual plaque samples were separated and analyzed on a Dionex Ultimate 3000 RSLCnano system coupled to a Q Exactive (Thermo Fisher, MA) in triplicate. Peptides were separated in a capillary column (75 µm x 10 cm) packed with C18 AQ (5 µm, 300Å; Bruker-Michrom, Auburn, CA) at room temperature. The flow rate was at 300 nl/min. Mobile phase A (0.1% FA in 5% ACN) and mobile phase B (0.1% FA in 90% ACN) were used to establish a 60 min gradient comprised of 1 min of 5-9% B, 46 min of 9-40% B, 5 min of 40-60% B, 0.1 min of 60-80% B and 2.9 min of 80% B followed by re-equilibration at 5% B for 5 min. Peptides were then analyzed on Q Exactive with a nanospray source (Thermo Fisher, MA) at an electrospray potential of 1.5 kV. PRM was done with an isolation width of 2 Th, 70,000 resolution at m/z 200, AGC target 1E6 and 250 ms maximum injection time as triggered by a scheduled inclusion list. For HCD, normalized collision energy was set to 25%. The fixed first mass is set to m/z 100.

5.3.7 Analysis of Data from Shotgun Proteomics

The raw data for pooled plaques were processed and searched with MaxQuant 1.3.0.5 with MS tolerance of 6 ppm and MS/MS tolerance of 0.02 Da. The UniProt human protein database (release 2012_05, 87187 sequences) and database for proteomics contaminants from MaxQuant were used for database searches. Reversed database searches were used to evaluate FDR of peptide and protein identifications. Two missed cleavage sites of trypsin were allowed. Carbamidomethylation (C) was set as a fixed modification. Oxidation (M), Acetyl (Protein N-term) and deamidation (NQ) were set as variable modifications. The FDR of both peptide identification and protein identification is set to be 1%. (77, 78) The option of “Second peptides” was enabled. The function of “Label-free quantification” was enabled in MaxQuant 1.3.0.5. Ingenuity Pathway Analysis (IPA, Ingenuity® Systems, www.ingenuity.com) was used to reveal canonical pathways associated with all identified proteins.

For label-free quantification of protein groups, only protein groups identified with at least 2 unique peptides are considered, and the cutoff is >1.5 times or <0.67 time with the relative standard deviation of the protein LFQ intensity values from both three technical replicates of test group and that of control group less than 20%. Alternatively, protein groups detected in all replicates of test group but not in all replicates of control group are also regarded as up-regulated ones. For label-free quantification of deamidated peptides, the cutoff is >1.6 times or <0.625 time with the relative standard deviation of the LFQ intensity values of deamidated peptides from both three technical replicates of test group and that of control group less than 30%. Alternatively, deamidated peptides detected in all replicates of test group but not in all replicates of control group are also regarded as up-regulated ones. Gene ontology analysis of up-regulated proteins in the pooled test group with secondary cerebrovascular events was done using the PANTHER (Protein ANalysis THrough Evolutionary Relationships) Classification System. (145, 146)

5.3.8 Analysis of Data from Parallel reaction monitoring (PRM)

Analysis of PRM data was done using Skyline (version 2.1.0.4936, University of Washington), (147) Xcalibur (version 2.2; Thermo Fisher Scientific) or Pinpoint (version 1.3; Thermo Fisher Scientific). For Pinpoint, ion chromatograms were extracted at a mass tolerance of 10 ppm; possible alignment error was set to 5 min; peak width was set to 1 min; complete peak area on smoothed data was used for calculation. Normalization of PRM data for individual plaques is based on the total area of their LC-MS/MS base peaks.

5.4 Results and Discussion

5.4.1 The Strategy for Proteomic Study of Protein Deamidation in Human Carotid Atherosclerotic Plaques for Predicting Secondary Cerebrovascular Events

As shown in Figure 5.1, this study is divided into two stages. In the stage I (discovery stage), 38 human carotid atherosclerotic plaques from patients with and without secondary cerebrovascular events were pooled into two groups, respectively. Each group

of pooled samples are digested into tryptic peptides, fractionated into multiple fractions using ERLIC, and subjected to 3 technical replicates of LC-MS/MS on a Q Exactive. Identification and label-free quantification of proteins and deamidated peptides are done using MaxQuant 1.3.0.5. Using the cutoff described in section 5.3.7, we selected up-regulated proteins and deamidated peptides which may be important to the development and progression of atherosclerotic plaques for further validation in both the pooled samples and each individual sample in the stage II (validation stage). They were also evaluated in predicting secondary cerebrovascular events.

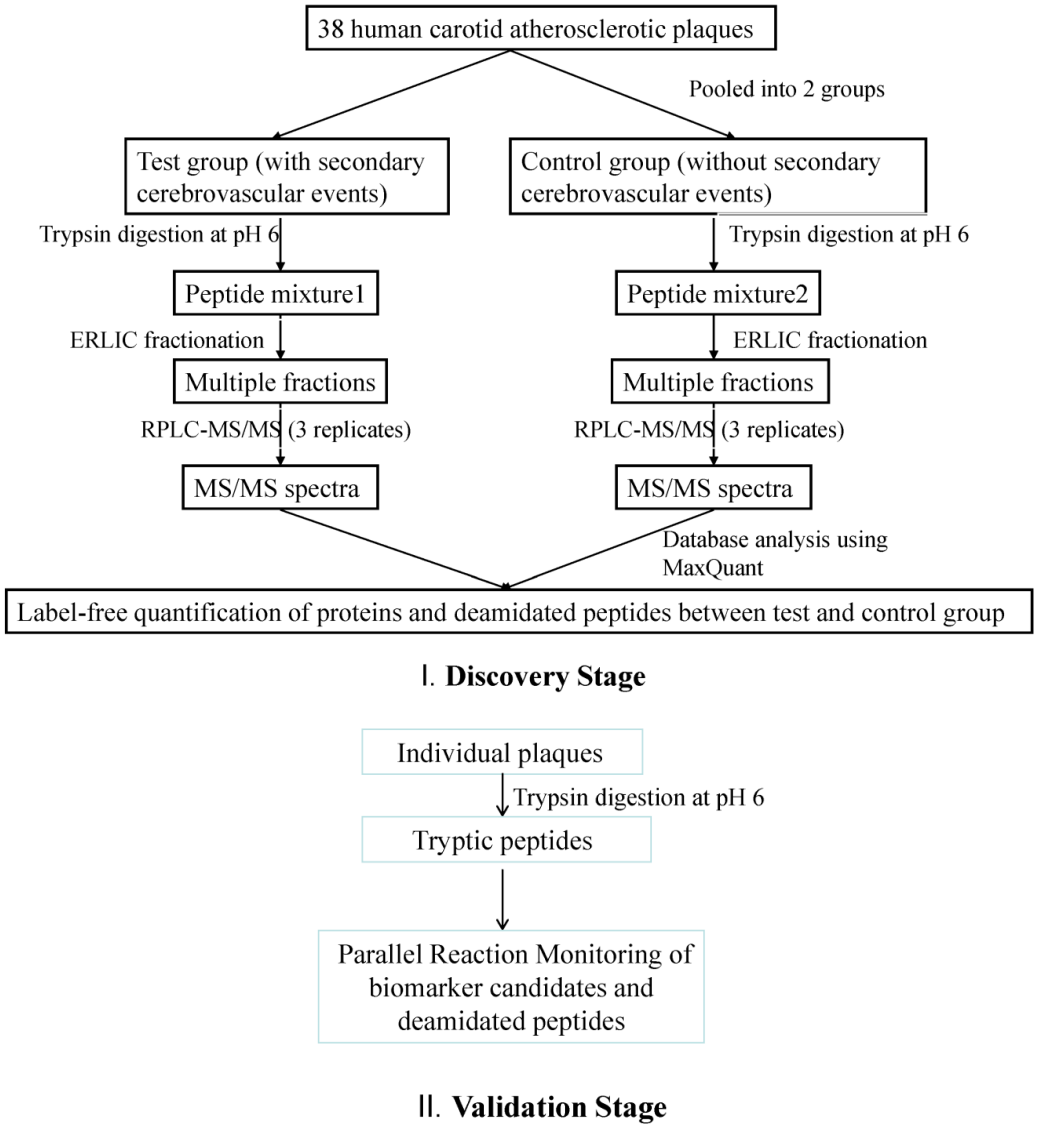

Figure 5.1 The strategy for proteomic study of protein deamidation in human carotid atherosclerotic plaques for predicting secondary cerebrovascular events. It includes two stages, i.e. I, Discovery stage on pooled samples and II, Validation stage on individual samples.

5.4.2 Protein Identification from Human Carotid Atherosclerotic Plaques

A total of 3846 protein groups were identified with at least 2 unique peptides (<1% FDR) from the two pooled samples of 38 human carotid atherosclerotic plaques using an offline multidimensional LC-MS/MS approach. (148) This figure is 4.77 and 3.21 times of that identified in two recent large-scale proteomic studies on human plaques (Figure 5.2A). (140, 141) Such a tremendous increase in proteome coverage of human plaques will be very useful to those researchers who aim to understand the composition and underlying mechanisms of atherosclerotic plaques. Importantly the proteins were identified with very high confidence. As shown in Figure 5.2B, a total of 4702 protein groups were identified at 1% FDR with at least 1 unique peptide, of which 1734 (36.9%) were identified with over 5 unique peptides, and a further 1323 (28.1%) were identified with 3-5 unique peptides. The identified proteins are listed in Supplemental Table 1 in Ref. (148). The identification of multiple unique peptides for each protein greatly improves the confidence of protein identification, and

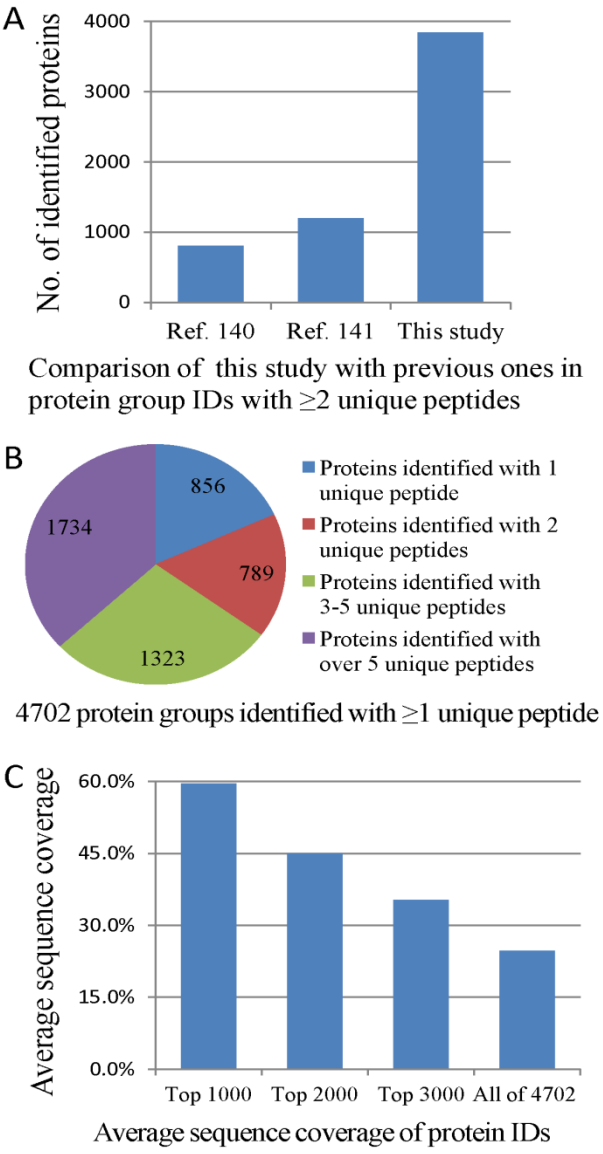

Figure 5.2 Proteome coverage of human carotid atherosclerotic plaques. A) Comparison of protein group identifications with previous large-scale proteomics studies on human plaques; B) Number of protein identifications with different numbers of unique peptides; C) Average sequence coverage of protein identification.

it will also improve the accuracy of relative or absolute quantification of proteins where necessary. Furthermore, Figure 5.2C shows that this study provided high sequence coverage for protein identification. For example, the average sequence coverage of the top 1000 proteins was 59.5%, which is comparable to that of the commonly-used proteomics standard for instrumental evaluation, bovine serum albumin (BSA). The theoretical maximum sequence coverage of 60% is well-accepted for many proteins as a consequence of the trypsin digestion step, which may produce peptides too long or too short for LC-MS/MS, and/or peptides with unknown modifications. Overall, the average sequence coverage for 4702 identified protein groups was 24.7%. Both ERLIC fractionation and the use of an up-to-date Q Exactive contributed to the significant increase in proteome coverage of atherosclerotic plaques achieved in this study. ERLIC is reported to be a promising alternative to SCX because ERLIC separates peptides based on both *p*I and GRAVY values through the simultaneous effect of electrostatic repulsion and hydrophilic interaction. (105)

5.4.3 Pathway Analysis of the Identified Proteins from Human Carotid Atherosclerotic Plaques

Figure 5.3 shows 24 IPA canonical pathways associated with the proteins we identified in human carotid atherosclerotic plaques, which were reported to be closely related to the development and progression of atherosclerosis.(149) Between 11 and 127 proteins were allocated within each pathway, which accounts for 24% to 57% of all proteins in the pathways. For example, 59 protein groups were identified within the atherosclerosis signaling pathway, which covers 42% of the proteins in the pathway. As shown in Supplemental Figure 1 in Ref. (148), nearly half of the gene products were identified in each step of the atherosclerosis signaling pathway, including ICAM1, VCAM1 and P-selectin in the monocyte endothelial cell adhesion, PDGF and TGF-β during the proliferation and intimal migration of smooth muscle cells, and MMP1 and MMP9 during the destabilization of plaques. For the pathway of inhibition of matrix metalloproteinases, 18 protein groups (45%) were identified (Figure 5.4), such as MMPs, TIMPs and ADAMs. MMPs and TIMPs modulate both cell-cell and cell-ECM

(extracellular matrix) interactions via proteolytic degradation or activation of cell surface and ECM proteins, which play an important role during the development of high-risk unstable plaques.(150) These proteins could potentially be tested for use as biomarkers for differentiating stable and unstable plaques in future. The list of all identified IPA canonical pathways can be found in Supplemental Table 2 in Ref. (148). The identification of these atherosclerosis-related pathways from human plaques gives a detailed picture of the plaque protein interaction network, facilitating a more comprehensive understanding of the mechanisms of atherosclerosis.

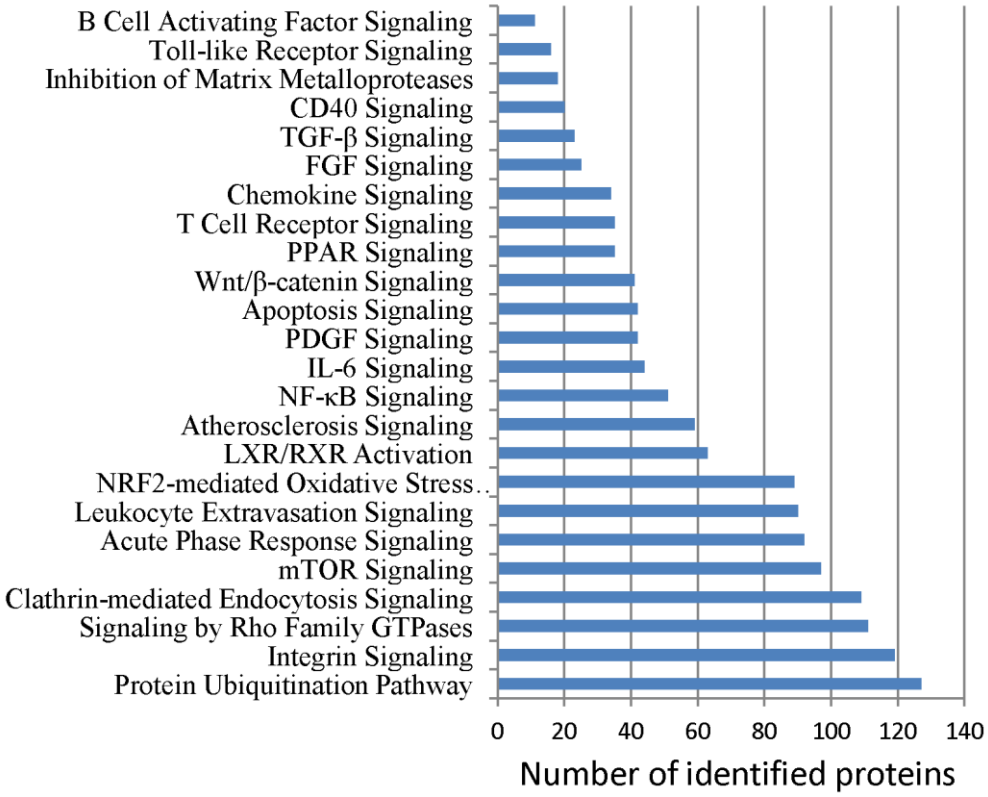

Figure 5.3 Number of identified proteins in 24 canonical pathways related to the development and progression of atherosclerosis according to IPA classification. 24% to 57% of the proteins in the listed pathways were identified in this study.

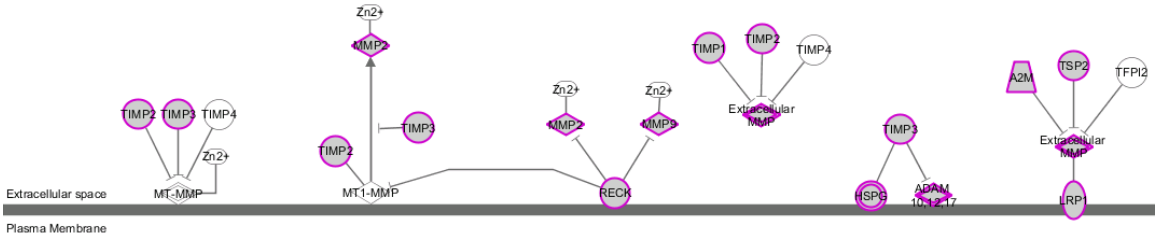

Figure 5.4 The proteins identified in the pathway of inhibition of matrix metalloproteinases

5.4.4 Identification of Potential Biomarkers and Low-abundance Proteins with Important Functions from Human Carotid Atherosclerotic Plaques

Table 5.1 lists 3 potential biomarkers and 25 low-abundance proteins identified in this study that are known to be crucial in the development and progression of atherosclerotic plaques, including adhesion molecules, growth factors, interleukins, inflammatory markers, MMPs and their inhibitors.(131, 151) The spectra for proteins identified with only 1 unique peptide are shown in Supplemental Figure 3 in Ref. (148). Most of these proteins could not be identified from human atherosclerotic plaques using mass spectrometry-based proteomics methods in previous studies.(139, 140) The identification of these proteins using LC-MS/MS facilitates the development of multiple reaction monitoring (MRM) assays for them and enables the relative or absolute quantification of them in stable and unstable plaques,(152) which in turn may lead to the discovery of novel biomarkers for diagnosing patients with high-risk unstable plaques in future. In addition to the list of low-abundance proteins with known functions, we speculate that the tremendous increase in proteome coverage may also lead to the identification of many low-abundance proteins with unknown functions, which will further contribute to advancing understanding of the mechanisms of atherosclerosis and biomarker discovery in future.

Table 5.1 Summary of the identified potential biomarkers and low-abundance proteins involved in atherosclerosis from human atherosclerotic plaques

Classification	Accession number	Protein Name	Gene Symbol	No. of identified unique peptides
Potential biomarkers	P05164	Myeloperoxidase	MPO	13
	P02679	Fibrinogen gamma chain	FGG	4
	P02675	Fibrinogen beta chain	FGB	59

Adhesion molecules	P19320	Vascular cell adhesion protein 1	VCAM1	10
	P05362	Intercellular adhesion molecule 1	ICAM1	8
Growth factors	P01137	Transforming growth factor beta-1	TGFB1	8
	P61812	Transforming growth factor beta-2	TGFB2	1
	Q5SZ07	Hepatoma-derived growth factor	HDGF	12
	P29279	Connective tissue growth factor	CTGF	12
	P05230	Fibroblast growth factor 1	FGF1	4
	P14210	Hepatocyte growth factor	HGF	10
	C9JAF2	Insulin-like growth factor II	IGF2	3
	Q9NRA1	Platelet-derived growth factor C	PDGFC	1
Interleukins and inflammatory markers	Q14005	Interleukin-16	IL16	4
	Q96PD4	Interleukin-17F	IL17F	1
	Q14116	Interleukin-18	IL18	7
	Q6ZMJ4	Interleukin-34	IL34	3
	P16109	P-selectin	SELP	3
MMPs and their inhibitors	P03956	Interstitial collagenase	MMP1	2
	P08253	72 kDa type IV collagenase	MMP2	32
	P09237	Matrilysin	MMP7	5
	P14780	Matrix metalloproteinase-9	MMP9	23
	P09238	Stromelysin-2	MMP10	1
	P39900	Macrophage metalloelastase	MMP12	17
	Q99542	Matrix metalloproteinase-19	MMP19	8
	P01033	Metalloproteinase inhibitor 1	TIMP1	10
	P16035	Metalloproteinase inhibitor 2	TIMP2	14
	P35625	Metalloproteinase inhibitor 3	TIMP3	10

5.4.5 Label-free Quantification of Protein Groups and Deamidated Peptides from Pooled Human Carotid Atherosclerotic Plaques between Patients with and without Secondary Cerebrovascular Events

In order to compare the identification of protein groups and deamidated peptides between the pooled test group and control group, the MaxQuant database search results from each technical replicate are averaged and shown in Figure 5.5. Only protein groups identified with at least 2 unique peptides are considered. Slightly less protein groups and Q-

deamidated peptides are identified from the test group than that from the control group, but slightly more Asn-deamidated peptides are identified from the test group. Using the strict cutoff described in section 5.3.7, we identified 91 up-regulated protein groups and 110 down-regulated protein groups in the pooled samples of atherosclerotic plaques from patients with secondary cerebrovascular events compared with that from patients without secondary events.

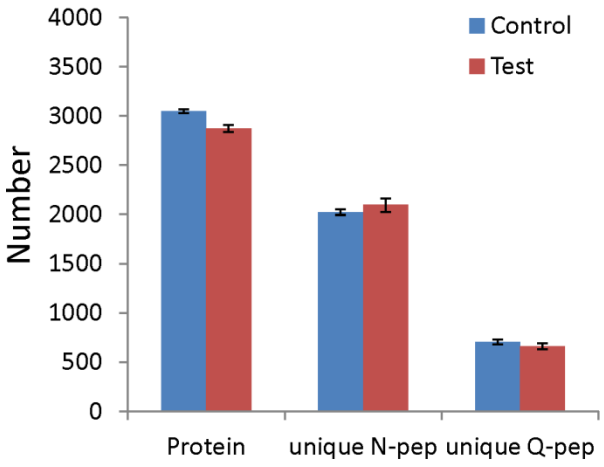

Figure 5.5 Comparison of the identification of protein groups and deamidated peptides between test and control group.

In addition, we identified 167 up-regulated unique deamidated peptides and 91 down-regulated unique deamidated peptides from the pooled test group. The identification of deamidated peptides is highly confident in this study since artificial deamidation is minimized by using our improved sample preparation protocol, and false positive identification of deamidated peptides is also minimized by using the spectrum extraction tool with the function of deisotoping and deconvolution of MS2 fragments embedded in MaxQuant 1.3.0.5. (77, 78, 153) The primary reason for the false positive identification of deamidated peptides from database searches is that the ^{13}C or $^{13}C_2$ peaks of unmodified peptides are selected as the precursor mass by spectrum extraction software and mismatched as deamidated peptides.(83, 84) In addition, the use of the ^{13}C or $^{13}C_2$ peaks of MS2 fragment ions in database searches also contributes to the false-positive identification of deamidated peptides as they can be mismatched as the monoisotopic peak or ^{13}C peak of the corresponding deamidated peptides due to the slight mass difference of 19.34 mDa between them (Figure 5.6). Therefore, MaxQuant is highly recommended as the spectrum extraction software because it performs the best in extracting correct monoisotopic peaks for peptide precursors. (153) In addition, MaxQuant also de-isotopes MS/MS fragments during spectrum extraction, which reduces

the possibility that the ^{13}C or $^{13}C_2$ peaks of fragment ions are matched during database searches. Alternatively, the MS/MS tolerance of less than 5 ppm may be used during database searches if MS/MS is acquired at a resolution of over 70,000, which reduces the possibility that the ^{13}C peak of the MS2 fragments of unmodified peptides is mismatched as the MS2 fragments of corresponding deamidated peptides. Q Exactive performs better than LTQ-FT Ultra in studying protein deamidation due to its high-resolution MS/MS. However, MaxQuant can only process raw files from mass spectrometers from Thermo Fisher. For raw files from mass spectrometers from other vendors, it is necessary to evaluate which software performs the best in extracting correct monoisotopic peaks for peptide precursors and fragments. Nevertheless, a cutoff of 5 ppm for precursor mass tolerance can be used to remove the false-positive identification of deamidated peptides no matter which software is used for spectrum extraction and database searches. (84)

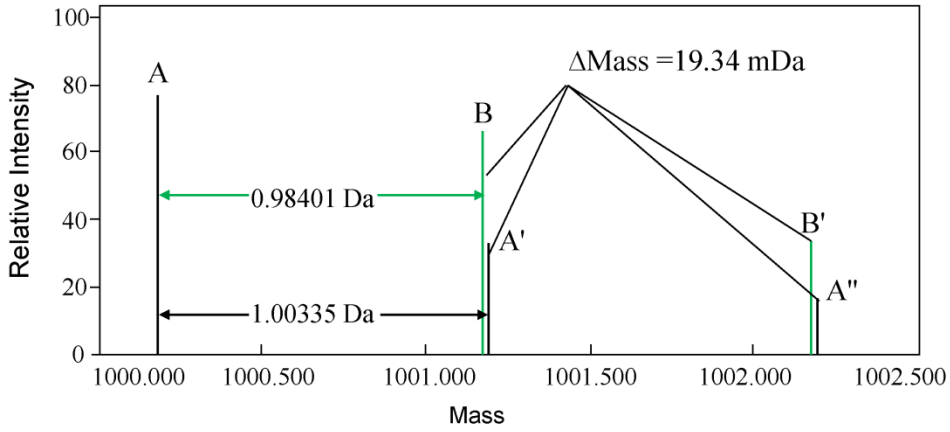

Figure 5.6: Schematic mass spectrum of the MS2 fragments of an unmodified peptide and its corresponding deamidated peptide. Peak A is the first isotopic peak of the MS2 fragment of the unmodified peptide; A' and A'' are its ^{13}C and $^{13}C_2$ peaks, respectively. Peak B is the first isotopic peak of the MS2 fragment of the corresponding deamidated peptide. Peak A' can be mismatched as the MS2 fragment of a deamidated peptide, i.e. Peak B.

5.4.5.1 Gene Ontology Analysis of Up-regulated Proteins in the Pooled Test Group with Secondary Cerebrovascular Events

In this study, we mainly focused on the study of the up-regulated proteins in the pooled test group with secondary cerebrovascular events in comparison to the control group without secondary cerebrovascular events due to the following considerations: 1, the up-

regulated proteins are potentially related to the mechanism of the disease; 2, the detection of up-regulated proteins is usually easier than that of down-regulated proteins if they can potentially be used as biomarkers in the future. The up-regulated proteins in the pooled test group were classified according to their cellular components, molecular function and protein class (Figure 5.7) using the PANTHER. (145, 146) The enriched cellular components, molecular function and protein class are found to play an important role in the initiation and progression of atherosclerosis.

As shown in Figure 5.7A, many of the up-regulated proteins in the pooled test group are from extracellular region or extracellular matrix (ECM) proteins. It was reported that smooth muscle cells release various matrix metalloproteinases (MMPs) that can digest ECM proteins and play an important role in the formation and development of atherosclerotic plaques. An excess of MMPs over TIMPs (tissue inhibitors of metalloproteinases) results in ECM destruction so that the plaque becomes unstable and prone to rupture. (154-156)

As shown in Figure 5.7B, most of the up-regulated proteins in the pooled test group are involved in the molecular function of binding and catalytic activity. Many of the up-regulated enzymes are reported to be important in the development of atherosclerosis, such as VCAM1, CTSF, MMP9 and MPO. The up-regulation of VCAM1 has been found to be associated

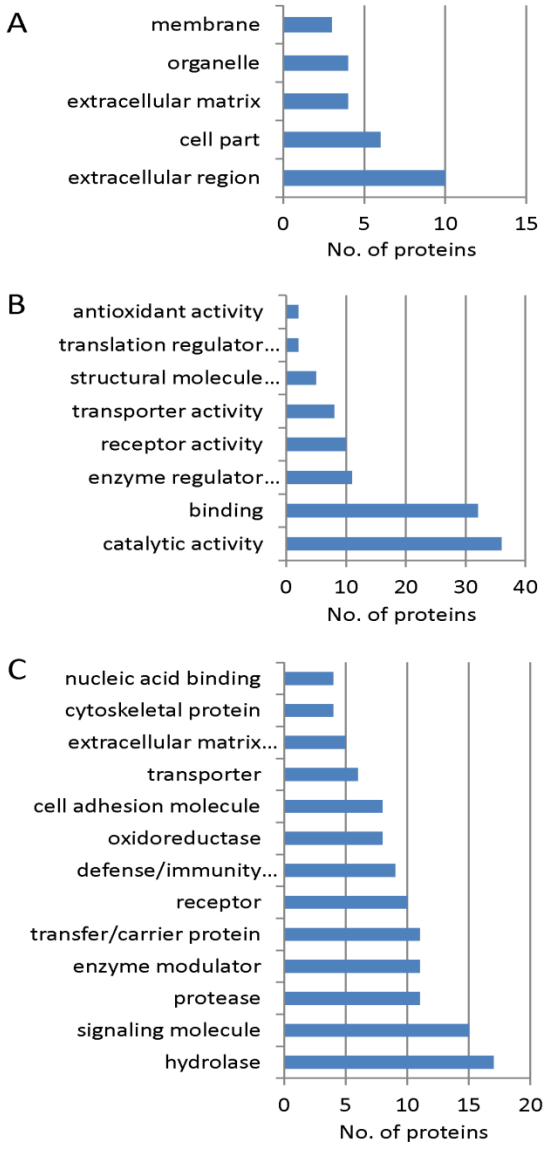

Figure 5.7 Gene ontology annotations of up-regulated proteins in test group according to their cellular components (A), molecular function (B) and protein class (C).

with atherosclerosis at the site of lesion formation. (157, 158) MPO is reported to be a major player in the initiation and progression of atherosclerotic cardiovascular disease (CVD). (159) It is an important enzyme to catalyze the production of oxidative reagents which kill pathogens. However, in chronic inflammation syndromes, MPO is also released into the extracellular space due to neutrophil activation and in turn causes tissue damage and plaque initiation.(160, 161)

Based on the classification of the up-regulated proteins in the pooled test group according to protein class (Figure 5.6C), protease, signaling molecule and hydrolase are three most identified protein class. The disorders of extracellular proteases have been reported to contribute to the growth of arterial plaques. (162, 163) They not only result in the degradation of extracellular matrix, but also have many other biological functions, such as angiogenesis, cytokine modulation, enhancing cell migration, proliferation, and apoptosis.

5.4.5.2 Analysis of Up-regulated Deamidated Peptides in the Pooled Test Group with Secondary Cerebrovascular Events

Among the 167 up-regulated unique deamidated peptides identified in the test group, 23 are from APOB (Apolipoprotein B-100, P04114); 4 are from MFGE8 (Lactadherin, Q08431); 3 are from PGK1 (Phosphoglycerate kinase 1, P00558). It is reported that these proteins are closely related to the initiation and progression of atherosclerosis. For example, APOB is the primary apolipoproteins of chylomicrons and low-density lipoproteins (LDL) that carry cholesterol to tissues. Although its exact role in LDL is not fully understood, high levels of APOB can result in plaque formation and atherosclerosis. It is reported that levels of APOB can be a better indicator of heart disease risk than total cholesterol or LDL. (164, 165) MFGE8 is involved in the phagocytic removal of apoptotic cells in many tissues. Apoptosis of macrophages may be good for plaque stability with apoptotic bodies removed, but apoptosis in the primary atherosclerosis may result in plaque rupture and thrombosis. (166, 167) Therefore, the increase of deamidation in these proteins may not be a random event but possibly have some

important biological functions and can potentially be used as biomarkers for predicting secondary cerebrovascular events. We also checked whether the deamidation of these proteins was consistent with their expression level. APOB increased 1.64 times in the test group, but MFGE8 and PGK1 showed no significant changes.

In addition, one deamidated peptides from TIMP1 and one from TIMP3 were found to be identified only in the test group. TIMPs are specific tissue inhibitors of MMPs, which inhibit the proteolytic activities of MMPs. The increased expression of several MMPs was reported to contribute to the weakening and instability of atherosclerotic plaques. (168, 169) Overexpression of TIMPs can inhibit MMP activity and reduce intimal thickening in different models.(170, 171) For example, the overexpression of TIMP1 led to the reduction of atherosclerotic lesions in mice. (172) Consequently, the reduction of TIMP3 in patients with type 2 diabetes resulted in the accelerated formation of atherosclerotic plaques. (173) TIMP1 and TIMP3 have been tested as the biomarker candidates for differentiating patients with stable or unstable plaques. (174, 175) In this study, TIMP1 increased 1.79 times in the test group compared with the control group, and TIMP3 was only identified in the test group. Since protein deamidation can affect its structure and function, we hypothesize that the increased deamidation of TIMP1 and TIMP3 may result in the function loss of them, thus decreasing the inhibition of MMPs and increasing the instability of plaques. Therefore, both the expression level and the deamidation of TIMP1 and TIMP3 were to be further validated as biomarker candidates for predicting secondary cerebrovascular events.

5.4.6 Application of Parallel Reaction Monitoring (PRM) to the Validation of the Up-regulated Proteins and Up-regulated Deamidated Peptides in Individual Plaques as Biomarker Candidates

As described in the section of 5.2, MRM cannot be used in the validation of deamidated peptides in individual samples since it cannot differentiate the MS2 fragments of

deamidated peptides and that of the ^{13}C peaks of their corresponding undeamidated peptides due to its low resolution, i.e. <2000. However, the newly introduced PRM can theoretically differentiate them depending on its high resolution, i.e. 70,000 to 140,000 on Q Exactive. Here, we first tested the applicability of PRM in validating deamidated peptides using simple tryptic digests, and then applied it to the validation of the up-regulated proteins and deamidated peptides in each individual plaque.

5.4.6.1 Application of PRM to the Validation of the Deamidated Peptides in Simple Tryptic Digests

We systematically optimized the parameters of PRM before applying it to the validation of deamidated peptides in simple tryptic digests of BSA and ovalbumin. As shown in Figure 5.8A, the use of different AGC targets has neglectable effect on the intensity of PRM transitions of the peptide of ELINSWVESQTNGIIR. In contrast, both Normalized Collisional Energy (NCE) and PRM isolation width have huge effect on peptide PRM transitions (Figure 5.8B and 5.8C). An increase of NCE to over 30 results in the remarkable decrease of the intensity of PRM transitions, thus decreasing the sensitivity of PRM. The use of the isolation width of 0.4 Th and 0.8 Th did not get any signals for PRM transitions. Increase of the resolution of PRM from 70,000 to 140,000 does not lead to the increase of sensitivity of PRM transitions (Figure 5.8D), but the optimal maximum ion

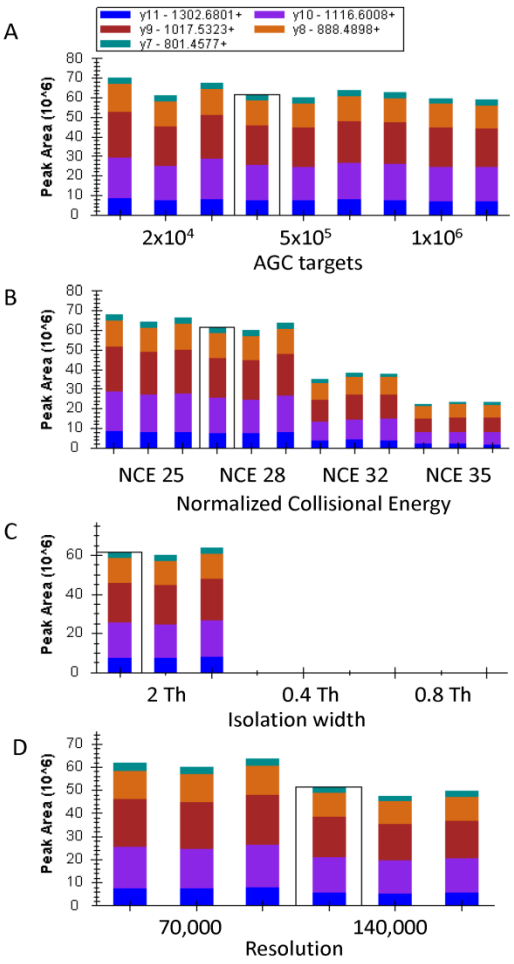

Figure 5.8 Effect of AGC targets (A), NCE, isolation width and resolution on PRM transitions of the tryptic peptide of ELINSWVESQTNGIIR.

injection time increases from 250 ms to 500 ms with less peptides quantified. Similar results were obtained from other tryptic peptides (data not shown). In the subsequent experiments, we used the optimized PRM parameters as described in the section of 5.3.6.

Using the optimized PRM parameters, we tested the specificity of the high-resolution PRM on quantifying deamidated peptides. As shown in Figure 5.9A, if the mass tolerance of 350 mmu, the typical resolution of tranditional MRM, was used to extract transitions for deamidated peptides, the ^{13}C peak of the corresponding undeamidated peptides was also extracted as a wrong transition due to the slight mass difference of 19.34 mDa between them, (81) which makes the accurate quantification of deamidated peptides impossible. It is still impossible to differentiate them even if a mass tolerance of 30 mmu is used (Figure 5.9B). Skyline (version 2.1.0.4936) used the mass resolution but not the extract mass tolerance to extract PRM transition. For example, for a fragment ion of 1000 Da acquired at the resolution of 70, 000, about 30 mmu is used to extract the PRM transition. Therefore, this version of Skyline cannot be used for accurately extracting PRM transitions for deamidated peptides, but Xcalibur and Pinpoint can be used to extract PRM transitions at very narrow mass tolerance. Depending on the high resolution of 70,000, a mass tolerance of 5 mmu can be used to extract the transitions so that the interference from the ^{13}C peak of the corresponding

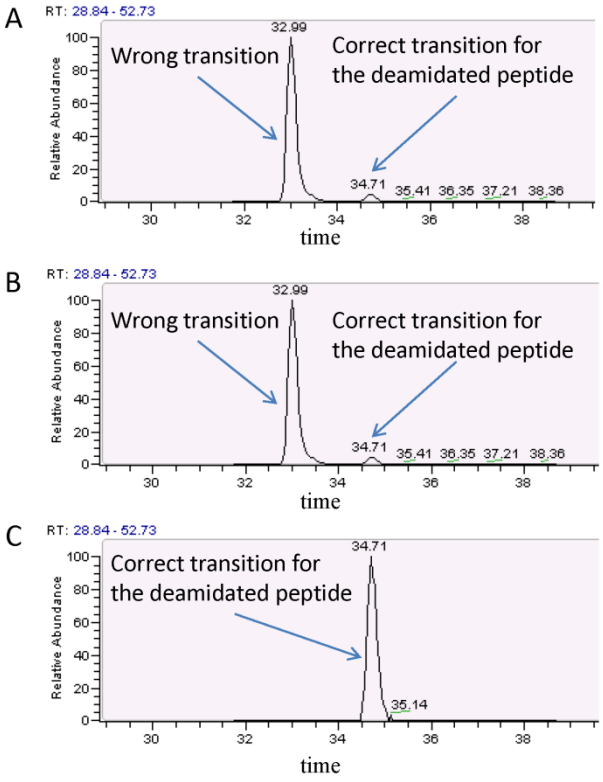

Figure 5.9 The y10 transition of LGEYGFQ(de)NALIVR extracted at the mass tolerance of 350 mmu (A), 30 mmu (B) and 5 mmu (C) using Xcalibur 2.2. Only the transition extracted at 5 mmu can differentiate the MS2 fragment of the deamidated peptide from that of the ^{13}C peak of the corresponding undeamidated peptide.

undeamidated peptides disappears completely (Figure 5.9C), which in turn leads to the accurate quantification of deamidated peptides. (28, 176) Since protein deamidation occurs spontaneously either *in vivo* or *in vitro* and generally produces a mixture of undeamidated and deamidated products, it is necessary to differentiate them using high-resolution PRM for accurate quantification of protein deamidation.

5.4.6.2 Selection and Refinement of Biomarker Candidates of Proteins and Deamidated Peptides for PRM Validation

We first used a relative low resolution of 17,500 and a time window to 25-29 min to conduct preliminary PRM on a large number of deamidated peptides and unmodified peptides from biomarker candidates, and then fine-tuned the PRM inclusion list by removing those with weak signals and determining the accurate elution time of target peptides. The refinement of PRM targets was done using pooled samples. Finally, dynamic PRM would be applied to both pooled samples and each individual sample using a resolution of 70,000 and a narrow time window of 5 min to ensure high mass accuracy of PRM transitions and monitor as many peptides as possible.

As discussed in the section of 5.4.5.2, the deamidated peptides of APOB, MFGE8, PGK1, TIMP1 and TIMP3 identified from the pooled samples in label-free experiments were selected as targets for PRM validation. Two to four unmodified peptides from each of these 5 proteins were also monitored to compare the difference between protein expression and deamidation. Since many more peptides can be quantified simultaneously in a single PRM experiment, we also selected other biomarker candidates which were up-regulated in the pooled test samples from label-free quantification as the targets for PRM. For example, some existing or potential biomarkers for unstable plaques, such as MPO, MMP7, MMP9, MMP12, FGB and FGG, were quantified using PRM. These biomarker candidates are not only indicators of unstable plaques, but also play an important role in the occurrence of cardiovascular and/or cerebrovascular events. Increasing evidence

indicates that MMPs are overproduced in the rupture-prone regions of atherosclerotic plaques and are closely related to plaque instability and consequent cardiovascular events. (177-180) The proteolytic activity of MMPs results in the rupture of plaques by destroying extracellular matrix and fibrous cap. MPO may work together with MMPs to degrade the collagen layer of atheroma, resulting in the instability and rupture of plaques.(181, 182) Since the instability of plaques was also the major cause for a secondary cerebrovascular event, these biomarkers for unstable plaques may also be valuable in predicting secondary cerebrovascular events.

In addition to the above-mentioned known biomarker candidates, we selected some novel biomarker candidates that were up-regulated in the pooled test samples from label-free quantification and were also considerably involved in the development and progression of atherosclerosis for PRM validation, such as ITGAM, PLTP, WISP2, CTSF and VCAM1. Studies in mouse models indicate that overexpression of PLTP (phospho-lipid transfer protein) accelerates the development of atherosclerosis by increasing hepatic VLDL level, decreasing plasma HDL levels and affecting the anti-inflammatory and antioxidative properties of HDL. (183-186) CTSF was found to expressed in human atherosclerotic lesions and modify low density lipoprotein particles *in vitro*. (187) VCAM1 was up-regulated at atherosclerosis-prone sites on the endothelium, and it promotes monocyte accumulation in the arterial intima in mouse models during the course of atherogenesis. (157, 188) To normalize the possible difference in sample preparation, loading amount and LC-MS/MS ionization efficiency, VCL and AKAP12 were selected as control proteins for PRM as its expression shows no significant difference between the pooled test samples and the pooled control samples. The complete list of biomarker candidates for PRM validation in each individual sample is shown in Table 5.2 and Table 5.3.

5.4.6.3 Application of PRM to the Validation of the Biomarker Candidates in Pooled Plaque Samples

To check the consistence between label-free quantification using extracted ion chromatography (XIC) and targeted parallel reaction monitoring (PRM) in quantifying proteins and deamidated peptides, we applied PRM to the validation of the results from label-free quantification on pooled plaques. Three technical replicates are includes in both label-free quantification and PRM. As shown in Table 5.2, the ratio of the protein biomarker candidates between pooled test samples and pooled control group is highly consistent between label-free quantification and PRM. Of 18 tested biomarker candidates, only CTSF had a different trend between label-free quantification and PRM. Similar results were obtained from peptide biomarker candidates (Table 5.3). Of 7 peptide biomarker candidates, only MWVTGVVTQ(de)GASR from MFGE8 showed a different trend between label-free quantification and PRM. It should be noted that the ratio of deamidated peptides has a larger difference between label-free quantification and PRM than that of proteins. The possible explanations are, 1, quantification of proteins is derived from multiple peptides, but quantification of deamidated peptides is based on only one peptide; 2, the abundance of deamidated peptides is lower than that of unmodified peptides used for protein quantification from the same proteins since deamidation generally does not occur at 100%, and the quantification of low-abundance peptides is generally not as accurate as that of peptides with higher abundance. In conclusion, PRM can be effectively used in the validation of peptide and protein biomarker candidates obtained from label-free quantification.

Table 5.2 Summary about quantification of protein biomarker candidates from label-free quantification and validation of them using PRM

Classification	Gene Symbol	S/C ratio from label-free quantification	S/C ratio from PRM	No. of unique peptides for PRM
Potential biomarkers	MPO	2.07±0.32	2.28±0.17	2
	FGB	1.54±0.09	1.42±0.05	3
	FGG	1.66±0.07	1.62±0.11	4
Control proteins	VCL	1.02±0.04	1.02±0.06	4
	AKAP12	1.02±0.05	1.02±0.06	2
Proteins up-	APOB	1.64±0.04	1.38±0.07	4

regulated in deamidation	PGK1	0.96±0.05	0.86±0.07	4
	MFGE8	1.27±0.04	1.16±0.19	4
New biomarker candidates	ITGAM	1.88±0.03	2.21±0.13	3
	PLTP	2.12±0.36	1.55±0.05	3
	WISP2	1.56±0.02	1.49±0.07	3
	CTSF	**1.77±0.16**	**1.02±0.06**	**2**
	VCAM1	1.52±0.07	1.28	1
MMPs and their inhibitors	MMP7	2.55±0.58	2.03±0.56	2
	MMP9	2.12±0.23	1.65±0.26	4
	MMP12	1.65±0.34	1.51±0.28	3
	TIMP1	1.81±0.22	1.45±0.02	2
	TIMP3	detected only in test group	1.78	1

Note: S/C ratio means the concentration in pooled test group divided by that in pooled control group.

Table 5.3 Summary about quantification of peptide biomarker candidates from label-free quantification and validation of them using PRM

Gene Symbol	Deamidated peptides	S/C ratio from label-free quantification	S/C ratio from PRM
APOB	IN(de)NQITIDSNTK	2.95	1.53
APOB	NFVASHIANIIN(de)SEEIDIQDIK	6.76	1.63
APOB	EYSGTIASEAN(de)TYIN(de)SK	1.81	2.31
APOB	AAIGKIPQQAN(de)DYIN(de)SFNWER	2.7	2.68
PGK1	IGDVYVN(de)DAFGTAHR	3.24	2.4
MFGE8	MWVTGVVTQ(de)GASR	detected only in test group	1.09
TIMP1	IQDGIIHITTCSFVAPWN(de)SISIAQR	detected only in test group	3.8
TIMP3	MYTGICN(1)FVER	detected only in test group	2.3

Note: S/C ratio means the concentration in pooled test group divided by that in pooled control group.

5.4.6.4 Application of PRM to the Validation of the Biomarker Candidates in Individual Plaque Samples

To determine the applicability of the protein and peptide biomarker candidates for predicting secondary cerebrovascular events, PRM is used to validate them in each individual plaque. As discussed in the section of 5.4.6.2, we proposed to use VCL and AKAP12 for normalization of PRM data for each individual sample. However, as shown in Figure 5.10, their concentration in each individual sample shows very large variations even if the average ratio of VCL and AKAP12 between patients with/without secondary cerebrovascular events is 1.05 for PRM data. Therefore, they cannot be used for normalization of PRM data. The commonly used housekeeping proteins for normalization in western blotting are also reported to be unusable in some diseases.(189) However, we found that the total area of the LC- MS/MS base peak for each individual plaque could be used to normalize PRM data to minimize the difference in trypsin digestion, sample loading amount, ionization efficiency, and so on. The underlying principle is that PRM collected many more ions than its targets with the isolation window of 2 Th and the AGC target of 1E6, and the total intensity of all these ions is identical for each plaque sample if all of the factors, including but not limited to trypsin digestion, sample loading amount and ionization efficiency, are the same. Similarly, the total loading amount is used as a control in fluorescent western blotting.(190)

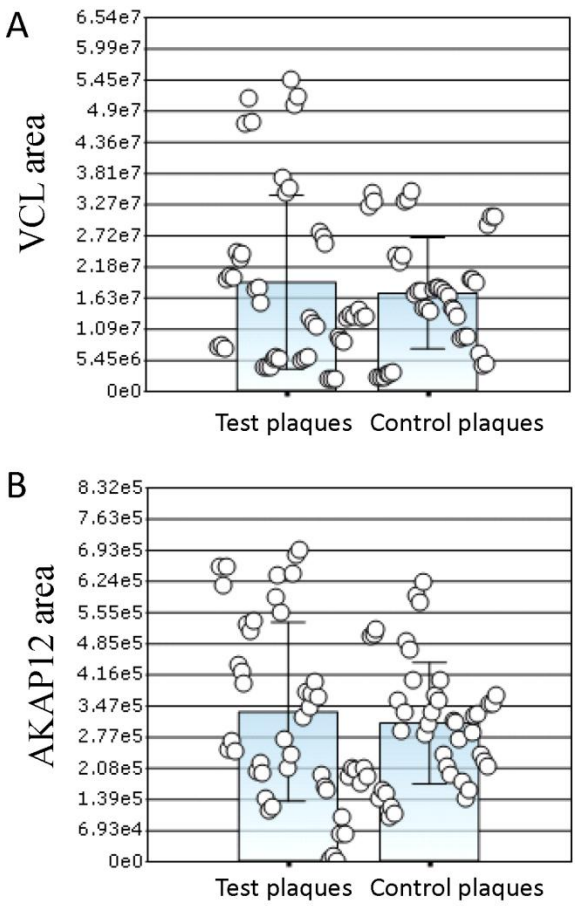

Figure 5.10 The concentration of VCL (A) and AKAP12 (B) in all individual patients with or without secondary events. They cannot be used for normalization of PRM due to the large individual variation.

After the peak area of all transitions for each protein is integrated and added together using Pinpoint 1.3 and normalized based on the total area of their LC-MS/MS base peaks,

receiver operating characteristic (ROC) is used to evaluate the biomarker candidates of proteins and deamidated peptides. Based on the area under the ROC curve (AUC) for all tested biomarker candidates (Table 5.4), none of them reach the criterion as an acceptable biomarker. We then analyzed the reasons. As shown in 5.11 A and B, the average concentration of MPO and MMP7 in pooled samples, two well-known biomarker candidates for unstable plaques, mainly attributes to a few plaques with extremely high concentration of MPO and MMP7. Therefore, the average concentration of MPO and MMP7 is not a good indicator of their concentration in individual samples. To eliminate the effect of a few plaques with extremely high concentration of some proteins and increase the success rate of biomarker discovery, the number of samples under test should be increased

Table 5.4 The AUCs of biomarker candidates of proteins and deamidated peptides from ROC curve analysis

Protein biomarker candidates	AUC	Biomarker candidates of deamidated peptides	AUC
AKAP12	0.561	IN(de)NQITIDSNTK_APOB	0.661
APOB	0.631	NFVASHIANIIN(de)SEEIDIQDIK_APOB	0.5
CTSF	0.519	EYSGTIASEAN(de)TYIN(de)SK_APOB	0.5
FGB	0.693	AAIGKIPQQAN(de)DYIN(de)SFNW_APOB ER	0.5
FGG	0.653	IGDVYVN(de)DAFGTAHR_PGK1	0.598
ITAM	0.539	MWVTGVVTQ(de)GASR_MFGE8	0.5
MFGE8	0.55	IQDGIIHITTCSFVAPWN(de)SISIAQ_TIMP1	0.5
MMP12	0.538	MYTGICN(de)FVER_TIMP3	0.627
MMP7	0.538		
MMP9	0.517		
MPO	0.504		
PGK1	0.623		
PLTP	0.532		
TIMP1	0.506		
TIMP3	0.611		
VCAM1	0.521		
VCL	0.541		
WISP2	0.638		

Note: excellent biomarkers: AUC>0.9; good biomarker, 0.9>AUC>0.8; acceptable biomarker, 0.8>AUC>0.7.

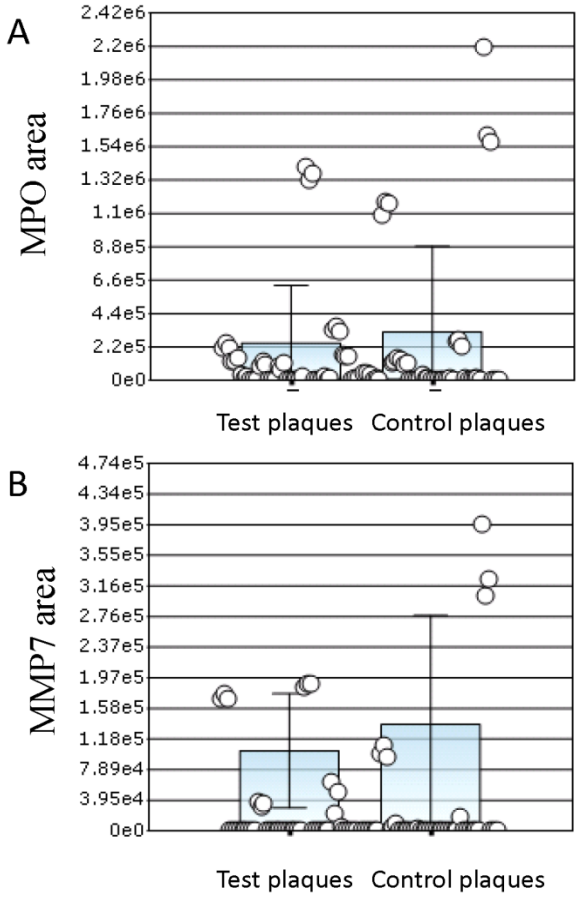

Figure 5.11 The concentration of MPO (A) and MMP7 (B) in all individual patients with or without secondary cerebrovascular events. The average concentration of them in pooled samples attributes to a few samples with extremely high concentrations.

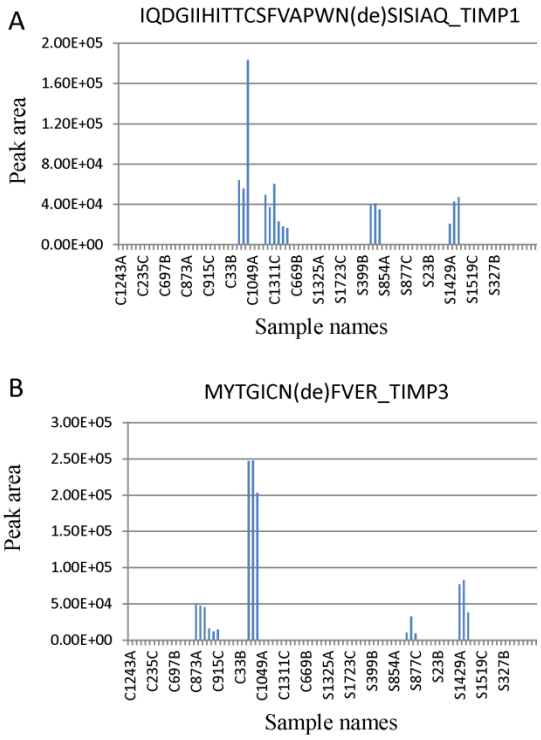

Figure 5.12 The XIC areas of the deamidated peptides from TIMP1 (A) and TIMP3 (B) in all individual patients with or without secondary cerebrovascular events. They cannot be detected in most individual samples due to

to a few hundred or more if possible.(191-193) We also checked the level of the deamidated peptides of IQDGIIHITTCSFVAPWN(de)SISIAQ_TIMP1 and MYTGICN(de)FVER_TIMP3 in each individual sample and found that they were detected only in some of the plaque samples (Figure 5.12 A and B) possibly due to their extremely low abundance in most samples. The ratio of deamidation is 6.3-20.1% and 7.7%-37.4% for IQDGIIHITTCSFVAPWN(de)SISIAQ and MYTGICN(de)FVER, respectively, in plaque samples from which the deamidated peptides are identified (Table

5.5). The low ratio of deamidation explains why it is much more difficult to identify and quantify deamidated peptides than unmodified peptides. The further increase of the sensitivity of mass spectrometry may contribute to the validation of deamidated peptides using PRM in the future. The traditional antibody based assays, such as Western Blot and ELISA, cannot be used in the validation of novel PTMs due to the lack of commercially available antibodies with high specificity. In this study, we did not validate the protein biomarker candidates using Western Blot or ELISA either due to the following two considerations: 1) PRM can be used as an alternative to Western Blot or ELISA for validation of biomarker candidates in individual samples according to experts in the area of proteomics; (194) 2) none of the biomarker candidates pass the PRM validation, and it will be a waste of resources to do further cross validation.

Table 5.5 Ratio of deamidation for deamidated peptides from TIMP1 and TIMP3 in individual plaque samples

Deamidated peptides	IQDGIIHITTCSFVAPWN(de)SISIAQ_TIMP1			MYTGICN(de)FVER_TIMP3		
Sample name	Ratio of deamidation	Asp%	isoAsp%	Ratio of deamidation	Asp%	isoAsp%
C3A	18.5%	2.6%	15.9%	35.3%	15.2%	20.1%
C3B	20.1%	4.3%	15.7%	37.4%	16.3%	21.1%
C3C	17.5%	2.4%	15.1%	34.6%	13.8%	20.9%
S1429A	7.3%	2.4%	4.9%	21.0%	9.9%	11.1%
S1429B	8.5%	2.9%	5.5%	20.6%	10.2%	10.5%
S1429C	8.2%	2.6%	5.6%	18.4%	6.6%	11.8%
S573A	7.7%	4.2%	3.5%			
S573B	7.0%	3.7%	3.3%			
S573C	6.3%	2.5%	3.7%			
C1311A	11.1%	5.8%	5.3%			
C1311B	10.0%	5.0%	4.9%			
C1311C	16.3%	6.1%	10.2%			
C1358A	8.3%	1.3%	6.9%			
C1358B	12.3%	1.3%	11.0%			
C1358C	8.4%	2.0%	6.4%			
C873A				17.4%	8.1%	9.3%
C873B				19.2%	6.3%	12.9%

C873C				18.1%	7.4%	10.7%
C915A				7.7%	6.5%	1.2%
C915B				18.6%	8.9%	9.6%
C915C				15.0%	9.2%	5.8%
S877A				28.7%	7.4%	21.3%
S877B				25.1%	11.5%	13.6%
S877C				20.8%	7.3%	13.5%

5.4.7 Fate of Deamidated Proteins in the Ageing Process

It is generally possible to utilize degradation pathways to convert a damaged protein into amino acids and then resynthesize it in most tissues. However, it is not the case for red blood cells or eye lens where the biosynthetic capacity is severely limited, (195) and it is also not the case in brains where it is necessary to keep specific PTMs associated with learning and memory. (196) As a complement to the degradation pathways, Protein L-isoaspartyl-O-methyltransferase (PIMT) can be employed to repair deamidated proteins containing isoAsp. (197) It seems that the PIMT repair can act as one part of proteolysis since protein degradation is more efficient on Asp containing proteins instead of isoAsp containing proteins. However, the failure to repair them during the ageing process results in the accumulation of isoAsp in proteins that affects the structure and function of proteins and triggers autoimmune responses. (198)

5.5 Conclusion

The proteome coverage of human atherosclerotic plaques obtained in this study is over 3 times of that in previously large-scale studies. (140, 141) Such a tremendous increase will be very useful to understand the composition and underlying mechanisms of atherosclerotic plaques. With our newly developed proteomics methods, the accurate identification, quantification and validation of endogenous protein deamidation in plaques were successfully achieved. No clinically usable biomarkers were identified in this study possibly due to the small sample size and high individual variation, but these newly developed methods can be applied to the study of protein deamidation in complex

samples for biomarker discovery and mechanism studies in the future. The further improvement in the sensitivity of PRM will contribute to the validation of peptide biomarker candidates in complex samples.

.

Chapter 6

6 Conclusion and future perspective

6.1 Conclusion and future perspective

Protein deamidation occurs nonenzymatically both *in vivo* and *in vitro* with the conversion of asparagine and glutamine into aspartic acid and glutamic acid, respectively. Endogenous deamidation has been reported to be related to aging and many diseases. *In vitro* deamidation results in the degradation of antibodies during inappropriate storage. LC-MS/MS is the method of choice for large-scale characterization of deamidation due to its high sensitivity, speed and specificity of detection. As a less studied PTM, there are still many technical challenges in studying protein deamidation using large-scale proteomic methods. Database search returns the identification of many false positive deamidated peptides due to the slight mass difference of 19.34 mDa between deamidated peptides and the ^{13}C peaks of their unmodified counterparts. Since deamidation occurs readily under the typical conditions of trypsin digestion, artificial deamidation may prevent the accurate identification and quantification of endogenous deamidation. Now, it is still very challenging to distinguish between the isomeric n-Asp and isoAsp deamidation products using large-scale proteomics methods because of their identical composition, mass and charge (Figure 1.1). The quantification of deamidated peptides cannot be validated using either ELISA or MRM. In this thesis, in order to overcome these obvious challenges, novel proteomic methods were developed and applied to the study of protein deamidation in human carotid atherosclerotic plaques from old patients for predicting secondary cerebrovascular events.

In Chapter 2, we developed a data analysis strategy to minimize the false positive identification of deamidated peptides from database searches by using the mass difference of 19.34 mDa between deamidated peptides and the ^{13}C peaks of their unmodified counterparts as a cutoff. Evaluation of 5 groups of proteomic data indicated that nonenzymatic Asn deamidation occurred on 4-9% of all peptides and resulted in the identification of many false positive N-glycosylation sites. The mild alkaline pH of the digestion buffer and prolonged incubation at 37ºC were proven to be the major causes of nonenzymatic Asn deamidation during proteomic sample preparations according to a

comprehensive study of many potential factors. Therefore, an improved protocol of trypsin digestion at pH 6 and deglycosylation at pH 5 was proposed and validated, and significant decrease of nonenzymatic Asn deamidation was achieved without affecting protein and peptide identification. We also identified the sequence motifs for glutamine deamidation, i.e. -Q-V-, -Q-L-, -Q-G-, -Q-A- and -Q-E-. It should be noted that artificial deamidation due to sample preparation cannot be avoided completely even with the improved protocol. In the future, $H_2{}^{18}O$ can also be used during PNGase F treatment in the improved protocol to further reduce the false positive identification of N-glycopeptides.

Because of the differences between in-gel and in-solution trypsin digestion, it is necessary to conduct a comprehensive evaluation on in-solution digestion before widely applying the sample preparation protocol developed in chapter 2 to proteomics studies. To evaluate the effect of trypsin digestion buffers on artificial deamidation and protein & peptide identification, we compared the commonly used buffers of Tris-HCl (pH 8), ammonium bicarbonate (ABB) and triethylammonium bicarbonate (TEAB), and ammonium acetate (pH 6) as developed in chapter 3. Both iTRAQ quantification and label-free results indicates that artificial Asn deamidation is produced in the order of ammonium acetate<Tris-HCl<ABB<TEAB, and Gln deamidation has no significant differences among all tested buffers. Determination of the half-time of Asn deamidation in the four buffers using synthetic peptides further validates the conclusion. Label-free experiments showed that protein and unique peptide identification is comparable during using these four buffers. However, targeted MRM or PRM validation may be used with caution while using Tris-HCl or ammonium acetate (pH 6) as digestion buffers due to the increase of tryptic miscleavages, i.e. the control and samples being digested under completely same conditions. In conclusion, the commonly used tryspin digestion buffers of ABB and TEAB are not suitable for studying Asn deamidation and N-glycosylation, but Tris-HCl may be used if trypsin digestion has to be done at around pH 8; Ammonium acetate (pH 6) is more suitable than other tested buffers for studying endogenous deamidation and N-glycosylation.

Chapter 6

In chapter 4, we proposed and validated a novel RP-ERLIC-MS/MS strategy for proteome-scale study of the triads of deamidation products. Protein Asn deamidation produces the mixture of protein isoforms containing asparaginyl, n-aspartyl and isoaspartyl residues at the deamidation sites, which results in function loss and protein degradation. The identification and quantification of these deamidation products are crucial to evaluate its biological effects, but it is difficult to distinguish between the isomeric n-Asp and isoAsp deamidation products in a proteome-wide analysis because of their similar physicochemical properties. The widely used RPLC-MS/MS cannot be effectively used in the separation and characterization of the structural isomers of deamidated peptides due to their identical polarities, but the newly introduced ERLIC is proven to separate them well based on their different *p*I. The RP-ERLIC-MS/MS method is featured by the use of offline RPLC in the first dimensional separation and the online coupling of electrostatic repulsion-hydrophilic interaction chromatography (ERLIC) to tandem MS. The three deamidation products from the same peptides are to be co-eluted and thus collected in the same fraction in offline RPLC. In the 2nd dimension of ERILC-MS/MS, they are separated according to their *p*I values, facilitating the identification and quantification of them using MS/MS. The co-elution of them in RPLC, the excellent separation of them in ERLIC and the performance of ERLIC-MS/MS were validated using synthetic peptides, simple tryptic digests and rat liver digests. The sensitivity of ERLIC-MS/MS still needs to be further improved before it can be used in characterizing low-abundance deamidated peptides from complex samples. For more reliable identification of isoAsp deamidation products, RP-ERLIC may be coupled to ECD or ETD in the future. RP-ERLIC may also be used for the analysis of whole proteome because of its remarkable resolution and compatibility with mass spectrometry.

Human carotid atherosclerotic plaques from old patients are good samples to test the applicability of our newly developed proteomic methods for studying deamidation since protein deamidation accumulates progressively with ages. In chapter 5, our newly developed proteomics methods as detailed in previous chapters were employed to ensure the accurate and reliable characterization of endogenous protein deamidation. With the

latest proteomics technologies, the proteome coverage of human atherosclerotic plaques obtained in this study is over 3 times of that in previously large-scale studies. (140, 141) A total of 3846 proteins were identified with at least 2 unique peptides from atherosclerotic plaques, and many low-abundance proteins with important functions in atherosclerosis were identified confidently using mass spectrometry for the first time. Such a tremendous increase will be very useful to understand the composition and underlying mechanisms of atherosclerotic plaques. Label-free quantification on pooled plaques from patients with/without secondary cerebrovascular events identified many up-regulated proteins and deamidated peptides that were either known biomarkers for unstable plaques or closely related to the initiation and progression of atherosclerosis as biomarker candidates. These candidates were then evaluated in 38 individual samples using PRM for predicting secondary cerebrovascular events after the applicability of PRM for validation of deamidated peptides was proven using simple tryptic digests. With our newly developed proteomics methods, the accurate identification, quantification and validation of endogenous protein deamidation in plaques were successfully achieved. No clinically usable biomarkers were identified in this study possibly due to the small sample size and high individual variation, but these newly developed methods can be applied to the accurate characterization of protein deamidation in complex samples for biomarker discovery and mechanism studies in the future. The further improvement in the sensitivity of PRM will contribute to the validation of peptide biomarker candidates in complex samples.

References

References

1. James, P. (1997) Protein identification in the post-genome era: the rapid rise of proteomics. *Q Rev Biophys* 30, 279-331.

2. Wilkins, M. R., Pasquali, C., Appel, R. D., Ou, K., Golaz, O., Sanchez, J. C., Yan, J. X., Gooley, A. A., Hughes, G., Humphery-Smith, I., Williams, K. L., and Hochstrasser, D. F. (1996) From proteins to proteomes: large scale protein identification by two-dimensional electrophoresis and amino acid analysis. *Biotechnology (N Y)* 14, 61-65.

3. Wasinger, V. C., Cordwell, S. J., Cerpa-Poljak, A., Yan, J. X., Gooley, A. A., Wilkins, M. R., Duncan, M. W., Harris, R., Williams, K. L., and Humphery-Smith, I. (1995) Progress with gene-product mapping of the Mollicutes: Mycoplasma genitalium. *Electrophoresis* 16, 1090-1094.

4. Cottrell, J. S. (2011) Protein identification using MS/MS data. *J Proteomics* 74, 1842-1851.

5. Dancik, V., Addona, T. A., Clauser, K. R., Vath, J. E., and Pevzner, P. A. (1999) De novo peptide sequencing via tandem mass spectrometry. *J Comput Biol* 6, 327-342.

6. Bandeira, N., Pham, V., Pevzner, P., Arnott, D., and Lill, J. R. (2008) Automated de novo protein sequencing of monoclonal antibodies. *Nat Biotechnol* 26, 1336-1338.

7. Gygi, S. P., Rochon, Y., Franza, B. R., and Aebersold, R. (1999) Correlation between protein and mRNA abundance in yeast. *Mol Cell Biol* 19, 1720-1730.

8. Mann, M., and Jensen, O. N. (2003) Proteomic analysis of post-translational modifications. *Nat Biotechnol* 21, 255-261.

9. Parker, K. C., Garrels, J. I., Hines, W., Butler, E. M., McKee, A. H., Patterson, D., and Martin, S. (1998) Identification of yeast proteins from two-dimensional gels: working out spot cross-contamination. *Electrophoresis* 19, 1920-1932.

10. Eymann, C., Dreisbach, A., Albrecht, D., Bernhardt, J., Becher, D., Gentner, S., Tam le, T., Buttner, K., Buurman, G., Scharf, C., Venz, S., Volker, U., and Hecker, M. (2004) A comprehensive proteome map of growing Bacillus subtilis cells. *Proteomics* 4, 2849-2876.

11. Wilkins, M. R., Gasteiger, E., Sanchez, J. C., Bairoch, A., and Hochstrasser, D. F. (1998) Two-dimensional gel electrophoresis for proteome projects: the effects of protein hydrophobicity and copy number. *Electrophoresis* 19, 1501-1505.

12. Wolters, D. A., Washburn, M. P., and Yates, J. R., 3rd (2001) An automated multidimensional protein identification technology for shotgun proteomics. *Anal Chem* 73, 5683-5690.

13. Yates, J. R., 3rd (1998) Mass spectrometry and the age of the proteome. *J Mass Spectrom* 33, 1-19.

14. Fang, X., Balgley, B. M., Wang, W., Park, D. M., and Lee, C. S. (2009) Comparison of multidimensional shotgun technologies targeting tissue proteomics. *Electrophoresis* 30, 4063-4070.

15. Sandra, K., Moshir, M., D'Hondt, F., Tuytten, R., Verleysen, K., Kas, K., Francois, I., and Sandra, P. (2009) Highly efficient peptide separations in proteomics. Part 2: bi- and multidimensional liquid-based separation techniques. *J Chromatogr B Analyt Technol Biomed Life Sci* 877, 1019-1039.

16. Pirmoradian, M., Budamgunta, H., Chingin, K., Zhang, B., Astorga-Wells, J., and Zubarev, R. A. (2013) Rapid and deep human proteome analysis by single-dimension shotgun proteomics. *Mol Cell Proteomics* 12, 3330-3338.

17. Hebert, A. S., Richards, A. L., Bailey, D. J., Ulbrich, A., Coughlin, E. E., Westphall, M. S., and Coon, J. J. (2014) The one hour yeast proteome. *Mol Cell Proteomics* 13, 339-347.

References

18. Geiger, T., Wehner, A., Schaab, C., Cox, J., and Mann, M. (2012) Comparative proteomic analysis of eleven common cell lines reveals ubiquitous but varying expression of most proteins. *Mol Cell Proteomics* 11, M111 014050.

19. Bantscheff, M., Schirle, M., Sweetman, G., Rick, J., and Kuster, B. (2007) Quantitative mass spectrometry in proteomics: a critical review. *Anal Bioanal Chem* 389, 1017-1031.

20. Ong, S. E., Blagoev, B., Kratchmarova, I., Kristensen, D. B., Steen, H., Pandey, A., and Mann, M. (2002) Stable isotope labeling by amino acids in cell culture, SILAC, as a simple and accurate approach to expression proteomics. *Mol Cell Proteomics* 1, 376-386.

21. Gygi, S. P., Rist, B., Gerber, S. A., Turecek, F., Gelb, M. H., and Aebersold, R. (1999) Quantitative analysis of complex protein mixtures using isotope-coded affinity tags. *Nat Biotechnol* 17, 994-999.

22. Ross, P. L., Huang, Y. N., Marchese, J. N., Williamson, B., Parker, K., Hattan, S., Khainovski, N., Pillai, S., Dey, S., Daniels, S., Purkayastha, S., Juhasz, P., Martin, S., Bartlet-Jones, M., He, F., Jacobson, A., and Pappin, D. J. (2004) Multiplexed protein quantitation in Saccharomyces cerevisiae using amine-reactive isobaric tagging reagents. *Mol Cell Proteomics* 3, 1154-1169.

23. Elliott, M. H., Smith, D. S., Parker, C. E., and Borchers, C. (2009) Current trends in quantitative proteomics. *J Mass Spectrom* 44, 1637-1660.

24. Fuzery, A. K., Levin, J., Chan, M. M., and Chan, D. W. (2013) Translation of proteomic biomarkers into FDA approved cancer diagnostics: issues and challenges. *Clin Proteomics* 10, 13.

25. Service, R. F. (2008) Proteomics. Will biomarkers take off at last? *Science* 321, 1760.

26. Picotti, P., and Aebersold, R. (2012) Selected reaction monitoring-based proteomics: workflows, potential, pitfalls and future directions. *Nat Methods* 9, 555-566.

27. Schiess, R., Wollscheid, B., and Aebersold, R. (2009) Targeted proteomic strategy for clinical biomarker discovery. *Mol Oncol* 3, 33-44.

28. Peterson, A. C., Russell, J. D., Bailey, D. J., Westphall, M. S., and Coon, J. J. (2012) Parallel reaction monitoring for high resolution and high mass accuracy quantitative, targeted proteomics. *Mol Cell Proteomics* 11, 1475-1488.

29. Jin, H., and Zangar, R. C. (2009) Protein modifications as potential biomarkers in breast cancer. *Biomark Insights* 4, 191-200.

30. Martin, L., Latypova, X., and Terro, F. (2011) Post-translational modifications of tau protein: implications for Alzheimer's disease. *Neurochem Int* 58, 458-471.

31. van Lummel, M., Duinkerken, G., van Veelen, P. A., de Ru, A., Cordfunke, R., Zaldumbide, A., Gomez-Tourino, I., Arif, S., Peakman, M., Drijfhout, J. W., and Roep, B. O. (2014) Posttranslational modification of HLA-DQ binding islet autoantigens in type 1 diabetes. *Diabetes* 63, 237-247.

32. Eom, G. H., and Kook, H. (2014) Posttranslational modifications of histone deacetylases: Implications for cardiovascular diseases. *Pharmacol Ther*.

33. Pena-Altamira, L. E., Polazzi, E., and Monti, B. (2013) Histone post-translational modifications in Huntington's and Parkinson's diseases. *Curr Pharm Des* 19, 5085-5092.

34. Jaisson, S., and Gillery, P. (2010) Evaluation of nonenzymatic posttranslational modification-derived products as biomarkers of molecular aging of proteins. *Clin Chem* 56, 1401-1412.

35. Huttlin, E. L., Jedrychowski, M. P., Elias, J. E., Goswami, T., Rad, R., Beausoleil, S. A., Villen, J., Haas, W., Sowa, M. E., and Gygi, S. P. (2010) A tissue-specific atlas of mouse protein phosphorylation and expression. *Cell* 143, 1174-1189.

36. Kim, W., Bennett, E. J., Huttlin, E. L., Guo, A., Li, J., Possemato, A., Sowa, M. E., Rad, R., Rush, J., Comb, M. J., Harper, J. W., and Gygi, S. P. (2011) Systematic and quantitative assessment of the ubiquitin-modified proteome. *Mol Cell* 44, 325-340.

37. Deeb, S. J., Cox, J., Schmidt-Supprian, M., and Mann, M. (2014) N-linked glycosylation enrichment for in-depth cell surface proteomics of diffuse large B-cell lymphoma subtypes. *Mol Cell Proteomics* 13, 240-251.

38. Burnett, G., and Kennedy, E. P. (1954) The enzymatic phosphorylation of proteins. *The Journal of biological chemistry* 211, 969-980.

39. Hay, R. T. (2005) SUMO: a history of modification. *Mol Cell* 18, 1-12.

40. Pickart, C. M. (2001) Mechanisms underlying ubiquitination. *Annual review of biochemistry* 70, 503-533.

41. Robinson, A. B., and Rudd, C. J. (1974) Deamidation of glutaminyl and asparaginyl residues in peptides and proteins. *Curr Top Cell Regul* 8, 247-295.

42. Wang, Z., Nicholls, S. J., Rodriguez, E. R., Kummu, O., Horkko, S., Barnard, J., Reynolds, W. F., Topol, E. J., DiDonato, J. A., and Hazen, S. L. (2007) Protein carbamylation links inflammation, smoking, uremia and atherogenesis. *Nature medicine* 13, 1176-1184.

43. Sevier, C. S., and Kaiser, C. A. (2002) Formation and transfer of disulphide bonds in living cells. *Nature reviews. Molecular cell biology* 3, 836-847.

44. Hunter, T. (2000) Signaling--2000 and beyond. *Cell* 100, 113-127.

45. Gnad, F., de Godoy, L. M., Cox, J., Neuhauser, N., Ren, S., Olsen, J. V., and Mann, M. (2009) High-accuracy identification and bioinformatic analysis of in vivo protein phosphorylation sites in yeast. *Proteomics* 9, 4642-4652.

46. Pawson, T., and Nash, P. (2003) Assembly of cell regulatory systems through protein interaction domains. *Science* 300, 445-452.

47. Morelle, W., Canis, K., Chirat, F., Faid, V., and Michalski, J. C. (2006) The use of mass spectrometry for the proteomic analysis of glycosylation. *Proteomics* 6, 3993-4015.

48. Lu, J. P., Knezevic, A., Wang, Y. X., Rudan, I., Campbell, H., Zou, Z. K., Lan, J., Lai, Q. X., Wu, J. J., He, Y., Song, M. S., Zhang, L., Lauc, G., and Wang, W. (2011) Screening novel biomarkers for metabolic syndrome by profiling human plasma N-glycans in Chinese Han and Croatian populations. *J Proteome Res* 10, 4959-4969.

49. Dube, D. H., and Bertozzi, C. R. (2005) Glycans in cancer and inflammation--potential for therapeutics and diagnostics. *Nat Rev Drug Discov* 4, 477-488.

50. Holst, S., Stavenhagen, K., Balog, C. I., Koeleman, C. A., McDonnell, L. M., Mayboroda, O. A., Verhoeven, A., Mesker, W. E., Tollenaar, R. A., Deelder, A. M., and Wuhrer, M. (2013) Investigations on aberrant glycosylation of glycosphingolipids in colorectal cancer tissues using liquid chromatography and matrix-assisted laser desorption time-of-flight mass spectrometry (MALDI-TOF-MS). *Mol Cell Proteomics* 12, 3081-3093.

51. Glozak, M. A., Sengupta, N., Zhang, X., and Seto, E. (2005) Acetylation and deacetylation of non-histone proteins. *Gene* 363, 15-23.

52. Yang, X. J., and Seto, E. (2008) Lysine acetylation: codified crosstalk with other posttranslational modifications. *Mol Cell* 31, 449-461.

53. Mertins, P., Qiao, J. W., Patel, J., Udeshi, N. D., Clauser, K. R., Mani, D. R., Burgess, M. W., Gillette, M. A., Jaffe, J. D., and Carr, S. A. (2013) Integrated proteomic analysis of post-translational modifications by serial enrichment. *Nat Methods* 10, 634-637.

54. Liddy, K. A., White, M. Y., and Cordwell, S. J. (2013) Functional decorations: post-translational modifications and heart disease delineated by targeted proteomics. *Genome Med* 5, 20.

55. Schmid, A. W., Fauvet, B., Moniatte, M., and Lashuel, H. A. (2013) Alpha-synuclein post-translational modifications as potential biomarkers for Parkinson disease and other synucleinopathies. *Mol Cell Proteomics* 12, 3543-3558.

56. Dunne, J. L., Overbergh, L., Purcell, A. W., and Mathieu, C. (2012) Posttranslational modifications of proteins in type 1 diabetes: the next step in finding the cure? *Diabetes* 61, 1907-1914.

57. Rush, J., Moritz, A., Lee, K. A., Guo, A., Goss, V. L., Spek, E. J., Zhang, H., Zha, X. M., Polakiewicz, R. D., and Comb, M. J. (2005) Immunoaffinity profiling of tyrosine phosphorylation in cancer cells. *Nat Biotechnol* 23, 94-101.

58. Larsen, M. R., Thingholm, T. E., Jensen, O. N., Roepstorff, P., and Jorgensen, T. J. (2005) Highly selective enrichment of phosphorylated peptides from peptide mixtures using titanium dioxide microcolumns. *Mol Cell Proteomics* 4, 873-886.

59. Heo, S. H., Lee, S. J., Ryoo, H. M., Park, J. Y., and Cho, J. Y. (2007) Identification of putative serum glycoprotein biomarkers for human lung adenocarcinoma by multilectin affinity chromatography and LC-MS/MS. *Proteomics* 7, 4292-4302.

60. Lewandrowski, U., Zahedi, R. P., Moebius, J., Walter, U., and Sickmann, A. (2007) Enhanced N-glycosylation site analysis of sialoglycopeptides by strong cation

exchange prefractionation applied to platelet plasma membranes. *Mol Cell Proteomics* 6, 1933-1941.

61. Calvano, C. D., Zambonin, C. G., and Jensen, O. N. (2008) Assessment of lectin and HILIC based enrichment protocols for characterization of serum glycoproteins by mass spectrometry. *J Proteomics* 71, 304-317.

62. Zhang, H., Guo, T., Li, X., Datta, A., Park, J. E., Yang, J., Lim, S. K., Tam, J. P., and Sze, S. K. (2010) Simultaneous characterization of glyco- and phosphoproteomes of mouse brain membrane proteome with electrostatic repulsion hydrophilic interaction chromatography. *Mol Cell Proteomics* 9, 635-647.

63. Cao, L., Yu, L., Guo, Z., Li, X., Xue, X., and Liang, X. (2013) Application of a strong anion exchange material in electrostatic repulsion-hydrophilic interaction chromatography for selective enrichment of glycopeptides. *Journal of chromatography. A* 1299, 18-24.

64. Boilly, B., Lheureux, E., Boilly-Marer, Y., and Bart, A. (1990) Cell interactions and regeneration control. *The International journal of developmental biology* 34, 219-231.

65. Roher, A. E., Lowenson, J. D., Clarke, S., Wolkow, C., Wang, R., Cotter, R. J., Reardon, I. M., Zurcher-Neely, H. A., Heinrikson, R. L., Ball, M. J., and et al. (1993) Structural alterations in the peptide backbone of beta-amyloid core protein may account for its deposition and stability in Alzheimer's disease. *The Journal of biological chemistry* 268, 3072-3083.

66. Takata, T., Oxford, J. T., Demeler, B., and Lampi, K. J. (2008) Deamidation destabilizes and triggers aggregation of a lens protein, betaA3-crystallin. *Protein Sci* 17, 1565-1575.

67. Wilmarth, P. A., Tanner, S., Dasari, S., Nagalla, S. R., Riviere, M. A., Bafna, V., Pevzner, P. A., and David, L. L. (2006) Age-related changes in human crystallins determined from comparative analysis of post-translational modifications in young and aged lens: does deamidation contribute to crystallin insolubility? *Journal of proteome research* 5, 2554-2566.

68. Mukhopadhyay, D., and Riezman, H. (2007) Proteasome-independent functions of ubiquitin in endocytosis and signaling. *Science* 315, 201-205.

69. Robinson, N. E., and Robinson, A. B. (2001) Deamidation of human proteins. *Proc Natl Acad Sci U S A* 98, 12409-12413.

70. Krokhin, O. V., Antonovici, M., Ens, W., Wilkins, J. A., and Standing, K. G. (2006) Deamidation of -Asn-Gly- sequences during sample preparation for proteomics: Consequences for MALDI and HPLC-MALDI analysis. *Anal Chem* 78, 6645-6650.

71. Solstad, T., and Flatmark, T. (2000) Microheterogeneity of recombinant human phenylalanine hydroxylase as a result of nonenzymatic deamidations of labile amide containing amino acids. Effects on catalytic and stability properties. *European journal of biochemistry / FEBS* 267, 6302-6310.

72. Huang, L., Lu, J., Wroblewski, V. J., Beals, J. M., and Riggin, R. M. (2005) In vivo deamidation characterization of monoclonal antibody by LC/MS/MS. *Analytical chemistry* 77, 1432-1439.

73. Geiger, T., and Clarke, S. (1987) Deamidation, isomerization, and racemization at asparaginyl and aspartyl residues in peptides. Succinimide-linked reactions that contribute to protein degradation. *The Journal of biological chemistry* 262, 785-794.

74. Motoyama, A., and Yates, J. R., 3rd (2008) Multidimensional LC separations in shotgun proteomics. *Analytical chemistry* 80, 7187-7193.

75. Perkins, D. N., Pappin, D. J., Creasy, D. M., and Cottrell, J. S. (1999) Probability-based protein identification by searching sequence databases using mass spectrometry data. *Electrophoresis* 20, 3551-3567.

76. Eng, J. K., McCormack, A. L., and Yates, J. R. (1994) An approach to correlate tandem mass spectral data of peptides with amino acid sequences in a protein database. *Journal of the American Society for Mass Spectrometry* 5, 976-989.

77. Cox, J., and Mann, M. (2008) MaxQuant enables high peptide identification rates, individualized p.p.b.-range mass accuracies and proteome-wide protein quantification. *Nat Biotechnol* 26, 1367-1372.

78. Cox, J., Neuhauser, N., Michalski, A., Scheltema, R. A., Olsen, J. V., and Mann, M. (2011) Andromeda: a peptide search engine integrated into the MaxQuant environment. *J Proteome Res* 10, 1794-1805.

79. Elias, J. E., and Gygi, S. P. (2007) Target-decoy search strategy for increased confidence in large-scale protein identifications by mass spectrometry. *Nat Methods* 4, 207-214.

80. Kall, L., Canterbury, J. D., Weston, J., Noble, W. S., and MacCoss, M. J. (2007) Semi-supervised learning for peptide identification from shotgun proteomics datasets. *Nat Methods* 4, 923-925.

81. Robinson, N. E., Lampi, K. J., McIver, R. T., Williams, R. H., Muster, W. C., Kruppa, G., and Robinson, A. B. (2005) Quantitative measurement of deamidation in lens betaB2-crystallin and peptides by direct electrospray injection and fragmentation in a Fourier transform mass spectrometer. *Mol Vis* 11, 1211-1219.

82. Segu, Z. M., Hussein, A., Novotny, M. V., and Mechref, Y. (2010) Assigning N-glycosylation sites of glycoproteins using LC/MSMS in conjunction with endo-M/exoglycosidase mixture. *Journal of proteome research* 9, 3598-3607.

References

83. Nepomuceno, A. I., Gibson, R. J., Randall, S. M., and Muddiman, D. C. (2014) Accurate identification of deamidated peptides in global proteomics using a quadrupole orbitrap mass spectrometer. *J Proteome Res* 13, 777-785.

84. Hao, P., Ren, Y., Alpert, A. J., and Sze, S. K. (2011) Detection, evaluation and minimization of nonenzymatic deamidation in proteomic sample preparation. *Mol Cell Proteomics* 10, O111 009381.

85. Ren, D., Pipes, G. D., Liu, D., Shih, L. Y., Nichols, A. C., Treuheit, M. J., Brems, D. N., and Bondarenko, P. V. (2009) An improved trypsin digestion method minimizes digestion-induced modifications on proteins. *Anal Biochem* 392, 12-21.

86. Palmisano, G., Melo-Braga, M. N., Engholm-Keller, K., Parker, B. L., and Larsen, M. R. (2012) Chemical deamidation: a common pitfall in large-scale N-linked glycoproteomic mass spectrometry-based analyses. *J Proteome Res* 11, 1949-1957.

87. Mann, M., and Kelleher, N. L. (2008) Precision proteomics: the case for high resolution and high mass accuracy. *Proc Natl Acad Sci U S A* 105, 18132-18138.

88. Li, X., Lin, C., and O'Connor, P. B. (2010) Glutamine deamidation: differentiation of glutamic acid and gamma-glutamic acid in peptides by electron capture dissociation. *Analytical chemistry* 82, 3606-3615.

89. Cournoyer, J. J., Pittman, J. L., Ivleva, V. B., Fallows, E., Waskell, L., Costello, C. E., and O'Connor, P. B. (2005) Deamidation: Differentiation of aspartyl from isoaspartyl products in peptides by electron capture dissociation. *Protein Sci* 14, 452-463.

90. Yang, H., Fung, E. Y., Zubarev, A. R., and Zubarev, R. A. (2009) Toward proteome-scale identification and quantification of isoaspartyl residues in biological samples. *Journal of proteome research* 8, 4615-4621.

91. Wolf-Yadlin, A., Hautaniemi, S., Lauffenburger, D. A., and White, F. M. (2007) Multiple reaction monitoring for robust quantitative proteomic analysis of cellular signaling networks. *Proc Natl Acad Sci U S A* 104, 5860-5865.

92. Unwin, R. D., Griffiths, J. R., Leverentz, M. K., Grallert, A., Hagan, I. M., and Whetton, A. D. (2005) Multiple reaction monitoring to identify sites of protein phosphorylation with high sensitivity. *Mol Cell Proteomics* 4, 1134-1144.

93. Sollid, L. M. (2000) Molecular basis of celiac disease. *Annu Rev Immunol* 18, 53-81.

94. Shimizu, T., Matsuoka, Y., and Shirasawa, T. (2005) Biological significance of isoaspartate and its repair system. *Biol Pharm Bull* 28, 1590-1596.

95. Powell, J. T., Vine, N., and Crossman, M. (1992) On the accumulation of D-aspartate in elastin and other proteins of the ageing aorta. *Atherosclerosis* 97, 201-208.

96. Robinson, N. E., and Robinson, A. B. (2001) Molecular clocks. *Proceedings of the National Academy of Sciences of the United States of America* 98, 944-949.

97. Robinson, N. E., and Robinson, A. B. (2004) Amide molecular clocks in drosophila proteins: potential regulators of aging and other processes. *Mechanisms of ageing and development* 125, 259-267.

98. Robinson, N. E., and Robinson, A. B. (2004) Prediction of primary structure deamidation rates of asparaginyl and glutaminyl peptides through steric and catalytic effects. *J Pept Res* 63, 437-448.

99. Catak, S., Monard, G., Aviyente, V., and Ruiz-Lopez, M. F. (2006) Reaction mechanism of deamidation of asparaginyl residues in peptides: effect of solvent molecules. *J Phys Chem A* 110, 8354-8365.

100. Zabrouskov, V., Han, X., Welker, E., Zhai, H., Lin, C., van Wijk, K. J., Scheraga, H. A., and McLafferty, F. W. (2006) Stepwise deamidation of ribonuclease A at five sites determined by top down mass spectrometry. *Biochemistry* 45, 987-992.

101. Li, X., Cournoyer, J. J., Lin, C., and O'Connor, P. B. (2008) Use of 18O labels to monitor deamidation during protein and peptide sample processing. *Journal of the American Society for Mass Spectrometry* 19, 855-864.

102. Gaza-Bulseco, G., Li, B., Bulseco, A., and Liu, H. C. (2008) Method to differentiate asn deamidation that occurred prior to and during sample preparation of a monoclonal antibody. *Analytical chemistry* 80, 9491-9498.

103. Robinson, N. E., Robinson, Z. W., Robinson, B. R., Robinson, A. L., Robinson, J. A., Robinson, M. L., and Robinson, A. B. (2004) Structure-dependent nonenzymatic deamidation of glutaminyl and asparaginyl pentapeptides. *J Pept Res* 63, 426-436.

104. Stroop, S. D. (2007) A modified peptide mapping strategy for quantifying site-specific deamidation by electrospray time-of-flight mass spectrometry. *Rapid Commun Mass Spectrom* 21, 830-836.

105. Hao, P., Guo, T., Li, X., Adav, S. S., Yang, J., Wei, M., and Sze, S. K. (2010) Novel application of electrostatic repulsion-hydrophilic interaction chromatography (ERLIC) in shotgun proteomics: comprehensive profiling of rat kidney proteome. *J Proteome Res* 9, 3520-3526.

106. Gonzalez, L. J., Shimizu, T., Satomi, Y., Betancourt, L., Besada, V., Padron, G., Orlando, R., Shirasawa, T., Shimonishi, Y., and Takao, T. (2000) Differentiating alpha- and beta-aspartic acids by electrospray ionization and low-energy tandem mass spectrometry. *Rapid Commun Mass Spectrom* 14, 2092-2102.

107. Robinson, N. E., Zabrouskov, V., Zhang, J., Lampi, K. J., and Robinson, A. B. (2006) Measurement of deamidation of intact proteins by isotopic envelope and mass

defect with ion cyclotron resonance Fourier transform mass spectrometry. *Rapid Commun Mass Spectrom* 20, 3535-3541.

108. Jung, H. J., Purvine, S. O., Kim, H., Petyuk, V. A., Hyung, S. W., Monroe, M. E., Mun, D. G., Kim, K. C., Park, J. M., Kim, S. J., Tolic, N., Slysz, G. W., Moore, R. J., Zhao, R., Adkins, J. N., Anderson, G. A., Lee, H., Camp, D. G., 2nd, Yu, M. H., Smith, R. D., and Lee, S. W. (2010) Integrated post-experiment monoisotopic mass refinement: an integrated approach to accurately assign monoisotopic precursor masses to tandem mass spectrometric data. *Analytical chemistry* 82, 8510-8518.

109. Dasari, S., Wilmarth, P. A., Rustvold, D. L., Riviere, M. A., Nagalla, S. R., and David, L. L. (2007) Reliable detection of deamidated peptides from lens crystallin proteins using changes in reversed-phase elution times and parent ion masses. *Journal of proteome research* 6, 3819-3826.

110. Liu, Y., Salas-Solano, O., and Gennaro, L. A. (2009) Investigation of sample preparation artifacts formed during the enzymatic release of N-linked glycans prior to analysis by capillary electrophoresis. *Analytical chemistry* 81, 6823-6829.

111. Rosenfeld, J., Capdevielle, J., Guillemot, J. C., and Ferrara, P. (1992) In-gel digestion of proteins for internal sequence analysis after one- or two-dimensional gel electrophoresis. *Anal Biochem* 203, 173-179.

112. Chen, E. I., Cociorva, D., Norris, J. L., and Yates, J. R., 3rd (2007) Optimization of mass spectrometry-compatible surfactants for shotgun proteomics. *J Proteome Res* 6, 2529-2538.

113. Ernoult, E., Gamelin, E., and Guette, C. (2008) Improved proteome coverage by using iTRAQ labelling and peptide OFFGEL fractionation. *Proteome Sci* 6, 27.

114. Hao, P., Qian, J., Ren, Y., and Sze, S. K. (2011) Electrostatic repulsion-hydrophilic interaction chromatography (ERLIC) versus strong cation exchange (SCX) for fractionation of iTRAQ-labeled peptides. *J Proteome Res* 10, 5568-5574.

115. Parker, B. L., Palmisano, G., Edwards, A. V., White, M. Y., Engholm-Keller, K., Lee, A., Scott, N. E., Kolarich, D., Hambly, B. D., Packer, N. H., Larsen, M. R., and Cordwell, S. J. (2011) Quantitative N-linked glycoproteomics of myocardial ischemia and reperfusion injury reveals early remodeling in the extracellular environment. *Mol Cell Proteomics* 10, M110 006833.

116. Ow, S. Y., Salim, M., Noirel, J., Evans, C., and Wright, P. C. (2011) Minimising iTRAQ ratio compression through understanding LC-MS elution dependence and high-resolution HILIC fractionation. *Proteomics* 11, 2341-2346.

117. Ow, S. Y., Salim, M., Noirel, J., Evans, C., Rehman, I., and Wright, P. C. (2009) iTRAQ underestimation in simple and complex mixtures: "the good, the bad and the ugly". *J Proteome Res* 8, 5347-5355.

118. Glatter, T., Ludwig, C., Ahrne, E., Aebersold, R., Heck, A. J., and Schmidt, A. (2012) Large-scale quantitative assessment of different in-solution protein digestion protocols reveals superior cleavage efficiency of tandem Lys-C/trypsin proteolysis over trypsin digestion. *J Proteome Res* 11, 5145-5156.

119. Patel, K., and Borchardt, R. T. (1990) Chemical pathways of peptide degradation. II. Kinetics of deamidation of an asparaginyl residue in a model hexapeptide. *Pharm Res* 7, 703-711.

120. Tyler-Cross, R., and Schirch, V. (1991) Effects of amino acid sequence, buffers, and ionic strength on the rate and mechanism of deamidation of asparagine residues in small peptides. *J Biol Chem* 266, 22549-22556.

References

121. Carr, S. A., Hemling, M. E., Bean, M. F., and Roberts, G. D. (1991) Integration of mass spectrometry in analytical biotechnology. *Anal Chem* 63, 2802-2824.

122. Andreazza, H. J., Wang, T., Bagley, C. J., Hoffmann, P., and Bowie, J. H. (2009) Negative ion fragmentations of deprotonated peptides. The unusual case of isoAsp: a joint experimental and theoretical study. Comparison with positive ion cleavages. *Rapid Commun Mass Spectrom* 23, 1993-2002.

123. Gan, C. S., Guo, T., Zhang, H., Lim, S. K., and Sze, S. K. (2008) A comparative study of electrostatic repulsion-hydrophilic interaction chromatography (ERLIC) versus SCX-IMAC-based methods for phosphopeptide isolation/enrichment. *J Proteome Res* 7, 4869-4877.

124. Hao, P., Guo, T., and Sze, S. K. (2011) Simultaneous analysis of proteome, phospho- and glycoproteome of rat kidney tissue with electrostatic repulsion hydrophilic interaction chromatography. *PLoS One* 6, e16884.

125. Wright, H. T. (1991) Nonenzymatic deamidation of asparaginyl and glutaminyl residues in proteins. *Critical reviews in biochemistry and molecular biology* 26, 1-52.

126. Bischoff, R., and Kolbe, H. V. (1994) Deamidation of asparagine and glutamine residues in proteins and peptides: structural determinants and analytical methodology. *Journal of chromatography* 662, 261-278.

127. Capasso, S. (2000) Estimation of the deamidation rate of asparagine side chains. *J Pept Res* 55, 224-229.

128. Hao, P., Qian, J., Dutta, B., Cheow, E. S., Sim, K. H., Meng, W., Adav, S. S., Alpert, A., and Sze, S. K. (2012) Enhanced separation and characterization of deamidated peptides with RP-ERLIC-based multidimensional chromatography coupled with tandem mass spectrometry. *J Proteome Res* 11, 1804-1811.

129. Peng, J., Elias, J. E., Thoreen, C. C., Licklider, L. J., and Gygi, S. P. (2003) Evaluation of multidimensional chromatography coupled with tandem mass spectrometry (LC/LC-MS/MS) for large-scale protein analysis: the yeast proteome. *Journal of proteome research* 2, 43-50.

130. Naghavi, M., Libby, P., Falk, E., Casscells, S. W., Litovsky, S., Rumberger, J., Badimon, J. J., Stefanadis, C., Moreno, P., Pasterkamp, G., Fayad, Z., Stone, P. H., Waxman, S., Raggi, P., Madjid, M., Zarrabi, A., Burke, A., Yuan, C., Fitzgerald, P. J., Siscovick, D. S., de Korte, C. L., Aikawa, M., Juhani Airaksinen, K. E., Assmann, G., Becker, C. R., Chesebro, J. H., Farb, A., Galis, Z. S., Jackson, C., Jang, I. K., Koenig, W., Lodder, R. A., March, K., Demirovic, J., Navab, M., Priori, S. G., Rekhter, M. D., Bahr, R., Grundy, S. M., Mehran, R., Colombo, A., Boerwinkle, E., Ballantyne, C., Insull, W., Jr., Schwartz, R. S., Vogel, R., Serruys, P. W., Hansson, G. K., Faxon, D. P., Kaul, S., Drexler, H., Greenland, P., Muller, J. E., Virmani, R., Ridker, P. M., Zipes, D. P., Shah, P. K., and Willerson, J. T. (2003) From vulnerable plaque to vulnerable patient: a call for new definitions and risk assessment strategies: Part I. *Circulation* 108, 1664-1672.

131. Hansson, G. K., and Hermansson, A. (2011) The immune system in atherosclerosis. *Nat Immunol* 12, 204-212.

132. van der Wal, A. C., and Becker, A. E. (1999) Atherosclerotic plaque rupture--pathologic basis of plaque stability and instability. *Cardiovasc Res* 41, 334-344.

133. Depre, C., Wijns, W., Robert, A. M., Renkin, J. P., and Havaux, X. (1997) Pathology of unstable plaque: correlation with the clinical severity of acute coronary syndromes. *J Am Coll Cardiol* 30, 694-702.

134. Lattimer, C. R., and Burnand, K. G. (1997) Recurrent carotid stenosis after carotid endarterectomy. *Br J Surg* 84, 1206-1219.

135. Sadideen, H., Taylor, P. R., and Padayachee, T. S. (2006) Restenosis after carotid endarterectomy. *Int J Clin Pract* 60, 1625-1630.

136. Frantzi, M., Bhat, A., and Latosinska, A. (2014) Clinical proteomic biomarkers: relevant issues on study design & technical considerations in biomarker development. *Clin Transl Med* 3, 7.

137. Whiteaker, J. R., Lin, C., Kennedy, J., Hou, L., Trute, M., Sokal, I., Yan, P., Schoenherr, R. M., Zhao, L., Voytovich, U. J., Kelly-Spratt, K. S., Krasnoselsky, A., Gafken, P. R., Hogan, J. M., Jones, L. A., Wang, P., Amon, L., Chodosh, L. A., Nelson, P. S., McIntosh, M. W., Kemp, C. J., and Paulovich, A. G. (2011) A targeted proteomics-based pipeline for verification of biomarkers in plasma. *Nat Biotechnol* 29, 625-634.

138. de la Cuesta, F., Alvarez-Llamas, G., Gil-Dones, F., Martin-Rojas, T., Zubiri, I., Pastor, C., Barderas, M. G., and Vivanco, F. (2009) Tissue proteomics in atherosclerosis: elucidating the molecular mechanisms of cardiovascular diseases. *Expert Rev Proteomics* 6, 395-409.

139. Eberini, I., Wait, R., Calabresi, L., Sensi, C., Miller, I., and Gianazza, E. (2013) A proteomic portrait of atherosclerosis. *J Proteomics* 82, 92-112.

140. Bagnato, C., Thumar, J., Mayya, V., Hwang, S. I., Zebroski, H., Claffey, K. P., Haudenschild, C., Eng, J. K., Lundgren, D. H., and Han, D. K. (2007) Proteomics analysis of human coronary atherosclerotic plaque: a feasibility study of direct tissue proteomics by liquid chromatography and tandem mass spectrometry. *Mol Cell Proteomics* 6, 1088-1102.

141. de Kleijn, D. P., Moll, F. L., Hellings, W. E., Ozsarlak-Sozer, G., de Bruin, P., Doevendans, P. A., Vink, A., Catanzariti, L. M., Schoneveld, A. H., Algra, A., Daemen, M. J., Biessen, E. A., de Jager, W., Zhang, H., de Vries, J. P., Falk, E., Lim, S. K., van der Spek, P. J., Sze, S. K., and Pasterkamp, G. (2010) Local atherosclerotic plaques are a source of prognostic biomarkers for adverse cardiovascular events. *Arterioscler Thromb Vasc Biol* 30, 612-619.

142. Hains, P. G., and Truscott, R. J. (2010) Age-dependent deamidation of lifelong proteins in the human lens. *Invest Ophthalmol Vis Sci* 51, 3107-3114.

143. Jin, L. L., Tong, J., Prakash, A., Peterman, S. M., St-Germain, J. R., Taylor, P., Trudel, S., and Moran, M. F. (2010) Measurement of protein phosphorylation stoichiometry by selected reaction monitoring mass spectrometry. *J Proteome Res* 9, 2752-2761.

144. Verhoeven, B. A., Velema, E., Schoneveld, A. H., de Vries, J. P., de Bruin, P., Seldenrijk, C. A., de Kleijn, D. P., Busser, E., van der Graaf, Y., Moll, F., and Pasterkamp, G. (2004) Athero-express: differential atherosclerotic plaque expression of mRNA and protein in relation to cardiovascular events and patient characteristics. Rationale and design. *Eur J Epidemiol* 19, 1127-1133.

145. Thomas, P. D., Campbell, M. J., Kejariwal, A., Mi, H., Karlak, B., Daverman, R., Diemer, K., Muruganujan, A., and Narechania, A. (2003) PANTHER: a library of protein families and subfamilies indexed by function. *Genome Res* 13, 2129-2141.

146. Mi, H., Lazareva-Ulitsky, B., Loo, R., Kejariwal, A., Vandergriff, J., Rabkin, S., Guo, N., Muruganujan, A., Doremieux, O., Campbell, M. J., Kitano, H., and Thomas, P. D. (2005) The PANTHER database of protein families, subfamilies, functions and pathways. *Nucleic Acids Res* 33, D284-288.

147. MacLean, B., Tomazela, D. M., Shulman, N., Chambers, M., Finney, G. L., Frewen, B., Kern, R., Tabb, D. L., Liebler, D. C., and MacCoss, M. J. (2010) Skyline: an open source document editor for creating and analyzing targeted proteomics experiments. *Bioinformatics* 26, 966-968.

148. Hao, P., Ren, Y., Pasterkamp, G., Moll, F. L., de Kleijn, D. P., and Sze, S. K. (2014) Deep proteomic profiling of human carotid atherosclerotic plaques using multidimensional LC-MS/MS. *Proteomics Clin Appl*.

149. Ghazalpour, A., Doss, S., Yang, X., Aten, J., Toomey, E. M., Van Nas, A., Wang, S., Drake, T. A., and Lusis, A. J. (2004) Thematic review series: The pathogenesis of atherosclerosis. Toward a biological network for atherosclerosis. *J Lipid Res* 45, 1793-1805.

150. Hansson, G. K. (2005) Inflammation, atherosclerosis, and coronary artery disease. *N Engl J Med* 352, 1685-1695.

151. Giannakopoulos, T., Avgerinos, E., Moulakakis, K., Kadoglou, N., Preza, O., Papapetrou, A., Papasideris, C., and Liapis, C. (2011) Biomarkers for diagnosis of the vulnerable atherosclerotic plaque. *Interventional Cardiology* 3, 223-233.

152. Lange, V., Picotti, P., Domon, B., and Aebersold, R. (2008) Selected reaction monitoring for quantitative proteomics: a tutorial. *Mol Syst Biol* 4, 222.

153. Hao, P., Ren, Y., Tam, J. P., and Sze, S. K. (2013) Correction of errors in tandem mass spectrum extraction enhances phosphopeptide identification. *J Proteome Res* 12, 5548-5557.

154. Katsuda, S., and Kaji, T. (2003) Atherosclerosis and extracellular matrix. *J Atheroscler Thromb* 10, 267-274.

155. MacLeod, D. C., Strauss, B. H., de Jong, M., Escaned, J., Umans, V. A., van Suylen, R. J., Verkerk, A., de Feyter, P. J., and Serruys, P. W. (1994) Proliferation and extracellular matrix synthesis of smooth muscle cells cultured from human coronary atherosclerotic and restenotic lesions. *J Am Coll Cardiol* 23, 59-65.

156. Johnson, J. L. (2007) Matrix metalloproteinases: influence on smooth muscle cells and atherosclerotic plaque stability. *Expert Rev Cardiovasc Ther* 5, 265-282.

157. Nakashima, Y., Raines, E. W., Plump, A. S., Breslow, J. L., and Ross, R. (1998) Upregulation of VCAM-1 and ICAM-1 at atherosclerosis-prone sites on the endothelium in the ApoE-deficient mouse. *Arterioscler Thromb Vasc Biol* 18, 842-851.

158. Iiyama, K., Hajra, L., Iiyama, M., Li, H., DiChiara, M., Medoff, B. D., and Cybulsky, M. I. (1999) Patterns of vascular cell adhesion molecule-1 and intercellular adhesion molecule-1 expression in rabbit and mouse atherosclerotic lesions and at sites predisposed to lesion formation. *Circ Res* 85, 199-207.

159. Karakas, M., and Koenig, W. (2012) Myeloperoxidase production by macrophage and risk of atherosclerosis. *Curr Atheroscler Rep* 14, 277-283.

160. Nicholls, S. J., and Hazen, S. L. (2009) Myeloperoxidase, modified lipoproteins, and atherogenesis. *J Lipid Res* 50 Suppl, S346-351.

161. Delporte, C., Van Antwerpen, P., Vanhamme, L., Roumeguere, T., and Zouaoui Boudjeltia, K. (2013) Low-density lipoprotein modified by myeloperoxidase in inflammatory pathways and clinical studies. *Mediators Inflamm* 2013, 971579.

162. Garcia-Touchard, A., Henry, T. D., Sangiorgi, G., Spagnoli, L. G., Mauriello, A., Conover, C., and Schwartz, R. S. (2005) Extracellular proteases in atherosclerosis and restenosis. *Arterioscler Thromb Vasc Biol* 25, 1119-1127.

163. Cudic, M., and Fields, G. B. (2009) Extracellular proteases as targets for drug development. *Curr Protein Pept Sci* 10, 297-307.

164. Lim, J. S., Lee, D. H., Park, J. Y., Jin, S. H., and Jacobs, D. R., Jr. (2007) A strong interaction between serum gamma-glutamyltransferase and obesity on the risk of prevalent type 2 diabetes: results from the Third National Health and Nutrition Examination Survey. *Clin Chem* 53, 1092-1098.

165. Jacobson, T. A. (2011) Opening a new lipid "apo-thecary": incorporating apolipoproteins as potential risk factors and treatment targets to reduce cardiovascular risk. *Mayo Clin Proc* 86, 762-780.

166. Kockx, M. M., and Herman, A. G. (2000) Apoptosis in atherosclerosis: beneficial or detrimental? *Cardiovasc Res* 45, 736-746.

167. Kockx, M. M., and Herman, A. G. (1998) Apoptosis in atherogenesis: implications for plaque destabilization. *Eur Heart J* 19 Suppl G, G23-28.

168. Galis, Z. S., Sukhova, G. K., Lark, M. W., and Libby, P. (1994) Increased expression of matrix metalloproteinases and matrix degrading activity in vulnerable regions of human atherosclerotic plaques. *J Clin Invest* 94, 2493-2503.

169. Galis, Z. S., and Khatri, J. J. (2002) Matrix metalloproteinases in vascular remodeling and atherogenesis: the good, the bad, and the ugly. *Circ Res* 90, 251-262.

170. Dollery, C. M., Humphries, S. E., McClelland, A., Latchman, D. S., and McEwan, J. R. (1999) Expression of tissue inhibitor of matrix metalloproteinases 1 by use of an adenoviral vector inhibits smooth muscle cell migration and reduces neointimal hyperplasia in the rat model of vascular balloon injury. *Circulation* 99, 3199-3205.

171. George, S. J., Baker, A. H., Angelini, G. D., and Newby, A. C. (1998) Gene transfer of tissue inhibitor of metalloproteinase-2 inhibits metalloproteinase activity and neointima formation in human saphenous veins. *Gene Ther* 5, 1552-1560.

172. Rouis, M., Adamy, C., Duverger, N., Lesnik, P., Horellou, P., Moreau, M., Emmanuel, F., Caillaud, J. M., Laplaud, P. M., Dachet, C., and Chapman, M. J. (1999) Adenovirus-mediated overexpression of tissue inhibitor of metalloproteinase-1 reduces atherosclerotic lesions in apolipoprotein E-deficient mice. *Circulation* 100, 533-540.

173. Cardellini, M., Menghini, R., Martelli, E., Casagrande, V., Marino, A., Rizza, S., Porzio, O., Mauriello, A., Solini, A., Ippoliti, A., Lauro, R., Folli, F., and Federici, M. (2009) TIMP3 is reduced in atherosclerotic plaques from subjects with type 2 diabetes and increased by SirT1. *Diabetes* 58, 2396-2401.

174. Romero, J. R., Vasan, R. S., Beiser, A. S., Polak, J. F., Benjamin, E. J., Wolf, P. A., and Seshadri, S. (2008) Association of carotid artery atherosclerosis with circulating biomarkers of extracellular matrix remodeling: the Framingham Offspring Study. *J Stroke Cerebrovasc Dis* 17, 412-417.

175. LA, V. B., Nakao, L. S., Ramos, S. G., Filho, A. P., Murta, L. O., Jr., Ingberman, M., Tefe-Silva, C., and Precoma, D. B. (2011) Assessment of MMP-9, TIMP-1, and COX-2 in normal tissue and in advanced symptomatic and asymptomatic carotid plaques. *Thromb J* 9, 6.

176. Kim, Y. J., Gallien, S., van Oostrum, J., and Domon, B. (2013) Targeted proteomics strategy applied to biomarker evaluation. *Proteomics Clin Appl* 7, 739-747.

177. Alvarez, B., Ruiz, C., Chacon, P., Alvarez-Sabin, J., and Matas, M. (2004) Serum values of metalloproteinase-2 and metalloproteinase-9 as related to unstable plaque and inflammatory cells in patients with greater than 70% carotid artery stenosis. *J Vasc Surg* 40, 469-475.

178. Eldrup, N., Gronholdt, M. L., Sillesen, H., and Nordestgaard, B. G. (2006) Elevated matrix metalloproteinase-9 associated with stroke or cardiovascular death in patients with carotid stenosis. *Circulation* 114, 1847-1854.

179. Libby, P., Ridker, P. M., and Hansson, G. K. (2009) Inflammation in atherosclerosis: from pathophysiology to practice. *J Am Coll Cardiol* 54, 2129-2138.

180. Halim, S. A., and Newby, L. K. (2009) Prognostic biomarkers in individuals with prevalent coronary heart disease. *Dis Markers* 26, 265-271.

181. Naruko, T., Ueda, M., Haze, K., van der Wal, A. C., van der Loos, C. M., Itoh, A., Komatsu, R., Ikura, Y., Ogami, M., Shimada, Y., Ehara, S., Yoshiyama, M., Takeuchi, K., Yoshikawa, J., and Becker, A. E. (2002) Neutrophil infiltration of culprit lesions in acute coronary syndromes. *Circulation* 106, 2894-2900.

182. Sugiyama, S., Okada, Y., Sukhova, G. K., Virmani, R., Heinecke, J. W., and Libby, P. (2001) Macrophage myeloperoxidase regulation by granulocyte macrophage colony-stimulating factor in human atherosclerosis and implications in acute coronary syndromes. *Am J Pathol* 158, 879-891.

183. Lie, J., de Crom, R., van Gent, T., van Haperen, R., Scheek, L., Sadeghi-Niaraki, F., and van Tol, A. (2004) Elevation of plasma phospholipid transfer protein increases the risk of atherosclerosis despite lower apolipoprotein B-containing lipoproteins. *J Lipid Res* 45, 805-811.

184. Lie, J., de Crom, R., van Gent, T., van Haperen, R., Scheek, L., Lankhuizen, I., and van Tol, A. (2002) Elevation of plasma phospholipid transfer protein in transgenic mice increases VLDL secretion. *J Lipid Res* 43, 1875-1880.

185. van Haperen, R., van Tol, A., van Gent, T., Scheek, L., Visser, P., van der Kamp, A., Grosveld, F., and de Crom, R. (2002) Increased risk of atherosclerosis by elevated plasma levels of phospholipid transfer protein. *J Biol Chem* 277, 48938-48943.

186. Jiang, X. C., Qin, S., Qiao, C., Kawano, K., Lin, M., Skold, A., Xiao, X., and Tall, A. R. (2001) Apolipoprotein B secretion and atherosclerosis are decreased in mice with phospholipid-transfer protein deficiency. *Nat Med* 7, 847-852.

187. Oorni, K., Sneck, M., Bromme, D., Pentikainen, M. O., Lindstedt, K. A., Mayranpaa, M., Aitio, H., and Kovanen, P. T. (2004) Cysteine protease cathepsin F is expressed in human atherosclerotic lesions, is secreted by cultured macrophages, and modifies low density lipoprotein particles in vitro. *J Biol Chem* 279, 34776-34784.

188. Cybulsky, M. I., Iiyama, K., Li, H., Zhu, S., Chen, M., Iiyama, M., Davis, V., Gutierrez-Ramos, J. C., Connelly, P. W., and Milstone, D. S. (2001) A major role for VCAM-1, but not ICAM-1, in early atherosclerosis. *J Clin Invest* 107, 1255-1262.

189. Li, R., and Shen, Y. (2013) An old method facing a new challenge: re-visiting housekeeping proteins as internal reference control for neuroscience research. *Life Sci* 92, 747-751.

190. Eaton, S. L., Roche, S. L., Llavero Hurtado, M., Oldknow, K. J., Farquharson, C., Gillingwater, T. H., and Wishart, T. M. (2013) Total protein analysis as a reliable loading control for quantitative fluorescent Western blotting. *PLoS One* 8, e72457.

191. Skates, S. J., Gillette, M. A., LaBaer, J., Carr, S. A., Anderson, L., Liebler, D. C., Ransohoff, D., Rifai, N., Kondratovich, M., Tezak, Z., Mansfield, E., Oberg, A. L., Wright, I., Barnes, G., Gail, M., Mesri, M., Kinsinger, C. R., Rodriguez, H., and Boja, E. S. (2013) Statistical design for biospecimen cohort size in proteomics-based biomarker discovery and verification studies. *J Proteome Res* 12, 5383-5394.

192. Di Camillo, B., Sanavia, T., Martini, M., Jurman, G., Sambo, F., Barla, A., Squillario, M., Furlanello, C., Toffolo, G., and Cobelli, C. (2012) Effect of size and heterogeneity of samples on biomarker discovery: synthetic and real data assessment. *PLoS One* 7, e32200.

193. Drucker, E., and Krapfenbauer, K. (2013) Pitfalls and limitations in translation from biomarker discovery to clinical utility in predictive and personalised medicine. *EPMA J* 4, 7.

194. Aebersold, R., Burlingame, A. L., and Bradshaw, R. A. (2013) Western blots versus selected reaction monitoring assays: time to turn the tables? *Mol Cell Proteomics* 12, 2381-2382.

195. Takemoto, L., and Boyle, D. (2000) Specific glutamine and asparagine residues of gamma-S crystallin are resistant to in vivo deamidation. *J Biol Chem* 275, 26109-26112.

196. Chain, D. G., Schwartz, J. H., and Hegde, A. N. (1999) Ubiquitin-mediated proteolysis in learning and memory. *Mol Neurobiol* 20, 125-142.

197. McFadden, P. N., and Clarke, S. (1987) Conversion of isoaspartyl peptides to normal peptides: implications for the cellular repair of damaged proteins. *Proc Natl Acad Sci U S A* 84, 2595-2599.

198. Young, A. L., Carter, W. G., Doyle, H. A., Mamula, M. J., and Aswad, D. W. (2001) Structural integrity of histone H2B in vivo requires the activity of protein L-isoaspartate O-methyltransferase, a putative protein repair enzyme. *J Biol Chem* 276, 37161-37165.

Appendix A

Publications

1. **Hao, P.**, Ren, Y., Datta, A., Tam, J. P., and Sze, S. K. (2014) Evaluation of the Effect of Trypsin Digestion Buffers on Artificial Deamidation. J Proteome Res. 2014 Dec 22. [Epub ahead of print]

2. **Hao, P.**, Ren, Y., Pasterkamp, G., Moll, F. L., de Kleijn, D. P., and Sze, S. K. (2014) Deep Proteomic Profiling of Human Carotid Atherosclerotic Plaques Using Multidimensional LC-MS/MS. *Proteomics Clin Appl.* 8, 631-5.

3. Ren, Y., **Hao, P.**, Law, S.K., and Sze, S. K. (2014) Hypoxia-induced changes to integrin alpha 3 glycosylation facilitate invasion in epidermoid carcinoma cell line A431. *Mol Cell Proteomics.* pii: mcp.M114.038505

4. Dutta, B., Ren, Y., **Hao, P.**, Sim, K. H., Cheow, E., Adav, S., Tam, J. P., and Sze, S. K. (2014) Profiling of the Chromatin-Associated Proteome Identifies HP1BP3 as a Novel Regulator of Cell Cycle Progression. *Mol Cell Proteomics.* pii: mcp.M113.034975.

5. **Hao, P.**, Ren, Y., Tam, J. P., and Sze, S. K. (2013) Correction of errors in tandem mass spectrum extraction enhances phosphopeptide identification. *J Proteome Res* 12, 5548-5557.

6. **Hao, P.**, Ren, Y., Dutta, B., and Sze, S. K. (2013) Comparative evaluation of electrostatic repulsion-hydrophilic interaction chromatography (ERLIC) and high-pH reversed phase (Hp-RP) chromatography in profiling of rat kidney proteome. *J Proteomics* 82, 254-262.

7. Li, Z., **Hao, P.**, Li, L., Tan, C. Y., Cheng, X., Chen, G. Y., Sze, S. K., Shen, H. M., and Yao, S. Q. (2013) Design and synthesis of minimalist terminal alkyne-containing diazirine photo-crosslinkers and their incorporation into kinase inhibitors for cell- and tissue-based proteome profiling. *Angew Chem Int Ed Engl* 52, 8551-8556.

8. Ren, Y., **Hao, P.**, Dutta, B., Cheow, E. S., Sim, K. H., Gan, C. S., Lim, S. K., and Sze, S. K. (2013) Hypoxia modulates A431 cellular pathways association to tumor radioresistance and enhanced migration revealed by comprehensive proteomic and functional studies. *Mol Cell Proteomics* 12, 485-498.

9. Ge, J., Zhang, C. J., Li, L., Chong, L. M., Wu, X., **Hao, P.**, Sze, S. K., and Yao, S. Q. (2013) Small molecule probe suitable for in situ profiling and inhibition of protein disulfide isomerase. *ACS Chem Biol* 8, 2577-2585.

10. **Hao, P.**, Qian, J., Dutta, B., Cheow, E. S., Sim, K. H., Meng, W., Adav, S. S., Alpert, A., and Sze, S. K. (2012) Enhanced separation and characterization of deamidated peptides with RP-ERLIC-based multidimensional chromatography coupled with tandem mass spectrometry. *J Proteome Res* 11, 1804-1811.

11. **Hao, P.**, Qian, J., Ren, Y., and Sze, S. K. (2011) Electrostatic repulsion-hydrophilic interaction chromatography (ERLIC) versus strong cation exchange (SCX) for fractionation of iTRAQ-labeled peptides. *J Proteome Res* 10, 5568-5574.

12. **Hao, P.**, Ren, Y., Alpert, A. J., and Sze, S. K. (2011) Detection, evaluation and minimization of nonenzymatic deamidation in proteomic sample preparation. *Mol Cell Proteomics* 10, O111 009381.

13. **Hao, P.**, Guo, T., and Sze, S. K. (2011) Simultaneous analysis of proteome, phospho- and glycoproteome of rat kidney tissue with electrostatic repulsion hydrophilic interaction chromatography. *PLoS One* 6, e16884.

14. **Hao, P.**, Guo, T., Li, X., Adav, S. S., Yang, J., Wei, M., and Sze, S. K. (2010) Novel application of electrostatic repulsion-hydrophilic interaction chromatography (ERLIC) in shotgun proteomics: comprehensive profiling of rat kidney proteome. *J Proteome Res* 9, 3520-3526.

Book Chapters:

1. **Hao, P.**, Sze, S.K. (2014) Proteomic analysis of protein deamidation. *Curr Protoc Protein Sci*. 2014 Nov 3;78:24.5.1-24.5.14

2. **Hao, P.**, Zhang, H., and Sze, S. K. (2011) Application of electrostatic repulsion hydrophilic interaction chromatography to the characterization of proteome, glycoproteome, and phosphoproteome using nano LC-MS/MS. *Methods Mol Biol* 790, 305-318.

Appendix B

Conference Presentations

Posters

1. 7th AOHUPO/9th PST, Bangkok, Thailand, August 6-8, 2014. **Piliang Hao,** Yan Ren, Siu Kwan Sze.

   Title: Evaluation of the Effect of Digestion Buffers on Artificial Deamidation in In-solution Trypsin Digestion

2. 62nd ASMS Conference on Mass Spectrometry and Allied Topics, Baltimore, USA, June 15-19, 2014. **Piliang Hao,** Yan Ren, James P. Tam, Siu Kwan Sze.

   Title: Correction of Errors in Tandem Mass Spectrum Extraction Enhances Phosphopeptide Identification

3. Inaugural SOCRATES Scientific Meeting 2013, Singapore, October 24-25, 2013. **Piliang Hao,** Yan Ren, Siu Kwan Sze.

   Title: Enhanced Separation and Characterization of Deamidated Peptides with RP-ERLIC-based Multidimensional Chromatography Coupled with Tandem Mass Spectrometry

4. International Conference on Natural Products and Health 2013, Singapore, September 5-7, 2013**. Piliang Hao,** Yan Ren, Siu Kwan Sze.

   Title: Enhanced Separation and Characterization of Deamidated Peptides with RP-ERLIC-based Multidimensional Chromatography Coupled with Tandem Mass Spectrometry

5. 60th ASMS Conference on Mass Spectrometry and Allied Topics, Vancouver, Canada, May 19-24, 2012. **Piliang Hao,** Yan Ren, Esther Sok Hwee Cheow, Kae Hwan Sim, Andrew Alpert, Siu Kwan Sze.

   Title: Global Profiling of Endogenous Deamidated Peptides with a RP-ERLIC Chromatography Sequence Coupled with Tandem Mass Spectrometry

6. 59th ASMS Conference on Mass Spectrometry and Allied Topics, Denver, USA, June 5-9, 2011. **Piliang Hao,** Jingru Qian, Wei Meng, Yan Ren, Andrew J. Alpert, Siu Kwan Sze.

   Title: Simultaneous Identification of Unmodified Tryptic Peptides and Phosphopeptides, Glycopeptides, and Deamidated Peptides by Electrostatic Repulsion-Hydrophilic Interaction Chromatography (ERLIC) and LC-MS/MS

Awards

The Bronze Award of the 1st Shimadzu Young Scientist Award